Accepted Manuscript

Design, synthesis and evaluation of scutellarein-*O*-alkylamines as multifunctional agents for the treatment of Alzheimer's disease

Zhipei Sang, Xiaoming Qiang, Yan Li, Wen Yuan, Qiang Liu, Yikun Shi, Wei Ang, Youfu Luo, Zhenghuai Tan, Yong Deng

PII: S0223-5234(15)00161-0

DOI: 10.1016/j.ejmech.2015.02.063

Reference: EJMECH 7747

To appear in: *European Journal of Medicinal Chemistry*

Received Date: 9 November 2014

Revised Date: 27 February 2015

Accepted Date: 28 February 2015

Please cite this article as: Z. Sang, X. Qiang, Y. Li, W. Yuan, Q. Liu, Y. Shi, W. Ang, Y. Luo, Z. Tan, Y. Deng, Design, synthesis and evaluation of scutellarein-*O*-alkylamines as multifunctional agents for the treatment of Alzheimer's disease, *European Journal of Medicinal Chemistry* (2015), doi: 10.1016/j.ejmech.2015.02.063.

Design, synthesis and evaluation of scutellarein-*O*-alkylamines as multifunctional agents for the treatment of Alzheimer's disease

Zhipei Sang[1,#], *Xiaoming Qiang*[1,#], *Yan Li*[1], *Wen Yuan*[1], *Qiang Liu*[1], *Yikun Shi*[3], *Wei Ang*[1], *Youfu Luo*[2], *Zhenghuai Tan*[3,*] *and Yong Deng*[1,*]

Graphical Abstract

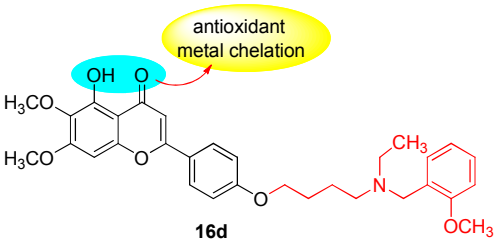

16d

Rat AChE IC_{50}: 0.62 μM
*Ee*AChE IC_{50}: 0.85 μM
*Hu*AChE IC_{50}: 0.25 μM
Rat BuChE IC_{50}: 62.0 μM
Blockade of CAS and PAS of AChE
ORAC-FL value: 0.84 (*Trolox* equiv)
Cytotoxicity (SH-SY5Y cells): IC_{50} >100 μM

Self-induced Aβ_{1-42} aggregation: 69.1% inhibition at 25 μM
Cu^{2+}-induced Aβ_{1-42} aggregation: 85.7% inhibition at 25 μM
AChE-induced Aβ_{1-40} aggregation: 62.2% inhibition at 100 μM
Disaggregation Cu^{2+}-induced Aβ_{1-42} aggregation: 81.3% disaggregation at 25 μM
Good protective effect against H_2O_2-induced PC12 cell injury

A series of scutellarein-*O*-alkylamine derivatives were designed, synthesized and tested as multifunctional agents for the treatment of Alzheimer's disease (AD). Compound **16d** was shown to be an interesting multifunctional lead compound for AD treatment.

Design, synthesis and evaluation of scutellarein-*O*-alkylamines as multifunctional agents for the treatment of Alzheimer's disease

Zhipei Sang[1,#], Xiaoming Qiang[1,#], Yan Li[1], Wen Yuan[1], Qiang Liu[1], Yikun Shi[3], Wei Ang[1], Youfu Luo[2], Zhenghuai Tan[3,] and Yong Deng[1,*]*

[1]Department of Medicinal Chemistry, Key Laboratory of Drug Targeting and Drug Delivery System of the Education Ministry, West China School of Pharmacy, Sichuan University, Chengdu, 610041, China

[2]State Key Laboratory of Biotherapy, West China Hospital, West China Medical School, Sichuan University, Chengdu, 610041, China

[3]Institute of Traditional Chinese Medicine Pharmacology and Toxicology, Sichuan Academy of Chinese Medicine Sciences, Chengdu, 610041, China

Abbreviations: AD, Alzheimer's disease; AChE, acetylcholinesterase; BuChE, butyrylcholinesterase; *Hu*AChE, human AChE; *Ee*AChE, *Electrophorus electricus* AChE; MTDL, multitarget-directed ligand; A*β*, *β*-amyloid peptide; CAS, catalytic active site; PAS, peripheral anionic site; MOM, methoxymethyl ether; PBS, phosphate-buffered saline; DTNB, 5,5'-dithiobis-2-nitrobenzoic acid; PDB, Protein Data Bank; *Tc*AChE, *Torpedo californica* AChE; ROS, reactive oxygen species; ORAC-FL, Oxygen Radicals Absorbance Capacity by Fluorescence; AAPH, 2,2'-Azobis (amidinopropane) dihydrochloride; ThT, thioflavin T; HEPES, 4-(2-Hydroxyethyl)-1-piperazineethanesulfonic acid; TEM, transmission electron microscopy.

# These authors contributed equally to this work.

* *Corresponding Author*.

Phone, +86-28-85258982; E-mail: tanzhh616@163.com (Zhenghuai Tan)

Phone, +86-28-85503790; E-mail: dengyong@scu.edu.cn (Yong Deng)

Abstract

A series of scutellarein-*O*-alkylamine derivatives were designed, synthesized and tested as multifunctional agents for the treatment of Alzheimer's disease (AD). The results showed that most of these compounds exhibited good multifunctional activities. Among them, compound **16d** demonstrated significant metal chelating properties, moderate acetylcholinesterase (AChE) inhibitory and anti-oxidative activity, and excellent inhibitory effects on self-induced A$\beta_{1\text{-}42}$ aggregation, Cu^{2+}-induced A$\beta_{1\text{-}42}$ aggregation, human AChE-induced A$\beta_{1\text{-}40}$ aggregation and disassembled Cu^{2+}-induced aggregation of the well-structured A$\beta_{1\text{-}42}$ fibrils. Both kinetic analysis of AChE inhibition and molecular modeling study suggested that **16d** binds simultaneously to the catalytic active site and peripheral anionic site of AChE. Moreover, compound **16d** showed a good protective effect against H_2O_2-induced PC12 cell injury, with low toxicity in SH-SY5Y cells. Furthermore, the step-down passive avoidance test showed this compound significantly reversed scopolamine-induced memory deficit in mice. Thus, **16d** was shown to be an interesting multifunctional lead compound worthy of further study.

Keywords: Alzheimer's disease; Scutellarein-*O*-alkylamines; Multifunctional agents; Acetylcholinesterase inhibitors; Metal-chelating agents; Aβ aggregation inhibitors.

1. Introduction

Alzheimer's disease (AD), the most common form of adult onset dementia affecting more than 44 million people worldwide, is a complex neurodegenerative process occurring in the central nervous system (CNS), characterized by progressive and irreversible cognitive impairment, severe behavioral abnormalities and ultimately causing death [1]. Current clinical treatment of AD is mainly focused on the symptomatic aspects. The drugs that are currently approved by the FDA include four acetylcholinesterase inhibitors (AChEs), tacrine (now withdrawn due hepatotoxicity), donepezil, rivastigmine and galantamine, and one *N*-methyl-*D*-aspartate (NMDA) receptor antagonist, memantine [2]. These agents can increase the levels of the neurotransmitter acetylcholine, which is depleted in AD brains, or prevent aberrant neuronal stimulation. Although these drugs are beneficial in improving cognitive, behavioral, and functional impairments they cannot prevent, halt, or reverse the progression of the disease. These are just palliative treatment and do not address the molecular mechanisms that underlie the pathogenic processes because of the multifactorial nature of AD [3]. However, treatment with a combination of an AChE inhibitor and memantine appears to produce an additional effect resulting in a well-tolerated, effective clinical strategy that increases the time before patients require nursing home care [4]. Thus, the development of agents that affect two or more AD-relevant targets has drawn considerable attention for their advancement in the treatment of AD [5,6]. In this regard, the multitarget-directed ligand strategy (MTDLs), i.e., single chemical entities able to hit different targets involved in the cascade of AD pathological events, has been applied by many research groups [7,8], and the results obtained have been encouraging and convince researchers that MTDLs might present the best pharmacological option for tackling the multifactorial nature of AD and for halting the progression of the disease. Several MTDLs candidate drugs with disease modifying potential are now in the pipeline and have reached testing stage in clinical trials [9].

Although the etiology of AD is still not completely known, several factors are considered to play definitive roles in AD pathogenesis. These include low levels of acetylcholine (ACh), oxidative

stress and free radical formation, the dyshomeostasis of biometals and *β*-amyloid (A*β*) deposits [10,11]. These insights have provided the rationale for therapies directly targeting the molecular causes of AD. Therefore the discovery of a lead compound that can modulate these four factors simultaneously is a crucial step in the search for a candidate for the clinical treatment of AD.

Scutellarin (4′,5,6-trihydroxyflavone-7-glucuronide), the major active component in breviscapine extracted from the Chinese herb *Erigeron breviscapus* (vant.) Hand.-Mazz., possesses a broad range of pharmacological properties related to neurological disorders, such as anti-inflammatory effect, metal chelating ability, neuroprotective action, A*β* fibril formation inhibition and free radical scavenging effect [12-14]. However, scutellarin's poor solubility, low oral absorption and difficultly of passing through the blood–brain barrier restricts its clinical uses as an anti-AD drug [15,16]. Recent studies have indicated that scutellarin is mainly hydrolyzed in the intestinal tract and is absorbed as aglycone scutellarein (**I**). This is the real bioactive component and much more easily absorbed [17]. Recently, our group has reported the synthesis of genistein-*O*-alkylbenzylamines and discovered a 7,4′-*O*-modified genistein derivative (**II**) as a potential multifunctional agent for the treatment of AD [18]. However, this compound has low inhibitory effects on self-induced A$\beta_{1\text{-}42}$ aggregation and human AChE-induced A$\beta_{1\text{-}40}$ aggregation. In this paper, 5,6,7-trimethoxy and 5-hydroxy-6,7-dimethoxy flavonoids were selected to combine with different length alkylbenzylamine or alkylpiperazine fragments to design a series of novel scutellarein-*O*-alkylamine derivatives, to test whether these novel molecules might possess more potency in various multifunctional activities.

In this study, a series of scutellarein-*O*-alkylamine derivatives were designed based on MTDLs (**Figure 1**). They were also synthesized and evaluated for their multifunctional biological activities. The biological evaluation included anti-oxidative effects, AChE and butyrylcholine esterase (BuChE) inhibition, the kinetics of enzyme inhibition, metal-chelating properties, effects on A*β* aggregation and disaggregation, protective effect against H_2O_2-induced PC12 cell injury, cytotoxic effects on SH-SY5Y cells, and neuroprotective effects in the mouse scopolamine model of memory

impairment. Finally, molecular modeling studies were also performed to afford insight into the binding mode and the structure-activity relationships of the novel scutellarein-*O*-alkylamine derivatives.

< Insert **Figure 1** >

2. Results and discussion

2.1. Chemistry

The synthesis of scutellarein-*O*-alkylamine derivatives (**15–18**) occurred via the general pathway, in which 6-hydroxy-2,3,4-trimethoxyacetophenone (**1**) was used as the starting material (**Scheme 1**). Compounds **7a–b** and **8a–b** were the key intermediates, usually prepared from condensation of compound **1** [19] with *para*-methoxymethoxybenzaldehyde (**2**) [20] or *m*-hydroxybenzaldehyde (**3**) in the presence of KOH at room temperature for 3 days to afford the chalcone intermediates **4** or **6**, respectively. Removal of the methoxymethyl ether (MOM) protection group was then carried out in a 10% aqueous hydrochloric acid solution at 50°C to obtain the corresponding 4′-OH chalcone compound (**5**). Subsequently, treatment of compound **5** or **6** with *conc.* H_2SO_4 and a catalytic amount of KI in DMSO at 100°C for 3–5 hours gave the flavonoids **7a** and **7b** respectively. Finally, removal of 5-methyl at flavonoid nucleus by anhydrous $AlCl_3$ in CH_3CN at 55–60°C for 1 h gave the corresponding 5-OH scutellarein derivatives **8a**–**b** [21]. Alkylation of **7a**–**b** or **8a**–**b** with excessive amounts of 1,3-dibromopropane, 1,4-dibromobutane or 1,6-dibromohexane in the presence of K_2CO_3 in CH_3CN at 60–65°C resulted in the intermediates, **10–13** [18]. In turn, these intermediates were reacted with the corresponding secondary amines **14A–F** in the presence of anhydrous K_2CO_3 at 60–65°C to provide the final scutellarein-*O*-alkylamine compounds, **15–18** [18]. All new compounds were purified by recrystallization or chromatography, and the analytical and spectroscopic data confirmed their structures, as detailed in the experimental section.

< Insert **Scheme 1** >

2.2. Pharmacology

2.2.1. Antioxidant activity

Reactive oxygen species (ROS) have been identified as important mediators of cell structure damage to lipids, proteins and nucleic acids. ROS have been associated with aging, AD and other neurodegenerative disorders [22]. In normal physiological conditions the host antioxidant defenses would control the level of reactive free radicals, but when free radicals have overwhelmed these defenses, cellular damage occurs [23]. Thus, an antioxidant might contribute to a therapeutic strategy that prevents the development of AD and other neurodegenerative disorders.

The antioxidant activities of all synthesized scutellarein-*O*-alkylamine derivatives were evaluated by following the well-established ORAC-FL method (oxygen radical absorbance capacity by fluorescein) [24] and the results were shown in **Table 1**. Trolox, a vitamin E analogue, was used as the standard, and the results were expressed as Trolox equivalents. Scutellarein was also tested, which has an ORAC-FL value of 10.0 Trolox equivalents. All the tested compounds exhibited potent peroxyl radical absorbance capacities, ranging from 0.12 to 0.84-fold of Trolox. As expected, the introduction of alkylamine group side chain in the flavonoid nucleus decreased the radical capture capacity but the different tertiary amine unit on the side chain has little influence on the radical capture capacity. Generally, the compounds with 5-hydroxyl at the flavonoid nucleus (**16** and **18**) exhibited higher radical capture capacity than that of 5-methoxyl (**15** and **17**). Compound **16d** showed the highest antioxidant activity, with an activity of 0.84 Trolox equivalents.

2.2.2. AChE and BuChE Inhibition

To evaluate the potential of the target compounds **15–18** for the treatment of AD, their cholinesterase inhibitory activities were determined by the modified Ellman method [25] using AChE from rat cortex homogenate (*Rat*AChE) and *electrophorus electricus* (*Ee*AChE) and BuChE from rat serum (*Rat*BuChE), with commercially available rivastigmine and donepezil as the reference standards. Furthermore, the most potent and representative compounds were reevaluated using human erythrocyte AChE (*Hu*AChE). The AChE and BuChE inhibitory activities of the synthesized scutellarein-*O*-alkylamine derivatives are listed in **Table 1** and **Table 2**, expressed as

IC_{50} values.

< Insert **Table 1** >

The tested target compounds displayed significant inhibitory activity against AChE. Almost all the compounds exhibited very weak activity against BuChE and showed higher selectivity for *rat*AChE over *rat*BuChE. The results showed that introduction of the *O*-alkylamines increased the ChEs inhibitory capacity and improved the selectivity for *rat*AChE over *rat*BuChE. This selectivity profile may be a limitation, but this also may be beneficial to diminish peripheral cholinergic side effects and provide lower toxicity. Because severe side effects of AChE inhibitors, such as tacrine, have been suggested to be attributed to their poor selectivity [26]. As shown in **Table 1** and **Figure 2**, the properties of the substitutions at flavonoid nucleus 5 position had significant effects on AChE inhibitory activities, 5-methoxy derivatives (**15c**, **15d**, **15i**, **15j**, **15o**, **15p**, **17h**, **17i**, **17n**, **17o**, **17t**, **17u**) showed higher activity than the 5-hydroxyl analogues (**16a–f**, **18a–f**). The 5-methoxy at the flavonoid nucleus may play a significant role in the AChE inhibitory activity.

< Insert **Figure 2** >

As shown in **Table 1**, compounds with different length alkyamino side chains at 4′ positon showed better AChE inhibitory activities than that at 3′ positon, but the compounds (**15e**, **15f**, **15k**, **15l**, **15q**, **17d**, **17e**, **17j**, **17k**, **17p**, **17q**, **17v**) containing two basic centers (methyl piperazine and benzylpiperazine group) demonstrated the opposite result. This phenomenon revealed that the alkyamino side chain can interact with catalytic active site (CAS) of AChE in different ways. The screening data also showed that the structure of terminal groups NR_1R_2 of side chain affected the inhibitory activities. The potencies to inhibit AChE were in the order *N*-(2-methoxybenzyl) ethanamine > *N*-(2-methoxybenzy)methanamine > *N*-benzylpiperazine > *N*-benzylethanamine > *N*-benzyl methanamine > 1-methylpiperazine. In most conditions，compounds (**15b**, **15d**, **15h**, **15j**, **15n**, **15p**, **16b**, **16d**, **16f**, **17b**, **17g**, **17i**, **17m**, **17o**, **17s**, **17u**, **18b**, **18d**, **18f**) possessing a *N*-ethyl group showed better AChE inhibitory activity than compounds (**15a**, **15c**, **15g**, **15i**, **15m**, **15o**, **16a**, **16c**, **16e**, **17a**, **17c**, **17f**, **17h**, **17l**, **17n**, **17r**, **17t**, **18a**, **18c**, **18e**) with a *N*-methyl group. The terminal

groups NR_1R_2 containing a methoxyl group showed more potent AChE inhibitory activity than that without a methoxyl. In particular, the *N*-(2-methoxybenzyl)ethanamine (**15j**, IC_{50} = 0.12±0.01μM) at the end of side chain expressed high inhibitory activity. As shown in **Table 1**, with the same scaffold and terminal groups NR_1R_2, AChE inhibitory activity increased with an increase in methylene chain length, except compounds **15j**, **16c** and **16d**, where the optimal chain length was four. However, inhibitory activity decreased with an increase of methylene chain length when the terminal groups NR_1R_2 was 1-benzylpiperazine, for example compounds (**15f**, **15l**, **15q**) and compounds (**17e**, **17k**, **17q**, **17v**). Finally, compound **15j** showed the most potent inhibition for *Rat*AChE with an IC_{50} value of 0.12μM and a 568.3-fold selectivity for AChE over BuChE. Furthermore, compound **16d** also exhibited a good AChE inhibition activity (IC_{50} = 0.62±0.01μM) and a high selectivity (100.0-fold of inhibition selectivity for AChE over BuChE). From the re-evaluated results by additional testing using *Ee*AChE and *Hu*AChE, it is notable that most of the tested compounds exhibited a 3–6-fold higher inhibitory activity towards *Rat*AChE than towards *Ee*AChE (**Table 1**). However, the inhibitory activity of compounds (**15j**, **16d**) against *Rat*AChE is about 2–4-fold lower than that against *Hu*AchE (**Table 2**).

2.2.3. Kinetic studies of AChE inhibition

To investigate the AChE inhibitory mechanism for this class of scutellarein-*O*-alkylamine derivatives, a kinetic study was carried out with a representative compound **16d** using *Ee*AChE (**Figure 3**). The Lineweaver–Burk plots exhibited that both inhibitions had rising slopes and increasing intercepts at higher concentration, which indicated a mixed-type inhibition. The result demonstrated that compound **16d** could bind to both CAS and PAS of AChE, which is similar to that of donepezil and consistent with the results of molecular modeling studies.

< Insert **Figure 3** >

2.2.4. Molecular modeling study

To explore the possible interacting mode of the scutellarein-*O*-alkylamine derivatives with *Torpedo californica (Tc)*AChE (PDB code: *1EVE*), a molecular modeling study was performed using the

docking program named AUTODOCK 4.2 package with Discovery Studio 2.1 [27]. As shown in **Figure 4**, the results indicated that **16d** occupied the entire enzymatic CAS, the mid-gorge sites and the PAS, and could simultaneously bind to both the catalytic site and the peripheral site thus providing an explanation for its highly potent inhibitory activity against AChE. In the **16d**-*Tc*AChE complex, the *N*-(2-methoxybenzyl)ethanamine moiety of **16d** was observed to bind to the CAS *via* a π-π interaction with Trp84 and potential hydrophobic interactions with residues Tyr130, Asn85, Ser81, Asp72, Gly123, Gly117, Gly118 and Ser122. The flavonoid moiety occupied the PAS of AChE, the benzene ring of flavonoid moiety in **16d** binding to the PAS *via* a π-π interaction with Trp279 and the benzene ring at 2-position of flavonoid nucleus could bind to the mid-gorge sites *via* a π-π interaction with Tyr334. The 5-hydroxy and 4-carbonyl group at the flavonoid nucleus could simultaneously bind to the Arg289 *via* two intermolecular hydrogen bonds, and the 4-chromanones moiety possessed potential hydrophobic interaction with residues Ser286, Leu282, Ile287 and Phe290. In addition, the long chain of methylene and the benzene ring at the 2-position of flavonoid nucleus could fold into a conformation in the gorge that allowed them to interact with Tyr70, Tyr121, Phe330 and Phe331 through hydrophobic interaction. The results of the docking also explained why 5-methoxy substituted derivatives showed higher AChE inhibition activity than that 5-hydroxyl substituted ones. It might be because the amino acid residues taking part in hydrogen bond interaction were different. As shown in **Fig 4**, **16d** took part in hydrogen bond interaction with Arg289, while **15j** formed hydrogen bond interaction with Phe288, a very important amino acid of the acyl pocket of AChE [28]. Another explanation for this phenomenon, that as with donepezil which has no direct hydrogen bond interaction, a water bridged hydrogen bonding may have occurred under biological circumstances between the 5-methoxy of compound **15j** and *Tc*AChE [29].

< Insert **Figure 4** >

*2.2.5. Metal-chelating properties of compounds **15j** and **16d***

The complexing ability of compounds **15j** and **16d** toward biometals such as Cu^{2+}, Fe^{2+}, Zn^{2+} and

Al^{3+} was studied by UV-visual spectrometry, and the results are shown in **Figure 5**. The electronic spectra of **16d** demonstrated a red shift (the peak at 330 nm shifted to 337 nm) after the addition of $CuCl_2$. The result indicated that compound **16d** could interact effectively with the Cu^{2+}. Similar results were also obtained when $AlCl_3$ was added, the peak in the electronic spectra of **16d** at 330 nm shift to 340 nm. When $FeSO_4$ and $ZnCl_2$ were added, the electronic spectra of **16d** showed no obvious change. Therefore, **16d** has the selectivity of metal chelation. However, when the same experiment was performed using compound **15j** and biometal ions, no significant differences were observed in the UV spectrum (see Supporting Information), suggesting little or no complex formation between **15j** with Cu^{2+}, Al^{3+}, Fe^{2+} or Zn^{2+}. The results revealed that the 5-hydroxyl and 4-carbonyl group of the flavonoid nucleus may contribute to the chelation.

The observed selectivity of the compound **16d** toward Cu^{2+} compared with Fe^{3+} may have interesting therapeutic applications. Several studies have shown that Cu^{2+} contributes more to the formation of senile plaques than iron does because of its superior affinity for $A\beta_{1\text{-}42}$ [30]. In addition, the complex $A\beta_{1\text{-}42}$-Cu^{2+} produces more reactive oxygen species due to its higher reduction potential (500 mV) than the corresponding complex with Fe^{3+} [31]. Therefore, the selective complexation of Cu^{2+} by the compound **16d** could simultaneously stop the formation of amyloid plaques and relieve oxidative stress.

< Insert **Figure 5** >

The stoichiometry of the **16d**-Cu^{2+} complex was determined using the molar ratio method, by preparing the solution of compound **16d** with ascending amounts of $CuCl_2$. The UV spectra were recorded and treated by numerical subtraction of $CuCl_2$ and **16d** at corresponding concentrations at 337nm. As shown in **Figure 6**, the absorbance linearly increased initially and then plateaued. The two straight lines intersected at a mole fraction of 0.95, indicating a 1:1 stoichiometry for the complex **16d**-Cu^{2+}.

< Insert **Figure 6** >

2.2.6. Effects on the self-induced $A\beta_{1\text{-}42}$ aggregation and HuAChE-induced $A\beta_{1\text{-}40}$ aggregation

A number of dual binding site AChE inhibitors have been found to exhibit a significant inhibitory activity on Aβ self-aggregation [32,33]. Therefore, some compounds (**15d**, **15g**, **15h**, **15i**, **15j**, **15p**, **16b**, **16d** and **16f**) that showed good potency for AChE inhibition were selected to assess their ability to inhibit self-induced A$\beta_{1\text{-}42}$ aggregation *via* the thioflavin T fluorescence method [18], using curcumin, a known active natural product that inhibits self-induced Aβ aggregation, as a reference compound. As summarized in **Table 2**, the tested compounds showed moderate (31.3–37.1%) to good (66.5–71.4%) inhibitory effect, compared with curcumin (43.1%). The marketed AD drug, donepezil, did not show any significant inhibitory activity under the same experimental conditions. The results also indicated that the 5-hydroxy at flavonoid nucleus (**16b**, **16d**, **16f**) showed remarkably higher inhibitory activity than that of 5-methoxyl (**15d**, **15g**, **15h**, **15i**, **15j** and **15p**), the inhibitory activity increased slightly as the length of the side chain carbon spacer increased, for example, **15d** (32.1%) < **15j** (34.3%) < **15p** (35.6%); **16b** (66.5%) < **16d** (69.1%) < **16f** (71.4%), and different tertiary amine units on the side chain had little influence on the inhibitory activity. The results revealed that the hydrogen bonds are crucial for the interactions between ligand and proteins. Compound **16d** also showed a dose-dependent inhibitory effect on self-induced A$\beta_{1\text{-}42}$ aggregation (43.5±0.8% at 12.5μM, 69.1±1.8% at 25μM, 87.2±2.6% at 50μM).

Numerous studies have revealed that AChE played an important role not only in the hydrolysis of ACh, but also in promoting the aggregation of Aβ into amyloid fibrils [33]. Furthermore, the PAS of AChE can bind to Aβ, accelerating the formation of amyloid fibrils [34]. Therefore, inhibition of AChE, particularly the inhibition of PAS of AChE, may affect Aβ aggregation. The kinetic study showed that compound **16d** exhibited a mix-type inhibition and was able to bind to both the catalytic and peripheral site of AChE. Therefore, to further explore the dual action, compound **15j** and **16d** were selected to assess their ability to inhibit the *Hu*AChE-induced A$\beta_{1\text{-}40}$ aggregation *via* the thioflavin T fluorescence method [18], using donepezil as the reference compound. As summarized in **Table 2**, compounds **15j** and **16d** (all at 100 μM) prevented *Hu*AChE-induced A$\beta_{1\text{-}40}$ aggregation by 37.0% and 62.2%, respectively, which was higher than that of donepezil (18.8%). It

revealed that **15j** and **16d** may had higher affinity for PAS than donepezil. The results also showed that compound **16d** has about two-fold more effective than that of **15j**, indicating that 5-hydroxy at flavonoid nucleus played an important role in binding to PAS of AChE.

< Insert **Table 2** >

2.2.7. Effects on Cu^{2+}-induced Aβ_{1-42} aggregation and disaggregation

To investigate the effects of the derivatives on Cu^{2+}-induced Aβ_{1-42} aggregation, we carried out two individual studies (**Table 2**): The inhibitory activity of Cu^{2+}-induced Aβ_{1-42} aggregation by the compounds (**15d**, **15g**, **15h**, **15i**, **15j**, **15p, 16b**, **16d** and **16f**) and the disaggregation effects of two representative compounds (**15j** and **16d**) on Cu^{2+}-induced Aβ_{1-42} aggregation, using Thioflavin T (ThT) binding assay with curcumin as the reference compound [35]. The degree of Aβ_{1-42} aggregation was probed mainly by transmission electron microscopy (TEM) [35]. The Aβ_{1-42} peptide (25μM) was first treated with one equivalent of Cu^{2+} for 2 min at room temperature and then incubated with or without the testing compounds for 24 h at 37°C. Cu^{2+} could accelerate the aggregation of Aβ. In contrast, the fluorescence was markedly reduced by 84.8± 1.1%, 85.7±2.5%, or 87.2± 1.7% when Aβ_{1-42} was treated with Cu^{2+} and compounds **16b**, **16d**, or **16f**, respectively, which exhibited more potency than that of curcumin (58.0±2.3%). However, the other tested compounds showed lower inhibition potent than that of curcumin (**Table 2**). Donepezil did not show any inhibitory activity under the same experimental conditions. Structure-activity relationship analysis indicated that the long carbon chain side-chain at flavonoid 4′-position might increase the inhibition activity, for example **15d** < **15j** < **15p** or **16b** < **16d** < **16f**. Moreover, compound **16d** significantly inhibited Cu^{2+}-induced Aβ_{1-42} aggregation in a concentration-dependent manner (46.5±3.5% at 5μM, 64.6±1.2% at 10μM and 85.7±2.5% at 25μM). Interestingly, the rate of inhibition of **16d** showed nearly two-fold greater potency than that of **15j** (46.8±1.5%). It revealed that the 5-hydroxyl and 4-carbonyl at the flavonoid nucleus were key structural units to chelate with Cu^{2+}. Further, the results of TEM are consistent with ThT binding assay results. More well-defined Aβ aggregates were observed in the presence of Cu^{2+} than Aβ alone, and fewer Aβ fibrils were

observed when compound **16d** was added to the samples (**Figure 7**). These observations suggest that the chelating properties of the tested compounds might be crucial to changing the structural organization of Aβ aggregation fibrils.

< Insert **Figure 7** >

For the disaggregation studies, compound **15j** or **16d** (25μM) were added to Aβ fibrils, which were generated by reacting A$\beta_{1\text{-}42}$ with one equivalent of Cu^{2+} for 24 h at 37°C. The ThT binding assay showed that **15j** exhibited lower disaggregation potency (41.3±1.7%) than that of curcumin (56.5±2.1%), but **16d** manifested good disaggregation potency (81.3±3.4%) (**Table 2**). The TEM figures illustrated that the sample of A$\beta_{1\text{-}42}$ alone had aggregated into amyloid fibrils after 24 h of incubation, while only small bulk aggregates were visible and no characteristic fibrils were observed after adding **16d** (**Figure 8**). This suggests that **16d** could decompose the structure of Cu^{2+}-mediated Aβ aggregation fibrils. In summary, we can conclude that compound **16d** can inhibit Cu^{2+}-induced Aβ aggregation and disassemble the well-structured Aβ fibrils.

< Insert **Figure 8** >

2.2.8. Cytotoxic effects on SH-SY5Y cells

To examine the cytotoxicity of the representative compounds **15j** and **16d**, human neuronal cell line SH-SY5Y cells were exposed to the test compounds at three different concentrations (1, 10 and 100μM) for 24 h and the cell viability was tested by the 3-(4,5-dimethylthiazol-2-yl)-2,5-diphenyltetrazolium (MTT) assays [36]. As shown in **Figure 9**, **15j** and **16d** did not show modified cell viability up to the concentration of 10μM. With increased concentration to 100μM, **15j** or **16d** induced a decrease of cell viability (73% and 80.8%, respectively), it may be that the compound with a 5-methoxy at flavonoid nucleus exhibited more cytotoxicity than that of a 5-hydroxy. These results showed that the target compounds had a wide therapeutic safety range. Moreover, these preliminary results should encourage further studies to elucidate the neuroprotective mechanisms of **15j** and **16d**.

< Insert **Figure 9** >

2.2.9. Cell protective effects on H_2O_2 induced PC12 cell injury

AD brains exhibit constant evidence of reactive oxygen species (ROS) and reactive nitrogen species (RNS) mediated injury. These, like H_2O_2 in the presence of transition metals, such as Fe^{2+}, generate hydroxyl radicals ($OH^{\cdot}$) which can feed into a self-propagating cascade of neurodegenerative events [22]. The protective effects of **15j** and **16d** against free radicals damage were assessed by measuring the ability of the compounds to protect against H_2O_2 injury according to the reported protocol [37]. After 100 μM H_2O_2 exposure, cell viability as determined by MTT reduction was markedly decreased to 56.1 % ($P < 0.01$ *vs* control), suggesting high sensitivity to H_2O_2-induced injury. However, compounds **15j** and **16d** showed protective effects in a dose-dependent manner against hydrogen peroxide-induced PC12 cell injury (**Figure 10**). At concentrations of 10.0 μM, compounds **15j** and **16d** exhibited significantly neuroprotective effects and the cell viabilities were 60.3% and 75.1%, respectively. When the concentration is reduced to 1.0 μM, these cell viabilities decreased to 58.7% and 65.9%, respectively. It suggested the compound with a 5-hydroxy on the flavonoid nucleus had higher cell survival ratio than that with a 5-methoxy group. This may be associated with the ease which the 5-hydroxy can capture the hydroxyl radical, generated by H_2O_2.

< Insert **Figure 10** >

2.2.10. In vivo assay

Scopolamine is a muscarinic receptor antagonist that inhibits central cholinergic neuronal activity and influences the expression of a broad spectrum of genes associated with muscarinic receptor signaling pathways, apoptosis, and cell differentiation in rat brain [38]. Scopolamine-induced amnesia has been used extensively to evaluate potential therapeutic agents for treating AD. To determine whether the treatment of **16d** improve the contextual memory in scopolamine-induced mice, we performed the step-down passive avoidance tests [39]. As shown in **Figure 11**, the latency of mice treated with scopolamine alone (1 mg/kg, control group) showed no significant differences compared with vehicle-treated mice (normal group), when the dose of scopolamine up to 3 mg/kg, the step-down latency of mice treated with scopolamine alone (control group) was significantly

shorter than that of vehicle-treated mice (normal group) ($p < 0.01$). Moreover, we found that the latency of mice showed no significant differences between the treatment with donepezil group (0.5 mg/kg, positive group) and scopolamine alone (3 mg/kg, control group), while treatment with donepezil group (5 mg/kg) showed longer latency time than the control group with scopolamine (3 mg/kg) ($p < 0.01$) and clearly reversed the cognitive deficit induced by scopolamine. This was in agreement with our previous work and other groups in which similar doses also increased the latency time [18, 40]. According to the screening data, treatment with compound **16d** (0.66, 2.2, 6.6 and 19.8 mg/kg) increased the latency time in a dose-dependent manner, but the medium dose group (6.6 mg/kg) presented the longest latency time (136.2 sec) ($p < 0.01$) of the four dose groups. The medium dose (6.6 mg/kg) of compound **16d** showed slightly longer latency time than the mole equivalent of donepezil (5 mg/kg) (132.8 sec), which was a representative AChE inhibitor and had been approved by FDA for treating AD. Meanwhile, the latency time of the high dose of **16d** (19.8 mg/kg) demonstrated slightly shorter (118.2 sec) than that of the medium dose and donepezil (5 mg/kg). The reason maybe that the high dose has some neurotoxicity, the medium dose may close to full saturate AChE and would be the optimal dose. The latency time of the lowest dose of **16d** (0.66 mg/kg) demonstrated no significant differences compared with scopolamine alone (3 mg/kg, control group). Therefore, the optimal dose of **16d** might be 6.6 mg/kg. These results indicated that compound **16d** might not only have reversed cognitive deficit induced by scopolamine through increasing brain cholinergic activity due to the inhibition of AChE but also revealed some other properties influencing memory processes.

< Insert **Figure 11** >

3. Conclusion

In summary, to explore for effective drugs for the treatment of Alzheimer's disease (AD), a novel series of scutellarein-*O*-alkylamine derivatives **15–18** were designed, synthesized and evaluated as multi-target anti-Alzheimer agents. Most of the synthesized compounds were potent in

inhibiting AChE activity *in vitro* and displayed high selectivity for AChE over BuChE. Compound **16d** demonstrated a useful inhibitory activity toward AChE with IC_{50} value of 0.62±0.01 μM. The kinetic analysis suggested that **16d** showed mixed-type inhibition, and could bind to both CAS and PAS of AChE, which was consistent with the molecular modeling study. Compound **16d** also possessed the modest antioxidant activity (0.84 *eq* of Trolox), excellent inhibitory effects on self-induced A$\beta_{1\text{-}42}$ aggregation (69.1±1.8%), Cu^{2+}-induced A$\beta_{1\text{-}42}$ aggregation (85.7±2.5%) and *Hu*AChE-induced A$\beta_{1\text{-}40}$ aggregation (62.2±1.8%). Moreover, **16d** was found to be able to bind Cu^{2+} and Al^{3+} and assemble into metal complexes, which disaggregated Cu^{2+}-induced A$\beta_{1\text{-}42}$ aggregation (81.3±3.4%). Furthermore, **16d** had a good neuroprotective effect against H_2O_2-induced PC12 cell injury and exhibited a low toxicity in SH-SY5Y cells. More interestingly, our *in vivo* study proved that mice treated with **16d** (6.6 mg/kg, *p.o.*) displayed slightly longer step-down latency time than the drug control group donepezil (5.0 mg/kg, *p.o.*) in the step-down passive avoidance test. The present study indicated that **16d** could be considered as an interesting multi-targeted lead compound for the further study in the treatment of AD. Further studies to evaluate compound **16d** *in vivo* and to develop structural refinements are underway and will be reported in due course.

4. Experimental section

4.1. Chemistry

Unless otherwise noted, all materials were obtained from commercial suppliers and used without further purification. The purity of all final compounds was determined by high-performance liquid chromatography (HPLC) analysis to be over 96%. HPLC analysis was carried out on a Shimadzu LC-10Avp plus system with the use of a Kromasil C_{18} column (4.6 mm × 250 mm, 5um). ^{1}H and ^{13}C NMR spectra were recorded using TMS as the internal standard in $CDCl_3$ or DMSO-d_6 with a Varian INOVA spectrometer at 400 and 100 MHz, respectively. Coupling constants were given in Hz. Multiplicities are given as s (singlet), d (doublet), dd (double-doublet), t (triplet), q (quadruplet),

m (multiplet), and br (broad signal). MS spectra data were obtained on an Agilent-6210 TOF LC-MS spectrometer. Melting points were recorded on YRT-3 melting-point apparatus (China) and are uncorrected. All the reactions were monitored by thin-layer chromatography (TLC) using silica gel GF_{254} plates from Qingdao Haiyang Chemical Co. Ltd. (China) with an UV lamp (254nm). Column chromatography using silica gel (230–400 mesh) purchased from Qingdao Haiyang Chemical Co. Ltd. (China).

*4.1.1. (E)-1-(6-Hydroxy-2,3,4-trimethoxyphenyl)-3-(4-methoxymethoxyphenyl)-2-propen-1-one (**4**).* To a stirred solution of 6-hydroxy-2,3,4-trimethoxyacetophenone (10.0 g, 44.0 mmol) and 4-methoxymethoxybenzaldehyde (8.10 g, 49.0 mmol) in ethanol (120 mL) was added a solution of KOH (7.4 g, 0.14 mol) in water (7.4 mL). The reaction mixture was stirred for 72 h at room temperature and quenched in ice-cold water, acidified with 10% HCl, filtered and washed with water. The crude product was recrystallized with alcohol to afford the title product as yellow solid (14.9 g, 90% yield), mp 94.2-94.5 °C. ^{1}H NMR (400 MHz, $CDCl_3$) δ 13.78 (s,1H, OH), 7.87 (d, *J* = 16.0 Hz, 1H, =CH), 7.81 (d, *J* = 16.0 Hz, 1H, =CH), 7.60 (d, *J* = 8.8Hz, 2H, Ar-H), 7.08 (d, *J* = 8.8Hz, 2H, Ar-H), 6.30 (s, 1H, Ar-H), 5.23 (s, 2H, OCH_2O), 3.93 (s, 3H, OCH_3), 3.91 (s, 3H, OCH_3), 3.84 (s, 3H, OCH_3), 3.50 (s, 3H, OCH_3).

*4.1.2. (E)-1-(6-Hydroxy-2,3,4-trimethoxyphenyl)-3-(4-hydroxyphenyl)-2-propen-1-one (**5**).* To a solution of compound **4** (3.74 g, 10.0 mmol) and 10%HCl (6.0 mL) in ethanol (8.0 mL), the mixture was heated for 4 h at 50 °C, cooled to room temperature. The reaction mixture was poured into crushed ice. The resulting precipitate was filtered and washed with water. The crude product was recrystallized with alcohol to give yellow solid (3.0 g, 91% yield), mp 146.2-147.2 °C. ^{1}H NMR (400 MHz, $CDCl_3$) δ 13.79 (s,1H, OH), 7.86 (d, *J* = 16.0 Hz, 1H, Ar-H), 7.81 (d, *J* = 16.0 Hz, 1H, Ar-H), 7.54 (d, *J* = 8.4Hz, 2H, Ar-H), 6.88 (d, *J* = 8.4Hz, 2H, Ar-H), 6.30 (s, 1H, Ar-H), 5.41 (brs, 1H, OH), 3.93 (s, 3H, OCH_3), 3.90 (s, 3H, OCH_3), 3.84 (s, 3H, OCH_3).

*4.1.3. (E)-1-(6-Hydroxy-2,3,4-trimethoxyphenyl)-3-(3-hydroxyphenyl)-2-propen-1-one (**6**).* To a stirred solution of 6-hydroxy-2,3,4-trimethoxyacetophenone (5.0 g, 22.0 mmol) and

m-hydroxybenzaldehyde (3.3 g, 26.4 mmol) in ethanol (40 mL) was added a solution of KOH (3.7 g, 66.0 mmol) in water (6.0 mL). The reaction mixture was stirred for 72 h at room temperature and quenched in ice-cold water, acidified with 10% HCl, filtered and washed with water. The crude product was recrystallized with alcohol to afford the title product as yellow solid (6.1 g, 83.0% yield), mp 87.8-88.9 °C. ^{1}H NMR (400 MHz, $CDCl_3$) δ 13.67 (brs,1H, OH), 7.91 (d, *J* = 15.6 Hz, 1H, =CH), 7.75 (d, *J* = 15.6 Hz, 1H, =CH), 7.29 (t, *J* = 8.0 Hz, 1H, Ar-H), 7.21 (d, *J* = 7.6 Hz, 1H, Ar-H), 7.11 (s, 1H, Ar-H), 6.88 (dd, *J* = 1.6 Hz, 7.6Hz, 1H, Ar-H), 6.29 (d, *J* = 5.6 Hz, 1H, Ar-H), 5.03 (brs, 1H, OH), 3.92 (s, 3H, OCH_3), 3.90 (s, 3H, OCH_3), 3.83 (s, 3H, OCH_3).

*4.1.4. General procedure for the synthesis of intermediates **7a-b**.* Chalcones compound **5** or **6** (3.6 g 10.8 mmol), potassium iodide (70 mg, 0.42 mmol) were added to a solution of *conc.* H_2SO_4 (0.2 mL) in DMSO (16 mL). The solution was heated to 100 °C for 3-5 h, and then the reaction mixture was poured into crushed ice. The resulting precipitate was collected and washed with 5% sodium thiosulfate solution (50 mL) and water. Recrystallization from 80% ethanol afforded the flavones compound **7a-b**, respectively.

*4.1.4.1. 4'-Hydroxy-5,6,7-trimethoxyflavone (**7a**).* Light yellow solid; 84.0 % yield; mp 224-225.4 °C. ^{1}H NMR (400 MHz, DMSO-d_6) δ 10.25 (s, 1H, OH), 7.91 (d, *J* = 8.4 Hz, 2H, Ar-H), 7.19 (s, 1H, Ar-H), 6.92 (d, *J* = 8.4 Hz, 2H, Ar-H), 6.64 (s, 1H, CH), 3.95 (s, 3H, OCH_3), 3.80 (s, 3H, OCH_3), 3.76 (s, 3H, OCH_3).

*4.1.4.2. 3'-Hydroxy-5,6,7-trimethoxyflavone (**7b**).* Light yellow solid; 90.0 % yield; mp 227-228.8 °C. ^{1}H NMR (400 MHz, DMSO-d_6) δ 9.85 (s,1H, OH), 7.48 (d, *J* = 7.6 Hz, 1H, Ar-H), 7.40 (s, 1H, Ar-H), 7.36 (t, *J* = 8.0 Hz, 1H, Ar-H), 7.20 (s, 1H, CH), 6.98 (dd, *J* = 2.0, 8.0 Hz, 1H, Ar-H), 6.69 (s, 1H, Ar-H), 3.96 (s, 3H, OCH_3), 3.81 (s, 3H, OCH_3), 3.77 (s, 3H, OCH_3).

*4.1.5. General procedure for the synthesis of intermediates **8a-b**.* Anhydrous $AlCl_3$ (1.62 g, 12.1 mmol) was added to a solution of compound **7a-b** (2.0 g, 6.1 mmol) in anhydrous acetonitrile (20 mL) at room temperature. The mixture was heated to 55-60 °C for 1 h, then added 10% HCl (20 mL) and refluxed for 40 min. Then the mixture was poured into ice water (50 mL). The resulting

precipitate was collected and washed with water. The residue was recrystallized with methoxyethanol to afford compounds **8a-b**, respectively.

*4.1.5.1. 5,4′-Dihydroxy-6,7-dimethoxyflavone (**8a**).* Light yellow solid; 88.0 % yield; mp 261-262.3 °C. ^{1}H NMR (400 MHz, DMSO-d_6) δ 12.94 (s, 1H, OH), 10.42 (s, 1H, OH), 7.98 (d, *J* =8.8 Hz, 2H, Ar-H), 6.94 (d, *J* = 8.8Hz, 2H, Ar-H), 6.93 (s, 1H, Ar-H), 6.87 (s, 1H, CH), 3.93 (s, 3H, OCH_3), 3.74 (s, 3H, OCH_3).

*4.1.5.2. 5,3′-Dihydroxy-6,7-dimethoxyflavone (**8b**).* Light yellow solid; 85.0 % yield; mp 210-211.4 °C. ^{1}H NMR (400 MHz, DMSO-d_6) δ 12.77 (s, 1H, OH), 9.85 (s, 1H, OH), 7.53 (d, *J* = 8.0 Hz, 1H, Ar-H), 7.45-7.42 (m, 1H, Ar-H), 7.38 (t, *J* = 8.0 Hz, 1H, Ar-H), 7.03 (d, *J* = 8.0 Hz, 1H, Ar-H), 6.94 (s, 1H, CH), 6.90 (s, 1H, Ar-H), 3.95 (s, 3H, OCH_3), 3.75 (s, 3H, OCH_3).

*4.1.6. General procedure for the synthesis of intermediates **10-13**.* The appropriate dibromoalkane derivative **9** (6.6 mmol) was added to a mixture of the intermediate **7a-b** or **8a-b** (3.0 mmol), anhydrous K_2CO_3 (430 mg, 3.1 mmol) and KI (53 mg, 0.32mmol) in CH_3CN (30 ml)**.** The reaction mixture was warmed to 60-65 °C and stirred for 8-10 h under an argon atmosphere. After complete reaction, the solvent was evaporated under reduced pressure. Water (30 mL) was added to the residue and the mixture was extracted with dichloromethane (30 mL×3). The combined organic phases were washed with saturated aqueous sodium chloride, dried over sodium sulfate, and filtered. The solvent was evaporated to dryness under reduced pressure. The residue was purified on a silica gel chromatography using petroleum ether/acetone (15:1) as eluent to give the intermediates **10-13**.

*4.1.6.1. 4′-(3-Bromopropoxy)-5,6,7-trimethoxyflavone (**10a**).* Light yellow solid; 68.7 % yield; mp 142.1-143.2 °C. ^{1}H NMR (400 MHz, $CDCl_3$) δ 7.83 (d, *J* = 8.8 Hz, 2H, Ar-H), 7.02 (d, *J* = 8.8 Hz, 2H, Ar-H), 6.80 (s, 1H, =CH), 6.59 (s, 1H, Ar-H), 4.19 (t, *J* = 6.0 Hz, 2H, OCH_2), 3.99 (s, 3H, OCH_3), 3.98 (s, 3H, OCH_3), 3.92 (s, 3H, OCH_3), 3.63 (t, *J* = 6.4 Hz, 2H, CH_2Br), 2.39-2.34 (m, 2H, CH_2).

*4.1.6.2. 4′-(4-Bromobutoxy)-5,6,7-trimethoxyflavone (**10b**).* Light yellow solid; 74.3 % yield; mp 157.3-158.4 °C. ^{1}H NMR (400 MHz, $CDCl_3$) δ 7.82 (d, *J* = 8.8 Hz, 2H, Ar-H), 6.99 (d, *J* = 8.8 Hz,

2H, Ar-H), 6.80 (s, 1H, =CH), 6.58 (s, 1H, Ar-H), 4.08 (t, *J* = 6.0 Hz, 2H, OCH_2), 3.99 (s, 3H, OCH_3), 3.98(s, 3H, OCH_3), 3.92(s, 3H, OCH_3), 3.51(t, *J* = 6.4 Hz, 2H, CH_2Br), 2.11-2.07(m, 2H, CH_2), 2.01-1.97(m, 2H, CH_2).

*4.1.6.3. 4'-(6-Bromohexyloxy)-5,6,7-trimethoxyflavone (**10c**).* Light yellow solid; 72.8 % yield, mp 117.3-118.2 °C. ^{1}H NMR (400 MHz, $CDCl_3$) δ 7.83 (d, *J* = 8.8 Hz, 2H, Ar-H), 6.99 (d, *J* = 8.8 Hz, 2H, Ar-H), 6.80 (s, 1H, =CH), 6.64 (s, 1H, Ar-H), 4.04 (t, *J* = 6.4 Hz, 2H, OCH_2), 3.99 (s, 3H, OCH_3), 3.99 (s, 3H, OCH_3), 3.92 (s, 3H, OCH_3), 3.44 (t, *J* = 6.8 Hz, 2H, CH_2Br), 1.92-1.88 (m, 2H, CH_2), 1.87-1.83 (m, 2H, CH_2), 1.56-1.52 (m, 4H, CH_2).

*4.1.6.4. 4'-(3-Bromopropoxy)-5-hydroxy-6,7-dimethoxyflavone (**11a**).* Yellow solid; 63.7 % yield; mp 143.1-144.5 °C. ^{1}H NMR (400 MHz, $CDCl_3$) δ 12.79 (brs, 1H, OH), 7.85 (d, *J* = 8.8 Hz, 2H, Ar-H), 7.03 (d, *J* = 9.2 Hz, 2H, Ar-H), 6.59 (s, 1H, =CH), 6.55 (s, 1H, Ar-H), 4.20 (t, *J* = 6.0 Hz, 2H, OCH_2), 3.97 (s, 3H, OCH_3), 3.93 (s, 3H, OCH_3), 3.63 (t, *J* = 6.4 Hz, 2H, CH_2Br), 2.39-2.34 (m, 2H, CH_2).

*4.1.6.5. 4'-(4-Bromobutoxy)-5-hydroxy-6,7-dimethoxyflavone (**11b**).* Yellow solid; 68.4 % yield; mp 149.1-150.5 °C. ^{1}H NMR (400 MHz, $CDCl_3$) δ 12.80 (brs, 1H, OH), 7.84 (d, *J* = 9.2 Hz, 2H, Ar-H), 7.00 (d, *J* = 9.2 Hz, 2H, Ar-H), 6.59 (s, 1H, =CH), 6.55 (s, 1H, Ar-H), 4.09 (t, *J* = 6.0 Hz, 2H, OCH_2), 3.97 (s, 3H, OCH_3), 3.93 (s, 3H, OCH_3), 3.51 (t, *J* = 6.4 Hz, 2H, CH_2Br), 2.12-2.08 (m, 2H, CH_2), 2.02-1.98 (m, 2H, CH_2).

*4.1.6.6. 4'-(6-Bromohexyloxy)-5-hydroxy-6,7-dimethoxyflavone (**11c**).* Yellow solid; 67.4 % yield; mp 133.3-134.5 °C. ^{1}H NMR (400 MHz, $CDCl_3$) δ 12.80 (brs, 1H, OH), 7.84 (d, *J* = 8.8 Hz, 2H, Ar-H), 7.00 (d, *J* = 8.8Hz, 2H, Ar-H), 6.59 (s, 1H, =CH), 6.55 (s, 1H, Ar-H), 4.05 (t, *J* = 6.4 Hz, 2H, OCH_2), 3.97 (s, 3H, OCH_3), 3.93 (s, 3H, OCH_3), 3.44 (t, *J* = 6.8 Hz, 2H, CH_2Br), 1.94-1.90 (m, 2H, CH_2), 1.87-1.83 (m, 2H, CH_2), 1.56-1.52 (m, 2H, CH_2).

*4.1.6.7. 3'-(2-Bromoethoxy)-5,6,7-trimethoxyflavone (**12a**).* Light yellow solid; 67.3 % yield; mp 94.5-95.9 °C. ^{1}H NMR (400 MHz, $CDCl_3$) δ 7.49 (d, *J* = 8.0 Hz, 1H, Ar-H), 7.43 (t, *J* = 8.0 Hz, 2H, Ar-H), 7.07 (d, *J* = 8.0 Hz 1H, Ar-H), 6.83 (s, 1H, =CH), 6.66 (s, 1H, Ar-H), 4.38 (t, *J* = 6.0 Hz, 2H,

OCH_2), 4.00 (s, 6H, 2 × OCH_3), 3.93 (s, 3H, OCH_3), 3.70 (t, *J* = 6.0 HZ, 2H, CH_2Br).

*4.1.6.8. 3′-(3-Bromopropoxy)-5,6,7-trimethoxyflavone (**12b**).* Light yellow solid; 70.6 % yield; mp 89.7-90.4 °C. ^{1}H NMR (400 MHz, $CDCl_3$) δ 7.47 (d, *J* = 8.0 Hz, 1H, Ar-H), 7.43-7.39 (m, 2H, Ar-H), 7.06 (dd, *J* = 1.6, 8.0 Hz, 1H, Ar-H), 6.83 (s, 1H, =CH), 6.74 (s, 1H, Ar-H), 4.19 (t, *J* = 6.4 Hz, 2H, OCH_2), 3.99 (s, 6H, 2 × OCH_3), 3.92 (s, 3H, OCH_3), 3.64 (t, *J* = 6.4 Hz, 2H, CH_2Br), 2.39-2.34 (m, 2H, CH_2).

*4.1.6.9. 3′-(4-Bromobutoxy)-5,6,7-trimethoxyflavone (**12c**).* Light yellow solid; 67.6 % yield; mp 108.2-109.1 °C. ^{1}H NMR (400 MHz, $CDCl_3$) δ 7.45 (d, *J* = 8.0 Hz, 1H, Ar-H), 7.42 (d, *J* = 8.0 Hz, 1H, Ar-H), 7.40-7.36 (m, 1H, Ar-H), 7.04 (dd, *J* = 1.6, 8.0 Hz, 2H, Ar-H), 6.82 (s, 1H, =CH), 6.67 (s, 1H, Ar-H), 4.08 (t, *J* = 6.4 Hz, 2H, OCH_2), 3.99 (s, 6H, 2 × OCH_3), 3.93 (s, 3H, OCH_3), 3.52 (t, *J* = 6.4 Hz, 2H, CH_2Br), 2.13-2.09 (m, 2H, CH_2), 2.02-1.98 (m, 2H, CH_2).

*4.1.6.10. 3′-(6-Bromohexyloxy)-5,6,7-trimethoxyflavone (**12d**).* Light yellow solid; 71.4 % yield; mp 128.9-130.2 °C. ^{1}H NMR (400 MHz, $CDCl_3$) δ 7.45 (d, *J* = 8.0 Hz, 1H, Ar-H), 7.41 (d, *J* = 8.0 Hz, 2H, Ar-H), 7.04 (dd, *J* = 1.6, 8.0 Hz, 1H, Ar-H), 6.82 (s, 1H, =CH), 6.69 (s, 1H, Ar-H), 4.04 (t, *J* = 6.4 Hz, 2H, OCH_2), 3.99 (s, 6H, 2 × OCH_3), 3.93 (s, 3H, OCH_3), 3.45 (t, *J* = 6.8 Hz, 2H, CH_2Br), 1.93-1.89 (m, 2H, CH_2), 1.87-1.82 (m, 2H, CH_2), 1.57-1.53 (m, 4H, CH_2).

*4.1.6.11. 3′-(3-Bromopropoxy)-5-hydroxy-6,7-dimethoxyflavone (**13a**).* Yellow solid; 68.7 % yield; mp 138.8-139.9 °C. 1H NMR (400 MHz, $CDCl_3$) δ 12.67 (brs, 1H, OH), 7.49-7.42 (m, 3H, Ar-H), 7.09 (dd, *J* = 1.2, 7.6 Hz, 1H, Ar-H), 6.67 (s, 1H, =CH), 6.58 (s, 1H, Ar-H), 4.21 (t, *J* = 5.6 Hz, 2H, OCH_2), 3.98 (s, 3H, OCH_3), 3.93 (s, 3H, OCH_3), 3.65 (t, *J* = 6.4 Hz, 2H, CH_2Br), 2.40-2.36 (m, 2H, CH_2).

*4.1.6.12. 3′-(3-Bromobutoxy)-5-hydroxy-6,7-dimethoxyflavone (**13b**).* Yellow solid; 63.4 % yield; mp 115.5-116.9 °C. ^{1}H NMR (400 MHz, $CDCl_3$) δ 12.67 (brs, 1H, OH), 7.47 (dt, *J* = 1.6, 8.0 Hz, 1H, Ar-H), 7.43 (d, *J* = 8.0 Hz, 1H, Ar-H), 7.41-7.36 (m, 1H, Ar-H), 7.07 (dd, *J* = 1.6, 8.0 Hz, 1H, Ar-H), 6.66 (s, 1H, =CH), 6.58 (s, 1H, Ar-H), 4.09 (t, *J* = 6.0 Hz, 2H, OCH_2), 3.98 (s, 3H, OCH_3), 3.93 (s, 3H, OCH_3), 3.52 (t, *J* = 6.4 Hz, 2H, CH_2Br), 2.14-2.10 (m, 2H, CH_2), 2.03-1.99 (m, 2H,

CH_2).

*4.1.6.13. 3'-(3-Bromohexyloxy)-5-hydroxy-6,7-dimethoxyflavone (**13c**).* Yellow solid; 69.3 % yield; mp 98.4-99.2 °C. ^{1}H NMR (400 MHz, $CDCl_3$) δ 12.68 (brs, 1H, OH), 7.46 (dt, *J* = 1.2, 8.0 Hz, 1H, Ar-H), 7.43 (d, *J* = 8.0 Hz, 1H, Ar-H), 7.42-7.38 (m, 1H, Ar-H), 7.07 (dd, *J* = 1.2, 8.0 Hz, 1H, Ar-H), 6.67 (s, 1H, =CH), 6.57 (s, 1H, Ar-H), 4.05 (t, *J* = 6.4 Hz, 2H, OCH_2), 3.98 (s, 3H, OCH_3), 3.93 (s, 3H, OCH_3), 3.47 (t, *J* = 6.4 Hz, 2H, CH_2Br), 1.94-1.90 (m, 2H, CH_2), 1.88-1.84 (m, 2H, CH_2), 1.56-1.52 (m, 2H, CH_2).

*4.1.7. General procedure for the synthesis of scutellarein-O-alkylamine derivatives **15**–**18*** [18]**.** To a mixture of the corresponding secondary amines **14A–F** (0.6 mmol), anhydrous K_2CO_3 (89.7 mg, 0.65 mmol) and KI (8.6 mg, 0.052 mmol) in anhydrous CH_3CN (12 ml) were added the appropriate intermediates **10–13** (0.5 mmol). The reaction mixture was warmed to 60-65 °C and stirred for 6–10 h under an argon atmosphere. After complete reaction, the solvent was evaporated under reduced pressure. The residue was dissolved in water (40 mL) and the mixture was extracted with dichloromethane (25 mL×3). The combined organic phases were washed with saturated aqueous sodium chloride (20 mL), dried over sodium sulfate, and filtered. The solvent was evaporated to dryness under reduced pressure. The residue was purified on a silica gel chromatography using mixtures of CH_2Cl_2/CH_3OH (100:1) as eluent to afford the corresponding scutellarein-*O*-alkylamine derivatives **15-18**.

*4.1.7.1. 4'-(3-(Benzyl(methyl)amino)propoxy)-5,6,7-trimethoxyflavone (**15a**).* Light yellow oil, 72.7 % yield, 97.6 % HPLC purity. ^{1}H NMR (400 MHz, $CDCl_3$) δ 7.81 (d, *J* = 8.8 Hz, 2H, Ar-H), 7.29-7.21 (m, 5H, Ar-H), 6.97 (d, *J* = 8.8 Hz, 2H, Ar-H), 6.80 (s, 1H, =CH), 6.59 (s, 1H, Ar-H), 4.10 (t, *J* = 6.4 Hz, 2H, OCH_2), 3.99 (s, 3H, OCH_3), 3.98 (s, 3H, OCH_3), 3.92 (s, 3H, OCH_3), 3.54 (s, 2H, CH_2Ph), 2.58 (t, *J* = 6.8 Hz, 2H, CH_2N), 2.56 (s, 3H, CH_3N), 2.06-2.00 (m, 2H, CH_2); HR-ESI-MS: Calcd. for $C_{29}H_{32}NO_6$ $[M+H]^+$: 490.2230, found: 490.2225.

*4.1.7.2. 4'-(3-(Benzyl(ethyl)amino)propoxy)-5,6,7-trimethoxyflavone (**15b**).* Light yellow oil, 77.5 % yield, 98.0 % HPLC purity. ^{1}H NMR (400 MHz, $CDCl_3$) δ 7.80 (d, *J* = 8.8 Hz, 2H, Ar-H), 7.34-7.26

(m, 5H, Ar-H), 6.95 (d, *J* = 8.8 Hz, 2H, Ar-H), 6.80 (s, 1H, =CH), 6.59 (s, 1H, Ar-H), 4.07 (t, *J* = 6.4 Hz, 2H, OCH_2), 3.99 (s, 3H, OCH_3), 3.98 (s, 3H, OCH_3), 3.92 (s, 3H, OCH_3), 3.62 (s, 2H, CH_2Ph), 2.65 (t, *J* = 6.4 Hz, 2H, CH_2N), 2.56 (*J* = 6.8 Hz, 2H, CH_2N), 2.00-1.96 (m, 2H, CH_2), 1.08 (t, *J* = 6.4 Hz, 3H, CH_3); HR-ESI-MS: Calcd. for $C_{30}H_{34}NO_6$ $[M+H]^+$: 504.2386, found: 504.2391.

4.1.7.3. 4′-(3-((2-Methoxybenzyl)(methyl)amino)propoxy)-5,6,7-trimethoxyflavone ***(15c)****.* Light yellow oil, 87.1 % yield, 98.9% HPLC purity. ^1H NMR (400 MHz, $CDCl_3$) δ 7.80 (d, *J* = 8.8 Hz, 2H, Ar-H), 7.41-7.35 (m, 1H, Ar-H), 7.29 (t, *J* = 7.2 Hz, 1H, Ar-H), 6.97 (d, *J* = 8.8 Hz, 2H, Ar-H), 6.92-6.88 (m, 2H, Ar-H), 6.79 (s, 1H, =CH), 6.57 (s, 1H, Ar-H), 4.14 (t, *J* = 6.4 Hz, 2H, OCH_2), 3.99 (s, 3H, OCH_3), 3.98 (s, 3H, OCH_3), 3.91 (s, 3H, OCH_3), 3.84 (s, 3H, OCH_3), 3.81 (s, 2H, CH_2Ph), 2.60-2.54 (m, 2H, CH_2N), 2.43 (s, 3H, CH_3N), 2.24-2.20 (m, 2H, CH_2); HR-ESI-MS: Calcd. for $C_{30}H_{34}NO_7$ $[M+H]^+$: 520.2335, found: 520.2342.

4.1.7.4. 4′-(3-((Ethyl)(2-methoxybenzyl)amino)propoxy)-5,6,7-trimethoxyflavone ***(15d)****.* Light yellow oil, 72.6 % yield, 98.6% HPLC purity. ^1H NMR (400 MHz, $CDCl_3$) δ 7.80 (d, *J* = 8.8 Hz, 2H, Ar-H), 7.43 (brs, 1H, Ar-H), 7.23 (t, *J* = 6.4 Hz, 1H, Ar-H), 6.96 (d, *J* = 8.8 Hz, 2H, Ar-H), 6.92 (t, *J* = 7.2 Hz, 1H, Ar-H), 6.86 (d, *J* = 8.0 Hz, 1H, Ar-H), 6.80 (s, 1H, =CH), 6.58 (s, 1H, Ar-H), 4.10 (t, *J* = 6.0 Hz, 2H, OCH_2), 3.99 (s, 3H, OCH_3), 3.98 (s, 3H, OCH_3), 3.92 (s, 3H, OCH_3), 3.82 (s, 3H, OCH_3), 3.69 (s, 2H, CH_2Ph), 2.74-2.70 (m, 2H, CH_2N), 2.65-2.61 (m, 2H, CH_2N), 2.06-2.02 (m, 2H, CH_2), 1.14-1.10 (m, 3H, CH_3); HR-ESI-MS: Calcd. for $C_{31}H_{36}NO_7$ $[M+H]^+$: 534.2492, found: 534.2484.

4.1.7.5. 4′-(3-(4-Benzylpiperazin-1-yl)propoxy)-5,6,7-trimethoxyflavone ***(15e)****.* Light yellow oil, 76.1 % yield, 97.8 % HPLC purity. ^1H NMR (400 MHz, $CDCl_3$) δ 7.81 (d, *J* = 8.8 Hz, 2H, Ar-H), 7.35-7.31 (m, 5H, Ar-H), 6.99 (d, *J* = 8.8 Hz, 2H, Ar-H), 6.80 (s, 1H, =CH), 6.58 (s, 1H, Ar-H), 4.10 (t, *J* = 6.0 Hz, 2H, OCH_2), 3.99 (s, 3H, OCH_3), 3.98 (s, 3H, OCH_3), 3.92 (s, 3H, OCH_3), 3.55 (s, 2H, CH_2Ph), 2.60-2.56 (m, 10H, CH_2N), 2.07-2.03 (m, 2H, CH_2); HR-ESI-MS: Calcd. for $C_{32}H_{37}N_2O_6$ $[M+H]^+$: 545.2652, found: 545.2645.

4.1.7.6. 4′-(3-(4-Methylpiperazin-1-yl)propoxy)-5,6,7-trimethoxyflavone ***(15f)****.* Light yellow oil,

70.9 % yield, 99.2 % HPLC purity. ^{1}H NMR (400 MHz, $CDCl_3$) δ 7.80 (d, *J* = 8.8 Hz, 2H, Ar-H), 6.99 (d, *J* = 8.8 Hz, 2H, Ar-H), 6.79 (s, 1H, =CH), 6.57 (s, 1H, Ar-H), 4.08 (t, *J* = 6.4 Hz, 2H, OCH_2), 3.98 (s, 3H, OCH_3), 3.97 (s, 3H, OCH_3), 3.91 (s, 3H, OCH_3), 2.58-2.54 (m, 10H, CH_2N), 2.33 (s, 3H, NCH_3), 2.03-1.99 (m, 2H, CH_2); HR-ESI-MS: Calcd. for $C_{26}H_{33}N_2O_6$ $[M+H]^+$: 469.2339, found: 469.2336.

*4.1.7.7. 4'-(4-(Benzyl(methyl)amino)butoxy)-5,6,7-trimethoxyflavone (**15g**).* Light yellow oil, 75.1 % yield, 97.5 % HPLC purity. ^{1}H NMR (400MHz, $CDCl_3$) δ 7.81 (d, *J* = 8.8 Hz, 2H, Ar-H), 7.33-7.26 (m, 5H, Ar-H), 6.97 (d, *J* = 8.8 Hz, 2H, Ar-H), 6.80 (s, 1H, =CH), 6.58 (s, 1H, Ar-H), 4.03 (t, *J* = 6.0 Hz, 2H, OCH_2), 3.99 (s, 3H, OCH_3), 3.98 (s, 3H, OCH_3), 3.92 (s, 3H, OCH_3), 3.56 (s, 2H, CH_2Ph), 2.49 (t, *J* = 6.8 Hz, 2H, CH_2N), 2.25 (s, 3H, NCH_3), 1.89-1.85 (m, 2H, CH_2), 1.77-1.73 (m, 2H, CH_2); HR-ESI-MS: Calcd. for $C_{30}H_{34}NO_6$ $[M+H]^+$: 504.2386, found: 504.2380.

*4.1.7.8. 4'-(4-(Benzyl(ethyl)amino)butoxy)-5,6,7-trimethoxyflavone (**15h**).* Light yellow oil, 70.7 % yield, 99.0% HPLC purity. ^{1}H NMR (400MHz, $CDCl_3$) δ 7.81 (d, *J* = 8.8 Hz, 2H, Ar-H), 7.46-7.42 (m, 2H, Ar-H), 7.36-7.30 (m, 3H, Ar-H), 6.96 (d, *J* = 8.8 Hz, 2H, Ar-H), 6.80 (s, 1H, =CH), 6.59 (s, 1H, Ar-H), 4.01 (t, *J* = 6.4 Hz, 2H, OCH_2), 3.99 (s, 3H, OCH_3), 3.98 (s, 3H, OCH_3), 3.92 (s, 3H, OCH_3), 3.79 (s, 2H, CH_2Ph), 2.72-2.68 (m, 4H, CH_2N), 1.87-1.83 (m, 4H, CH_2), 1.21 (t, *J* = 6.4 Hz, 3H, CH_3); HR-ESI-MS: Calcd. for $C_{31}H_{36}NO_6$ $[M+H]^+$: 518.2543, found: 518.2552.

*4.1.7.9. 4'-(4-((2-Methoxybenzyl)(methyl)amino)butoxy)-5,6,7-trimethoxyflavone (**15i**).* Light yellow oil, 77.5 % yield, 99.2 % HPLC purity. ^{1}H NMR (400MHz, $CDCl_3$) δ 7.81 (d, *J* = 8.8 Hz, 2H, Ar-H), 7.36 (d, *J* = 7.6 Hz, 1H, Ar-H), 7.26 (t, *J* = 7.6 Hz, 1H, Ar-H), 6.98 (d, *J* = 8.8 Hz, 2H, Ar-H), 6.94 (t, *J* = 7.6 Hz, 2H, Ar-H), 6.88 (d, *J* = 8.0 Hz, 1H, Ar-H), 6.80 (s, 1H, =CH), 6.58 (s, 1H, Ar-H), 4.05 (t, *J* = 6.0 Hz, 2H, OCH_2), 3.99 (s, 3H, OCH_3), 3.98 (s, 3H, OCH_3), 3.92 (s, 3H, OCH_3), 3.83 (s, 3H, OCH_3), 3.64 (s, 2H, CH_2Ph), 2.59-2.55 (m, 2H, CH_2N), 2.31 (s, 3H, NCH_3), 1.90-1.86 (m, 2H, CH_2), 1.82-1.78 (m, 2H, CH_2); HR-ESI-MS: Calcd. for $C_{31}H_{36}NO_7$ $[M+H]^+$: 534.2492, found: 534.2480.

*4.1.7.10. 4'-(4-((Ethyl)(2-methoxybenzyl)amino)butoxy)-5,6,7-trimethoxyflavone (**15j**).* Light yellow

oil, 72.7 % yield, 99.5% HPLC purity. ^{1}H NMR (400MHz, $CDCl_3$) δ 7.80 (d, *J* = 8.8 Hz, 2H, Ar-H), 7.42 (d, *J* = 7.2 Hz, 1H, Ar-H), 7.20 (t, *J* = 6.8 Hz, 1H, Ar-H), 6.97 (d, *J* = 8.8 Hz, 2H, Ar-H), 6.92 (t, *J* = 7.2 Hz, 1H, Ar-H), 6.86 (d, *J* = 8.0 Hz, 1H, Ar-H), 6.80 (s, 1H, =CH), 6.58 (s, 1H, Ar-H), 4.01 (t, *J* = 6.4 Hz, 2H, OCH_2), 3.99 (s, 3H, OCH_3), 3.98 (s, 3H, OCH_3), 3.92 (s, 3H, OCH_3), 3.82 (s, 3H, OCH_3), 3.62 (s, 2H, CH_2Ph), 2.57-2.53 (m, 4H, CH_2N), 1.86-1.84 (m, 2H, CH_2), 1.71-1.67 (m, 2H, CH_2), 1.08 (t, *J* = 6.8 Hz, 3H, CH_3); ^{13}C NMR (100MHz, $CDCl_3$) δ 177.2, 161.4, 161.1, 157.8, 157.5, 154.4, 152.4, 140.2, 131.3, 129.1, 127.5, 123.6, 120.6, 114.9, 114.8, 112.7, 110.4, 106.9, 96.2, 67.7, 62.1, 61.5, 56.2, 55.4, 52.2, 50.7, 47.4, 26.8, 22.4, 10.7; HR-ESI-MS: Calcd. for $C_{32}H_{38}NO_7$ $[M+H]^+$: 548.2648, found: 548.2657.

4.1.7.11. 4'-(4-(4-Benzylpiperazin-1-yl)butoxy)-5,6,7-trimethoxyflavone ***(15k)****.* Light yellow oil, 72.8% yield, 98.3% HPLC purity. ^{1}H NMR (400MHz, $CDCl_3$) δ 7.81 (d, *J* = 8.8 Hz, 2H, Ar-H), 7.33-7.27 (m, 5H, Ar-H), 6.98 (d, *J* = 8.8 Hz, 2H, Ar-H), 6.80 (s, 1H, =CH), 6.58 (s, 1H, Ar-H), 4.06 (t, *J* = 6.0 Hz, 2H, OCH_2), 3.99 (s, 3H, OCH_3), 3.98 (s, 3H, OCH_3), 3.92 (s, 3H, OCH_3), 3.54 (s, 2H, CH_2Ph), 2.52-2.48 (m, 10H, CH_2N), 1.85-1.81 (m, 2H, CH_2), 1.76-1.72 (m, 2H, CH_2); HR-ESI-MS: Calcd. for $C_{33}H_{39}N_2O_6$ $[M+H]^+$: 559.2808, found: 559.2820.

4.1.7.12. 4'-(4-(4-Methylpiperazin-1-yl)butoxy)-5,6,7-trimethoxyflavone ***(15l)****.* Light yellow oil, 78.8% yield, 98.9% HPLC purity. ^{1}H NMR (400MHz, $CDCl_3$) δ 7.82 (d, *J* = 8.8 Hz, 2H, Ar-H), 6.99 (d, *J* = 8.8 Hz, 2H, Ar-H), 6.80 (s, 1H, =CH), 6.58 (s, 1H, Ar-H), 4.06 (t, *J* = 6.0 Hz, 2H, OCH_2), 3.99 (s, 3H, OCH_3), 3.98 (s, 3H, OCH_3), 3.92 (s, 3H, OCH_3), 2.70-2.63 (m, 6H, CH_2N), 2.52 (t, *J* = 7.2 Hz, 4H, CH_2N), 2.41 (s, 3H, NCH_3), 1.88-1.84 (m, 2H, CH_2), 1.77-1.73 (m, 2H, CH_2); HR-ESI-MS: Calcd. for $C_{27}H_{35}N_2O_6$ $[M+H]^+$: 483.2495, found: 483.2490.

4.1.7.13. 4'-(6-(Benzyl(methyl)amino)hexyloxy)-5,6,7-trimethoxyflavone ***(15m)****.* Light yellow oil, 82.5 % yield, 98.7% HPLC purity. ^{1}H NMR (400MHz, $CDCl_3$) δ 7.81 (d, *J* = 8.8 Hz, 2H, Ar-H), 7.35-7.26 (m, 5H, Ar-H), 6.99 (d, *J* = 8.8 Hz, 2H, Ar-H), 6.80 (s, 1H, =CH), 6.58 (s, 1H, Ar-H), 4.02 (t, *J* = 6.4 Hz, 2H, OCH_2), 3.99 (s, 3H, OCH_3), 3.98 (s, 3H, OCH_3), 3.92 (s, 3H, OCH_3), 3.59 (s, 2H, CH_2Ph), 2.49-2.45 (m, 2H, CH_2N), 2.27 (s, 3H, NCH_3), 1.82-1.78 (m, 2H, CH_2), 1.65-1.61

(m, 2H, CH_2), 1.52-1.46 (m, 2H, CH_2), 1.44-1.40 (m, 2H, CH_2); HR-ESI-MS: Calcd. for $C_{32}H_{38}NO_6$ $[M+H]^+$: 532.2699, found: 532.2706.

*4.1.7.14. 4′-(6-(Benzyl(ethyl)amino)hexyloxy)-5,6,7-trimethoxyflavone (**15n**).* Light yellow oil, 76.5 % yield, 98.6 % HPLC purity. ^{1}H NMR (400MHz, $CDCl_3$) δ 7.81 (d, *J* = 8.8 Hz, 2H, Ar-H), 7.35-7.26 (m, 5H, Ar-H), 6.98 (d, *J* = 8.8 Hz, 2H, Ar-H), 6.79 (s, 1H, =CH), 6.58 (s, 1H, Ar-H), 4.00 (t, *J* = 6.4 Hz, 2H, OCH_2), 3.98 (s, 6H, 2 × OCH_3), 3.91 (s, 3H, OCH_3), 3.64 (s, 2H, CH_2Ph), 2.61-2.57 (m, 2H, CH_2N), 2.53-2.49 (m, 2H, CH_2N), 1.82-1.78 (m, 2H, CH_2), 1.58-1.54 (m, 2H, CH_2), 1.52-1.46 (m, 2H, CH_2), 1.39-1.35 (m, 2H, CH_2), 1.11-1.07 (m, 3H, CH_3); HR-ESI-MS: Calcd. for $C_{33}H_{40}NO_6$ $[M+H]^+$: 546.2856, found: 546.2848.

*4.1.7.15. 4′-(6-((2-Methoxybenzyl)(methyl)amino)hexyloxy)-5,6,7-trimethoxyflavone (**15o**).* Light yellow oil, 71.0 % yield, 97.9 % HPLC purity. ^{1}H NMR (400MHz, $CDCl_3$) δ 7.81 (d, *J* = 8.8 Hz, 2H, Ar-H), 7.38 (d, *J* = 7.2 Hz, 1H, Ar-H), 7.26 (t, *J* = 6.8 Hz, 1H, Ar-H), 6.99 (d, *J* = 8.8 Hz, 2H, Ar-H), 6.94 (t, *J* = 7.2 Hz, 1H, Ar-H), 6.88 (d, *J* = 8.0 Hz, 1H, Ar-H), 6.80 (s, 1H, =CH), 6.58 (s, 1H, Ar-H), 4.03 (t, *J* = 6.8 Hz, 2H, OCH_2), 3.99 (s, 3H, OCH_3), 3.98 (s, 3H, OCH_3), 3.92 (s, 3H, OCH_3), 3.83 (s, 3H, OCH_3), 3.65 (s, 2H, CH_2Ph), 2.54-2.50 (m, 2H, CH_2N), 2.30 (s, 3H, NCH_3), 1.85-1.81 (m, 2H, CH_2), 1.68-1.64 (m, 2H, CH_2), 1.51-1.47 (m, 2H, CH_2), 1.43-1.39 (m, 2H, CH_2); HR-ESI-MS: Calcd. for $C_{33}H_{40}NO_7$ $[M+H]^+$: 562.2805, found: 562.2799.

*4.1.7.16. 4′-(6-((Ethyl)(2-methoxybenzyl)amino)hexyloxy)-5,6,7-trimethoxyflavone (**15p**).* Light yellow oil, 76.5 % yield, 99.0 % HPLC purity. ^{1}H NMR (400MHz, $CDCl_3$) δ 7.81 (d, *J* = 8.8 Hz, 2H, Ar-H), 7.52 (brs, 1H, Ar-H), 7.29-7.25 (m, 1H, Ar-H), 6.98 (d, *J* = 8.8 Hz, 2H, Ar-H), 6.99-6.94 (m, 1H, Ar-H), 6.88 (d, *J* = 8.0 Hz, 1H, Ar-H), 6.80 (s, 1H, =CH), 6.58 (s, 1H, Ar-H), 4.02 (t, *J* = 6.4 Hz, 2H, OCH_2), 4.00 (s, 3H, OCH_3), 3.99 (s, 3H, OCH_3), 3.92 (s, 3H, OCH_3), 3.84 (s, 3H, OCH_3), 3.82 (s, 2H, CH_2Ph), 2.73-2.69 (m, 2H, CH_2N), 2.65-2,61 (m, 2H, CH_2N), 1.84-1.80 (m, 2H, CH_2), 1.70-1.66 (m, 2H, CH_2), 1.52-1.48 (m, 2H, CH_2), 1.40-1.36 (m, 2H, CH_2), 1.21-1.17 (m, 3H, CH_3); HR-ESI-MS: Calcd. for $C_{34}H_{42}NO_7$ $[M+H]^+$: 576.2961, found: 576.2972.

*4.1.7.17. 4′-(6-(4-Benzylpiperazin-1-yl)hexyloxy)-5,6,7-trimethoxyflavone (**15q**).* Light yellow oil,

76.4 yield, 98.0% HPLC purity. ^{1}H NMR (400MHz, $CDCl_3$) δ 7.79 (d, *J* = 9.2 Hz, 2H, Ar-H), 7.30-7.22 (m, 5H, Ar-H), 6.96 (d, *J* = 9.2 Hz, 2H, Ar-H), 6.78 (s, 1H, =CH), 6.56 (s, 1H, Ar-H), 4.00 (t, *J* = 6.4 Hz, 2H, OCH_2), 3.97 (s, 3H, OCH_3), 3.96 (s, 3H, OCH_3), 3.90 (s, 3H, OCH_3), 3.51 (s, 2H, CH_2Ph), 2.53-2.49 (m, 6H, CH_2N), 2.42-2.38 (m, 4H, CH_2N), 1.82-1.78 (m, 2H, CH_2), 1.54-1.50 (m, 2H, CH_2), 1.50-1.45 (m, 2H, CH_2), 1.38-1.34 (m, 2H, CH_2); HR-ESI-MS: Calcd. for $C_{35}H_{43}N_2O_6$ $[M+H]^+$: 587.3121, found: 587.3120.

*4.1.7.18. 5-Hydroxy-4′-(3-((2-Methoxybenzyl)(methyl)amino)propoxy)-6,7-dimethoxyflavone (**16a**).* Light yellow oil, 80.6% yield, 98.5% HPLC purity. ^{1}H NMR (400MHz, $CDCl_3$) δ 12.80 (s, 1H, OH), 7.83 (d, *J* = 8.8 Hz, 2H, Ar-H), 7.32 (d, *J* = 7.6 Hz, 1H, Ar-H), 7.23 (d, *J* = 8.0 Hz, 1H, Ar-H), 7.00 (d, *J* = 8.8 Hz, 2H, Ar-H), 6.90 (t, *J* = 7.6 Hz, 1H, Ar-H), 6.86 (d, *J* = 8.0 Hz, 1H, Ar-H), 6.59 (s, 1H, =CH), 6.55 (s, 1H, Ar-H), 4.14 (t, *J* = 6.4 Hz, 2H, OCH_2), 3.97 (s, 3H, OCH_3), 3.93 (s, 3H, OCH_3), 3.81 (s, 3H, OCH_3), 3.58 (s, 2H, CH_2Ph), 2.68-2.62 (m, 2H, CH_2N), 2.29 (s, 3H, NCH_3), 2.12-2.08 (m, 2H, CH_2); ^{13}C NMR (100MHz, $CDCl_3$) δ 182.5, 163.9, 162.1, 158.5, 157.6, 153.1, 152.9, 132.4, 130.5, 128.1, 127.8, 126.4, 123.0, 120.1, 114.9, 110.3, 105.9, 103.8, 90.5, 66.4, 60.7, 56.2, 55.3, 55.2, 53.8, 42.4, 26.9; HR-ESI-MS: Calcd. for $C_{29}H_{32}NO_7$ $[M+H]^+$: 506.2179, found: 506.2176.

*4.1.7.19. 5-Hydroxy-4′-(3-((ethyl)(2-Methoxybenzyl) amino)propoxy)-6,7-dimethoxyflavone (**16b**).* Light yellow oil, 78.7% yield, 99.2% HPLC purity. ^{1}H NMR (400MHz, $CDCl_3$) δ 12.80 (s, 1H, OH), 7.82 (d, *J* = 8.4 Hz, 2H, Ar-H), 7.40 (d, *J* = 6.4Hz, 1H, Ar-H), 7.22 (t, *J* = 7.6 Hz, 1H, Ar-H), 6.98 (d, *J* = 8.4 Hz, 2H, Ar-H), 6.91 (t, *J* = 7.6 Hz, 1H, Ar-H), 6.85 (d, *J* = 8.0 Hz, 1H, Ar-H), 6.59 (s, 1H, =CH), 6.55 (s, 1H, Ar-H), 4.10 (t, *J* = 6.0 Hz, 2H, OCH_2), 3.97 (s, 3H, OCH_3), 3.93 (s, 3H, OCH_3), 3.82 (s, 3H, OCH_3), 3.64 (s, 2H, CH_2Ph), 2.72-2.68 (m, 2H, CH_2N), 2.62-2.58 (m, 2H, CH_2N), 2.04-2.00 (m, 2H, CH_2), 1.08 (t, *J* = 7.2 Hz, 3H, CH_3); ^{13}C NMR (100MHz, $CDCl_3$) δ 182.5, 164.0, 162.1, 158.5, 157.5, 153.0, 152.9, 132.4, 130.0, 127.8, 127.3, 126.7, 123.0, 120.2, 114.8, 110.1, 105.9, 103.7, 90.4, 66.4, 60.7, 56.2, 55.2, 51.3, 49.5, 47.7, 26.7, 11.7; HR-ESI-MS: Calcd. for $C_{30}H_{34}NO_7$ $[M+H]^+$: 520.2335, found: 520.2328.

*4.1.7.20. 5-Hydroxy-4′-(3-((2-Methoxybenzyl)(methyl)amino)butoxy)-6,7-dimethoxyflavone (**16c**).* Light yellow oil, 71.2% yield, 98.2% HPLC purity. ^{1}H NMR (400MHz, $CDCl_3$) δ 12.79 (s, 1H, OH), 7.83 (d, *J* = 8.8 Hz, 2H, Ar-H), 7.37 (d, *J* = 6.0 Hz, 1H, Ar-H), 7.28-7.24 (m, 1H, Ar-H), 6.99 (d, *J* = 8.8 Hz, 2H, Ar-H), 6.94 (t, *J* = 7.6 Hz, 1H, Ar-H), 6.88 (d, *J* = 8.4 Hz, 1H, Ar-H), 6.59 (s, 1H, =CH), 6.55 (s, 1H, Ar-H), 4.06 (t, *J* = 6.0 Hz, 2H, OCH_2), 3.97 (s, 3H, OCH_3), 3.93 (s, 3H, OCH_3), 3.83 (s, 3H, OCH_3), 3.62 (s, 2H, CH_2Ph), 2.59-2.54 (m, 2H, CH_2N), 2.31 (s, 3H, NCH_3), 1.89-1.85 (m, 2H, CH_2), 1.83-1.79 (m, 2H, CH_2); ^{13}C NMR (100MHz, $CDCl_3$) δ 182.5, 163.9, 162.0, 158.6, 157.7, 153.1, 152.9, 132.4, 130.8, 128.3, 127.8, 125.8, 123.1, 120.2, 114.8, 110.3, 105.9, 103.8, 90.5, 67.9, 60.7, 56.9, 56.2, 55.3, 55.1, 42.0, 26.8, 23.4; HR-ESI-MS: Calcd. for $C_{30}H_{34}NO_7$ $[M+H]^+$: 520.2335, found: 520.2325.

*4.1.7.21. 5-Hydroxy-4′-(3-((ethyl)(2-Methoxybenzyl) amino)butoxy)-6,7-dimethoxyflavone (**16d**).* Light yellow oil, 71.5% yield, 97.9% HPLC purity. ^{1}H NMR (400MHz, $CDCl_3$) δ 12.80 (s, 1H, OH), 7.83 (d, *J* = 8.8 Hz, 2H, Ar-H), 7.44 (d, *J* = 6.8 Hz, 1H, Ar-H), 7.23 (t, *J* = 7.2 Hz, 1H, Ar-H), 6.98 (d, *J* = 8.8 Hz, 2H, Ar-H), 6.93 (t, *J* = 7.2 Hz, 1H, Ar-H), 6.86 (d, *J* = 8.0 Hz, 1H, Ar-H), 6.59 (s, 1H, =CH), 6.55 (s, 1H, Ar-H), 4.02 (t, *J* = 6.4 Hz, 2H, OCH_2), 3.97 (s, 3H, OCH_3), 3.93 (s, 3H, OCH_3), 3.83 (s, 3H, OCH_3), 3.65 (s, 2H, CH_2Ph), 2.60-2.56 (m, 4H, CH_2N), 1.87-1.83 (m, 2H, CH_2), 1.74-1.70 (m, 2H, CH_2), 1.12-1.08 (m, 3H, CH_3); ^{13}C NMR (100MHz, $CDCl_3$) δ 182.5, 164.0, 162.1, 158.6, 157.6, 153.1, 152.9, 132.4, 130.2, 127.8, 127.6, 126.6, 123.0, 120.2, 114.8, 110.2, 105.9, 103.8, 90.5, 68.0, 60.7, 56.2, 55.2, 52.7, 51.1, 47.5, 26.9, 23.2, 11.5; HR-ESI-MS: Calcd. for $C_{31}H_{36}NO_7$ $[M+H]^+$: 534.2492, found: 534.2489.

*4.1.7.22. 5-Hydroxy-4′-(3-((2-Methoxybenzyl)(methyl)amino)hexyloxy)-6,7-dimethoxyflavone (**16e**).* Light yellow oil, 72.6% yield, 98.8% HPLC purity. ^{1}H NMR (400MHz, $CDCl_3$) δ 12.80 (s, 1H, OH), 7.84 (d, *J* = 8.8 Hz, 2H, Ar-H), 7.39 (d, *J* = 7.2 Hz, 1H, Ar-H), 7.26 (t, *J* = 7.2 Hz, 1H, Ar-H), 7.00 (d, *J* = 8.8 Hz, 2H, Ar-H), 6.95 (t, *J* = 7.6 Hz, 1H, Ar-H), 6.88 (d, *J* = 8.0 Hz, 1H, Ar-H), 6.59 (s, 1H, =CH), 6.55 (s, 1H, Ar-H), 4.04 (t, *J* = 6.0 Hz, 2H, OCH_2), 3.97 (s, 3H, OCH_3), 3.93 (s, 3H, OCH_3), 3.84 (s, 3H, OCH_3), 3.66 (s, 2H, CH_2Ph), 2.56-2.52 (m, 2H, CH_2N), 2.32 (s, 3H, NCH_3),

1.86-1.82 (m, 2H, CH_2), 1.71-1.66 (m, 2H, CH_2), 1.53-1.48 (m, 2H, CH_2), 1.45-1.40 (m, 2H, CH_2); ^{13}C NMR (100MHz, $CDCl_3$) δ 182.5, 163.9, 162.1, 158.5, 157.7, 153.0, 152.8, 132.4, 131.0, 128.5, 127.8, 125.3, 123.0, 120.2, 114.8, 110.3, 105.9, 103.7, 90.4, 68.1, 60.7, 57.3, 56.2, 55.3, 55.0, 41.9, 28.9, 27.0, 26.7, 25.8; HR-ESI-MS: Calcd. for $C_{32}H_{38}NO_7$ $[M+H]^+$: 548.2648, found: 548.2640.

*4.1.7.23. 5-Hydroxy-4'-(3-((ethyl)(2-Methoxybenzyl) amino)hexyloxy)-6,7-dimethoxyflavone (**16f**).* Light yellow oil, 77.1% yield, 98.6% HPLC purity. ^{1}H NMR (400MHz, $CDCl_3$) δ 12.80 (s, 1H, OH), 7.83 (d, *J* = 8.8 Hz, 2H, Ar-H), 7.45 (d, *J* = 6.8 Hz, 1H, Ar-H), 7.23 (t, *J* = 8.0 Hz, 1H, Ar-H), 6.99 (d, *J* = 8.8 Hz, 2H, Ar-H), 6.94 (t, *J* = 7.6 Hz, 1H, Ar-H), 6.86 (d, *J* = 8.0 Hz, 1H, Ar-H), 6.59 (s, 1H, =CH), 6.55 (s, 1H, Ar-H), 4.02 (t, *J* = 6.4 Hz, 2H, OCH_2), 3.97 (s, 3H, OCH_3), 3.93 (s, 3H, OCH_3), 3.83 (s, 3H, OCH_3), 3.66 (s, 2H, CH_2Ph), 2.63-2.58 (m, 2H, CH_2N), 2.55-2.50 (m, 2H, CH_2N), 1.84-1.79 (m, 2H, CH_2), 1.61-1.56 (m, 2H, CH_2), 1.52-1.48 (m, 2H, CH_2), 1.43-1.38 (m, 2H, CH_2), 1.10 (t, *J* = 6.8 Hz, 3H, CH_3); ^{13}C NMR (100MHz, $CDCl_3$) δ 182.4, 163.8, 162.0, 158.5, 157.5, 152.9, 152.8, 132.3, 130.2, 127.8, 127.7, 126.7, 122.9, 120.2, 114.7, 110.1, 105.8, 103.6, 90.4, 68.0, 60.6, 56.1, 55.1, 53.0, 51.0, 47.4, 28.9, 27.0, 26.4, 25.7, 11.3; HR-ESI-MS: Calcd. for $C_{33}H_{40}NO_7$ $[M+H]^+$: 562.2805, found: 562.2812.

*4.1.7.24. 3'-(3-(Benzyl(methyl)amino)ethoxy)-5,6,7-trimethoxyflavone (**17a**).* Light yellow oil, 75.5% yield, 97.8% HPLC purity. ^{1}H NMR (400 MHz, $CDCl_3$) δ 7.44 (d, *J* = 8.0 Hz, 1H, Ar-H), 7.41-7.26 (m, 7H, Ar-H), 7.03 (dd, *J* = 1.6, 8.0 Hz, 1H, Ar-H), 6.82 (s, 1H, =CH), 6.65 (s, 1H, Ar-H), 4.20 (t, *J* = 6.0 Hz, 2H, OCH_2), 3.99 (s, 3H, OCH_3), 3.98 (s, 3H, OCH_3), 3.92 (s, 3H, OCH_3), 3.69 (s, 2H, CH_2Ph), 2.92 (t, *J* = 6.0 Hz, 2H, CH_2N), 2.41 (s, 3H, NCH_3); HR-ESI-MS: Calcd. for $C_{28}H_{30}NO_6$ $[M+H]^+$: 476.2073, found: 476.2062.

*4.1.7.25. 3'-(3-(Benzyl(ethyl)amino)ethoxy)-5,6,7-trimethoxyflavone (**17b**).* Light yellow oil, 77.8% yield, 98.5% HPLC purity. ^{1}H NMR (400 MHz, $CDCl_3$) δ 7.44 (d, *J* = 8.0 Hz, 1H, Ar-H), 7.40-7.25 (m, 7H, Ar-H), 6.99 (dd, *J* = 1.6, 8.0 Hz, 1H, Ar-H), 6.82 (s, 1H, =CH), 6.64 (s, 1H, Ar-H), 4.12-4.07 (m, 2H, OCH_2), 3.99 (s, 3H, OCH_3), 3.99 (s, 3H, OCH_3), 3.92 (s, 3H, OCH_3), 3.74 (s, 2H, CH_2Ph), 2.97-2.93 (m, 2H, CH_2N), 2.72-2.68 (m, 2H, CH_2N), 1.14 (t, *J* = 6.4 Hz, 3H, CH_3);

HR-ESI-MS: Calcd. for $C_{29}H_{32}NO_6$ $[M+H]^+$: 490.2230, found: 490.2234.

*4.1.7.26. 3′-(3-((2-Methoxybenzyl)(methyl)amino)ethoxy)-5,6,7-trimethoxyflavone (**17c**).* Light yellow oil, 74.9% yield, 98.8% HPLC purity. ^{1}H NMR (400 MHz, $CDCl_3$) δ 7.46-7.38 (m, 4H, Ar-H), 7.29-7.24 (m, 1H, Ar-H), 7.07 (dd, *J* = 1.6, 8.0 Hz, 1H, Ar-H), 6.96 (t, *J* = 7.2 Hz, Ar-H), 6.89 (d, *J* = 8.0 Hz, Ar-H), 6.84 (s, 1H, =CH), 6.65 (s, 1H, Ar-H), 4.28 (t, *J* =6.0 Hz, 2H, OCH_2), 3.99 (s, 6H, 2 × OCH_3), 3.92 (s, 3H, OCH_3), 3.83 (s, 3H, OCH_3), 3.79 (s, 2H, CH_2Ph), 3.02-2.98 (m, 2H, CH_2N), 2.47 (s, 3H, NCH_3); HR-ESI-MS: Calcd. for $C_{29}H_{32}NO_7$ $[M+H]^+$: 506.2179, found: 406.2188.

*4.1.7.27. 3′-(3-(4-Benzylpiperazin-1-yl)ethoxy)-5,6,7-trimethoxyflavone (**17d**).* Light yellow oil, 72.3% yield, 98.3% HPLC purity. ^{1}H NMR (400 MHz, $CDCl_3$) δ 7.45 (d, *J* = 7.6 Hz, 1H, Ar-H), 7.42-7.27 (m, 7H, Ar-H), 7.04 (dd, *J* = 1.6, 8.0 Hz, 1H, Ar-H), 6.83 (s, 1H, =CH), 6.65 (s, 1H, Ar-H), 4.22 (t, *J* = 6.4 Hz, 2H, OCH_2), 4.00 (s, 3H, OCH_3), 3.99 (s, 3H, OCH_3), 3.92 (s, 3H, OCH_3), 3.60 (s, 1H, CH_2Ph), 2.92 (t, *J* = 6.4 Hz, 2H, CH_2N), 2.78-2.73 (m, 4H, CH_2N), 2.65-2.61 (m, 4H, CH_2N); HR-ESI-MS: Calcd. for $C_{31}H_{35}N_2O_6$ $[M+H]^+$: 531.2495, found: 531.2486.

*4.1.7.28. 3′-(3-(4-Methylpiperazin-1-yl)ethoxy)-5,6,7-trimethoxyflavone (**17e**).* Light yellow oil, 78.3% yield, 98.4% HPLC purity. ^{1}H NMR (400 MHz, $CDCl_3$) δ 7.46 (d, *J* = 7.6 Hz, 1H, Ar-H), 7.43-7.38 (m, 2H, Ar-H), 7.05 (dd, *J* = 1.2, 8.0 Hz, 1H, Ar-H), 6.82 (s, 1H, =CH), 6.65 (s, 1H, Ar-H), 4.19 (t, *J* = 6.0 Hz, 2H, OCH_2), 4.00 (s, 3H, OCH_3), 3.99 (s, 3H, OCH_3), 3.92 (s, 3H, OCH_3), 2.89 (t, *J* = 6.0 Hz, 2H, CH_2N), 2.77-2.71 (m, 4H, CH_2N), 2.65-2.60 (m, 4H, CH_2N), 2.37 (s, 3H, NCH_3); HR-ESI-MS: Calcd. for $C_{25}H_{31}N_2O_6$ $[M+H]^+$: 455.2182, found: 455.2180.

*4.1.7.29. 3′-(3-(Benzyl(methyl)amino)propoxy)-5,6,7-trimethoxyflavone (**17f**).* Light yellow oil, 76.4% yield, 98.0% HPLC purity. ^{1}H NMR (400 MHz, $CDCl_3$) δ 7.45 (d, *J* = 7.6 Hz, 1H, Ar-H), 7.41 (d, *J* = 8.0 Hz, 1H, Ar-H), 7.38-7.34 (m, 1H, Ar-H), 7.32-7.28 (m, 5H, Ar-H), 7.02 (dd, *J* = 1.6, 7.6 Hz, 1H, Ar-H), 6.82 (s, 1H, =CH), 6.66 (s, 1H, Ar-H), 4.11 (t, *J* = 6.4 Hz, 2H, OCH_2), 4.00 (s, 3H, OCH_3), 3.98 (s, 3H, OCH_3), 3.93 (s, 3H, OCH_3), 3.57 (s, 2H, CH_2Ph), 2.64-2.60 (m, 2H, CH_2N), 2.28 (s, 3H, NCH_3), 2.09-2.04 (m, 2H, CH_2); HR-ESI-MS: Calcd. for $C_{29}H_{32}NO_6$ $[M+H]^+$:

490.2230, found: 490.2239.

*4.1.7.30. 3′-(3-(Benzyl(ethyl)amino)propoxy)-5,6,7-trimethoxyflavone (**17g**).* Light yellow oil, 75.3% yield, 98.1% HPLC purity. ^{1}H NMR (400 MHz, $CDCl_3$) δ 7.45 (d, *J* = 8.0 Hz, 1H, Ar-H), 7.40 (d, *J* = 8.0 Hz, 1H, Ar-H), 7.39-7.35 (m, 2H, Ar-H), 7.36-7.32 (m, 1H, Ar-H), 7.30 (t, *J* = 7.2 Hz, 2H, Ar-H), 7.26-7.22 (m, 1H, Ar-H), 7.00 (dd, *J* = 1.6, 8.0 Hz, 1H, Ar-H), 6.83 (s, 1H, =CH), 6.65 (s, 1H, Ar-H), 4.08 (t, *J* = 6.0 Hz, 2H, OCH_2), 4.00 (s, 3H, OCH_3), 3.99 (s, 3H, OCH_3), 3.93 (s, 3H, OCH_3), 3.70 (s, 2H, CH_2Ph), 2.77-2.72 (m, 2H, CH_2N), 2.68-2.63 (m, 2H, CH_2N), 2.08-2.04 (m, 2H, CH_2), 1.14 (t, *J* = 6.4 Hz, 3H, CH_3); HR-ESI-MS: Calcd. for $C_{30}H_{34}NO_6$ $[M+H]^+$: 504.2386, found: 504.2392.

*4.1.7.31. 3′-(3-((2-Methoxybenzyl)(methyl)amino)propoxy)-5,6,7-trimethoxyflavone (**17h**).* Light yellow oil, 77.7% yield, 99.0% HPLC purity. ^{1}H NMR (400 MHz, $CDCl_3$) δ 7.44 (d, *J* = 8.0 Hz, 1H, Ar-H), 7.40 (d, *J* = 8.0 Hz, 1H, Ar-H), 7.39-7.34 (m, 1H, Ar-H), 7.35 (d, *J* = 7.2 Hz, 1H, Ar-H), 7.23 (d, *J* = 7.2 Hz, 1H, Ar-H), 7.03 (dd, *J* = 1.2, 7.6 Hz, 1H, Ar-H), 6.91 (t, *J* = 7.6 Hz, Ar-H), 6.86 (d, *J* = 8.4 Hz, Ar-H), 6.83 (s, 1H, =CH), 6.66 (s, 1H, Ar-H), 4.13 (t, *J* = 6.0 Hz, 2H, OCH_2), 4.00 (s, 3H, OCH_3), 3.99 (s, 3H, OCH_3), 3.93 (s, 3H, OCH_3), 3.81 (s, 3H, OCH_3), 3.64 (s, 2H, CH_2Ph), 2.72-2.68 (m, 2H, CH_2N), 2.33 (s, 3H, NCH_3), 2.14-2.10 (m, 2H, CH_2); HR-ESI-MS: Calcd. for $C_{30}H_{34}NO_7$ $[M+H]^+$: 520.2335, found: 520.2328.

*4.1.7.32. 3′-(3-((Ethyl)(2-methoxybenzyl)amino)propoxy)-5,6,7-trimethoxyflavone (**17i**).* Light yellow oil, 80.2% yield, 98.7% HPLC purity. ^{1}H NMR (400 MHz, $CDCl_3$) δ 7.45-7.39 (m, 3H, Ar-H), 7.38-7.34 (m, 1H, Ar-H), 7.21 (t, *J* = 6.8 Hz, 1H, Ar-H), 7.01 (dd, *J* = 1.2, 8.0 Hz, 1H, Ar-H), 6.91 (t, *J* = 7.2 Hz, 1H, Ar-H), 6.85 (d, *J* = 8.4 Hz, 1H, Ar-H), 6.82 (s, 1H, =CH), 6.66 (s, 1H, Ar-H), 4.10 (t, *J* = 6.4 Hz, 2H, OCH_2), 4.00 (s, 3H, OCH_3), 3.99 (s, 3H, OCH_3), 3.93 (s, 3H, OCH_3), 3.82 (s, 3H, OCH_3), 3.67 (s, 2H, CH_2Ph), 2.73-2.69 (m, 2H, CH_2N), 2.63-2.59 (m, 2H, CH_2N), 2.06-2.02 (m, 2H, CH_2), 1.13-1.09 (m, 3H, CH_3); HR-ESI-MS: Calcd. for $C_{31}H_{36}NO_7$ $[M+H]^+$: 534.2492, found: 534.2496.

*4.1.7.33. 3′-(3-(4-Benzylpiperazin-1-yl)propoxy)-5,6,7-trimethoxyflavone (**17j**).* Light yellow oil,

71.8% yield, 98.9% HPLC purity. ^{1}H NMR (400 MHz, $CDCl_3$) δ 7.44 (d, *J* = 7.6 Hz, 1H, Ar-H), 7.40 (d, *J* = 8.0 Hz, 1H, Ar-H), 7.39-7.34 (m, 1H, Ar-H), 7.33-7.26 (m, 5H, Ar-H), 7.03 (dd, *J* = 1.6, 7.6 Hz, 1H, Ar-H), 6.82 (s, 1H, =CH), 6.65 (s, 1H, Ar-H), 4.10 (t, *J* = 6.0 Hz, 2H, OCH_2), 3.99 (s, 6H, 2 × OCH_3), 3.92 (s, 3H, OCH_3), 3.57 (s, 2H, CH_2Ph), 2.68-2.64 (m, 10H, CH_2N), 2.12-2.06 (m, 2H, CH_2); HR-ESI-MS: Calcd. for $C_{32}H_{37}N_2O_6$ $[M+H]^+$: 545.2652, found: 545.2646.

*4.1.7.34. 3'-(3-(4-Methylpiperazin-1-yl)propoxy)-5,6,7-trimethoxyflavone (**17k**).* Light yellow oil, 77.9% yield, 98.2% HPLC purity. ^{1}H NMR (400 MHz, $CDCl_3$) δ 7.45 (d, *J* = 7.6 Hz, 1H, Ar-H), 7.41 (d, *J* = 8.0 Hz, 1H, Ar-H), 7.40-7.35 (m, 1H, Ar-H), 7.04 (dd, *J* = 1.6, 8.0 Hz, 1H, Ar-H), 6.82 (s, 1H, =CH), 6.66 (s, 1H, Ar-H), 4.10 (t, *J* = 6.4 Hz, 2H, OCH_2), 3.99 (s, 6H, 2 × OCH_3), 3.93 (s, 3H, OCH_3), 2.63-2.59 (m, 10H, CH_2N), 2.37 (s, 3H, NCH_3), 2.06-2.02 (m, 2H, CH_2); HR-ESI-MS: Calcd. for $C_{26}H_{33}N_2O_6$ $[M+H]^+$: 469.2339, found: 469.2350.

*4.1.7.35. 3'-(4-(Benzyl(methyl)amino)butoxy)-5,6,7-trimethoxyflavone (**17l**).* Light yellow oil, 77.2% yield, 98.3% HPLC purity. ^{1}H NMR (400MHz, $CDCl_3$) δ 7.44 (d, *J* = 7.6 Hz, 1H, Ar-H), 7.40 (d, *J* = 8.0 Hz, 1H, Ar-H), 7.39-7.35 (m, 1H, Ar-H), 7.30-7.26 (m, 5H, Ar-H), 7.02 (dd, *J* = 1.2, 8.0 Hz, 1H, Ar-H), 6.81 (s, 1H, =CH), 6.65 (s, 1H, Ar-H), 4.03 (t, *J* = 6.0 Hz, 2H, OCH_2), 3.99 (s, 3H, OCH_3), 3.98 (s, 3H, OCH_3), 3.92 (s, 3H, OCH_3), 3.52 (s, 2H, CH_2Ph), 2.46 (t, *J* = 6.8 Hz, 2H, CH_2N), 2.23 (s, 3H, NCH_3), 1.87-1.83 (m, 2H, CH_2), 1.76-1.72 (m, 2H, CH_2); HR-ESI-MS: Calcd. for $C_{30}H_{34}NO_6$ $[M+H]^+$: 504.2386, found: 504.2385.

*4.1.7.36. 3'-(4-(Benzyl(ethyl)amino)butoxy)-5,6,7-trimethoxyflavone (**17m**).* Light yellow oil, 80.1% yield, 97.9% HPLC purity. ^{1}H NMR (400MHz, $CDCl_3$) δ 7.44 (d, *J* = 8.0 Hz, 1H, Ar-H), 7.40 (d, *J* = 8.0 Hz, 1H, Ar-H), 7.38-7.34 (m, 3H, Ar-H), 7.30 (t, *J* = 7.2 Hz, 2H, Ar-H), 7.25-7.20 (m, 1H, Ar-H), 7.00 (dd, *J* = 1.6, 8.0 Hz, 1H, Ar-H), 6.81 (s, 1H, =CH), 6.65 (s, 1H, Ar-H), 4.01 (t, *J* = 6.0 Hz, 2H, OCH_2), 4.00 (s, 3H, OCH_3), 3.98 (s, 3H, OCH_3), 3.92 (s, 3H, OCH_3), 3.61 (s, 2H, CH_2Ph), 2.57-2.53 (m, 4H, CH_2N), 1.87-1.83 (m, 2H, CH_2), 1.72-1.68 (m, 2H, CH_2), 1.08 (t, *J* = 6.4 Hz, 3H, CH_3); HR-ESI-MS: Calcd. for $C_{31}H_{36}NO_6$ $[M+H]^+$: 518.2543, found: 518.2547.

*4.1.7.37. 3'-(4-((2-Methoxybenzyl)(methyl)amino)butoxy)-5,6,7-trimethoxyflavone (**17n**).* Light

yellow oil, 78.8% yield, 98.6% HPLC purity. ^{1}H NMR (400MHz, $CDCl_3$) δ 7.44 (d, *J* = 7.6 Hz, 1H, Ar-H), 7.40 (d, *J* = 7.6 Hz, 1H, Ar-H), 7.40-7.36 (m, 1H, Ar-H), 7.37-7.33 (m, 1H, Ar-H), 7.23 (d, *J* = 7.2 Hz, 1H, Ar-H), 7.03 (dd, *J* = 1.2, 7.6 Hz, 1H, Ar-H), 6.93 (t, *J* = 7.6 Hz, Ar-H), 6.87 (d, *J* = 8.4 Hz, Ar-H), 6.82 (s, 1H, =CH), 6.65 (s, 1H, Ar-H), 4.05 (t, *J* = 6.0 Hz, 2H, OCH_2), 3.99 (s, 6H, 2 × OCH_3), 3.92 (s, 3H, OCH_3), 3.83 (s, 3H, OCH_3), 3.61 (s, 2H, CH_2Ph), 2.57-2.53 (m, 2H, CH_2N), 2.29 (s, 3H, NCH_3), 1.89-1.83 (m, 2H, CH_2), 1.82-1.78 (m, 2H, CH_2); HR-ESI-MS: Calcd. for $C_{31}H_{36}NO_7$ $[M+H]^+$: 534.2492, found: 534.2580.

*4.1.7.38. 3′-(4-((Ethyl)(2-methoxybenzyl)amino)butoxy)-5,6,7-trimethoxyflavone (**17o**).* Light yellow oil, 79.3% yield, 98.0% HPLC purity. ^{1}H NMR (400MHz, $CDCl_3$) δ 7.44-7.39 (m, 3H, Ar-H), 7.39-7.34 (m, 1H, Ar-H), 7.21 (t, *J* = 7.2 Hz, 1H, Ar-H), 7.01 (dd, *J* = 1.2, 8.0 Hz, 1H, Ar-H), 6.92 (t, *J* = 7.6 Hz, 1H, Ar-H), 6.85 (d, *J* = 8.4 Hz, 1H, Ar-H), 6.82 (s, 1H, =CH), 6.65 (s, 1H, Ar-H), 4.01 (t, J = 6.0 Hz, 2H, OCH_2), 3.99 (s, 3H, OCH_3), 3.98 (s, 3H, OCH_3), 3.92 (s, 3H, OCH_3), 3.80 (s, 3H, OCH_3), 3.65 (s, 2H, CH_2Ph), 2.60-2.56 (m, 4H, CH_2N), 1.86-1.82 (m, 2H, CH_2), 1.74-1.70 (m, 2H, CH_2), 1.09 (t, *J* = 6.8 Hz, 3H, CH_3); HR-ESI-MS: Calcd. for $C_{32}H_{38}NO_7$ $[M+H]^+$: 548.2648, found: 548.2644.

*4.1.7.39. 3′-(4-(4-Benzylpiperazin-1-yl)butoxy)-5,6,7-trimethoxyflavone (**17p**).* Light yellow oil, 83.2% yield, 97.6% HPLC purity. ^{1}H NMR (400MHz, $CDCl_3$) δ 7.45 (d, *J* = 8.0 Hz, 1H, Ar-H), 7.40 (d, *J* = 8.0 Hz, 1H, Ar-H), 7.40-7.36 (m, 1H, Ar-H), 7.33-7.26 (m, 5H, Ar-H), 7.02 (dd, *J* = 1.6, 8.0 Hz, 1H, Ar-H), 6.84 (s, 1H, =CH), 6.65 (s, 1H, Ar-H), 4.07 (t, *J* = 6.0 Hz, 2H, OCH_2), 3.99 (s, 6H, 2 × OCH_3), 3.92 (s, 3H, OCH_3), 3.58 (s, 2H, CH_2Ph), 2.73-2.69 (m, 10H, CH_2N), 1.89-1.84 (m, 4H, CH_2); HR-ESI-MS: Calcd. for $C_{33}H_{39}N_2O_6$ $[M+H]^+$: 559.2808, found: 559.2800.

*4.1.7.40. 3′-(4-(4-Methylpiperazin-1-yl)butoxy)-5,6,7-trimethoxyflavone (**17q**).* Light yellow oil, 86.6% yield, 97.8% HPLC purity. ^{1}H NMR (400MHz, $CDCl_3$) δ 7.45 (d, *J* = 7.6 Hz, 1H, Ar-H), 7.41 (d, *J* = 8.0 Hz, 1H, Ar-H), 7.40-7.36 (m, 2H, Ar-H), 7.04 (dd, *J* = 1.6, 8.0 Hz, 1H, Ar-H), 6.82 (s, 1H, =CH), 6.65 (s, 1H, Ar-H), 4.06 (t, *J* = 6.0 Hz, 2H, OCH_2), 3.99 (s, 6H, 2 × OCH_3), 3.93 (s, 3H, OCH_3), 2.58-2.53 (m, 6H, CH_2N), 2.48 (t, *J* = 7.6 Hz, 4H, CH_2N), 2.34 (s, 3H, NCH_3),

1.88-1.84 (m, 2H, CH_2), 1.76-1.72 (m, 2H, CH_2); HR-ESI-MS: Calcd. for $C_{27}H_{35}N_2O_6$ $[M+H]^+$: 483.2495, found: 483.2488.

*4.1.7.41. 3′-(6-(Benzyl(methyl)amino)hexyloxy)-5,6,7-trimethoxyflavone (**17r**).* Light yellow oil, 77.2% yield, 98.5% HPLC purity. ^{1}H NMR (400MHz, $CDCl_3$) δ 7.45 (d, *J* = 8.0 Hz, 1H, Ar-H), 7.41 (d, *J* = 8.0 Hz, 1H, Ar-H), 7.40-7.36 (m, 1H, Ar-H), 7.33-7.28 (m, 5H, Ar-H), 7.03 (dd, *J* = 1.2, 7.6 Hz, 1H, Ar-H), 6.82 (s, 1H, =CH), 6.66 (s, 1H, Ar-H), 4.02 (t, *J* = 6.4 Hz, 2H, OCH_2), 3.99 (s, 3H, OCH_3), 3.98 (s, 3H, OCH_3), 3.92 (s, 3H, OCH_3), 3.60 (s, 2H, CH_2Ph), 2.48 (t, *J* = 6.8 Hz, 2H, CH_2N), 2.28 (s, 3H, NCH_3), 1.85-1.80 (m, 2H, CH_2), 1.66-1.62 (m, 2H, CH_2), 1.51-1.47 (m, 2H, CH_2), 1.43-1.38 (m, 2H, CH_2); HR-ESI-MS: Calcd. for $C_{32}H_{38}NO_6$ $[M+H]^+$: 532.2699, found: 532.2709.

*4.1.7.42. 3′-(6-(Benzyl(ethyl)amino)hexyloxy)-5,6,7-trimethoxyflavone (**17s**).* Light yellow oil, 85.2% yield, 99.3% HPLC purity. ^{1}H NMR (400MHz, $CDCl_3$) δ 7.46-7.26 (m, 8H, Ar-H), 7.03 (dd, *J* = 1.2, 8.8 Hz, 1H, Ar-H), 6.82 (s, 1H, =CH), 6.65 (s, 1H, Ar-H), 4.01 (t, *J* = 6.0 Hz, 2H, OCH_2), 3.99 (s, 3H, OCH_3), 3.98 (s, 3H, OCH_3), 3.90 (s, 3H, OCH_3), 3.74 (s, 2H, CH_2Ph), 2.62-2.58 (m, 4H, CH_2N), 1.85-1.81 (m, 2H, CH_2), 1.66-1.62 (m, 2H, CH_2), 1.53-1.48 (m, 2H, CH_2), 1.35-1.30 (m, 2H, CH_2), 1.17-1.13 (m, 3H, CH_3); HR-ESI-MS: Calcd. for $C_{33}H_{40}NO_6$ $[M+H]^+$: 546.2856, found: 546.2852.

*4.1.7.43. 3′-(6-((2-Methoxybenzyl)(methyl)amino)hexyloxy)-5,6,7-trimethoxyflavone (**17t**).* Light yellow oil, 79.5% yield, 98.0% HPLC purity. ^{1}H NMR (400MHz, $CDCl_3$) δ 7.44 (d, *J* = 8.0 Hz, 1H, Ar-H), 7.41 (d, *J* = 8.0 Hz, 1H, Ar-H), 7.41-7.36 (m, 2H, Ar-H), 7.32-7.28 (m, 1H, Ar-H), 7.03 (dd, *J* = 1.2, 8.0 Hz, 1H, Ar-H), 6.95 (t, *J* = 7.2 Hz, 1H, Ar-H), 6.88 (d, *J* = 8.0 Hz, 1H, Ar-H), 6.82 (s, 1H, =CH), 6.66 (s, 1H, Ar-H), 4.03 (t, *J* = 6.4 Hz, 2H, OCH_2), 3.99 (s, 3H, OCH_3), 3.98 (s, 3H, OCH_3), 3.92 (s, 3H, OCH_3), 3.84 (s, 3H, OCH_3), 3.71 (s, 2H, CH_2Ph), 2.59-2.54 (m, 2H, CH_2N), 2.34 (s, 3H, NCH_3), 1.86-1.82 (m, 2H, CH_2), 1.72-1.68 (m, 2H, CH_2), 1.55-1.50 (m, 2H, CH_2), 1.45-1.41 (m, 2H, CH_2); HR-ESI-MS: Calcd. for $C_{33}H_{40}NO_7$ $[M+H]^+$: 562.2805, found: 562.2797.

*4.1.7.44. 3′-(6-((Ethyl)(2-methoxybenzyl)amino)hexyloxy)-5,6,7-trimethoxyflavone (**17u**).* Light

yellow oil, 77.6% yield, 98.1% HPLC purity. ^{1}H NMR (400MHz, $CDCl_3$) δ 7.45-7.38 (m, 4H, Ar-H), 7.26-7.21 (m, 1H, Ar-H), 7.03 (dd, *J* = 1.2, 8.0 Hz, 1H, Ar-H), 6.95 (t, *J* = 7.2 Hz, 1H, Ar-H), 6.86 (d, *J* = 8.0 Hz, 1H, Ar-H), 6.82 (s, 1H, =CH), 6.65 (s, 1H, Ar-H), 4.02 (t, *J* = 6.4 Hz, 2H, OCH_2), 3.99 (s, 3H, OCH_3), 3.98 (s, 3H, OCH_3), 3.92 (s, 3H, OCH_3), 3.83 (s, 3H, OCH_3), 3.65 (s, 2H, CH_2Ph), 2.59-2.54 (m, 4H, CH_2N), 1.84-1.80 (m, 2H, CH_2), 1.64-1.60 (m, 2H, CH_2), 1.53-1.48 (m, 2H, CH_2), 1.41-1.38 (m, 2H, CH_2), 1.14-1.10 (m, 3H, NCH_3); HR-ESI-MS: Calcd. for $C_{34}H_{42}NO_7$ $[M+H]^+$: 576.2961, found: 576.2958.

*4.1.7.45. 3′-(6-(4-Benzylpiperazin-1-yl)hexyloxy)-5,6,7-trimethoxyflavone (**17v**).* Light yellow oil, 78.3% yield, 98.4% HPLC purity. ^{1}H NMR (400MHz, $CDCl_3$) δ 7.44 (d, *J* = 7.6 Hz, 1H, Ar-H), 7.41 (d, *J* = 8.0 Hz, 1H, Ar-H), 7.39-7.34 (m, 1H, Ar-H), 7.32-7.26 (m, 5H, Ar-H), 7.03 (dd, *J* = 1.6, 8.0 Hz, 1H, Ar-H), 6.82 (s, 1H, =CH), 6.65 (s, 1H, Ar-H), 4.02 (t, *J* = 6.0 Hz, 2H, OCH_2), 3.99 (s, 6H, OCH_3), 3.92 (s, 3H, OCH_3), 3.55 (s, 2H, CH_2Ph), 2.58-2.54 (m, 10H, CH_2N), 1.85-1.80 (m, 2H, CH_2), 1.66-1.61 (m, 2H, CH_2), 1.55-1.51 (m, 2H, CH_2), 1.43-1.39 (m, 2H, CH_2); HR-ESI-MS: Calcd. for $C_{35}H_{43}N_2O_6$ $[M+H]^+$: 587.3121, found: 587.3127.

*4.1.7.46. 5-Hydroxy-3′-(3-((2-Methoxybenzyl)(methyl)amino)propoxy)-6,7-dimethoxyflavone (**18a**).* Light yellow oil, 81.4% yield, 98.6% HPLC purity. ^{1}H NMR (400MHz, $CDCl_3$) δ 12.69 (s, 1H, OH), 7.45 (dt, *J* = 1.2, 7.6 Hz, 1H, Ar-H), 7.42 (d, *J* = 7.6 Hz, 1H, Ar-H), 7.42-7.38 (m, 1H, Ar-H), 7.32 (d, *J* = 7.2 Hz, 1H, Ar-H), 7.22 (t, *J* = 7.2 Hz, 1H, Ar-H), 7.07 (dd, *J* = 1.2, 7.6 Hz, 1H, Ar-H), 6.89 (t, *J* = 7.6 Hz, Ar-H), 6.85 (d, *J* = 8.4 Hz, Ar-H), 6.67 (s, 1H, =CH), 6.58 (s, 1H, Ar-H), 4.13 (t, *J* = 6.0 Hz, 2H, OCH_2), 3.97 (s, 3H, OCH_3), 3.93 (s, 3H, OCH_3), 3.80 (s, 3H, OCH_3), 3.58 (s, 2H, CH_2Ph), 2.64 (t, *J* = 6.0 Hz, 2H, CH_2N), 2.29 (s, 3H, NCH_3), 2.10-2.06 (m, 2H, CH_2); ^{13}C NMR (100MHz, $CDCl_3$) δ 182.6, 163.7, 159.5, 158.8, 157.7, 153.2, 152.9, 132.5, 132.4, 130.6, 130.0, 128.1, 126.6, 120.1, 118.3, 117.7, 112.3, 110.3, 106.2, 105.6, 90.6, 66.4, 60.8, 56.3, 55.4, 55.3, 53.9, 42.5, 27.1; HR-ESI-MS: Calcd. for $C_{29}H_{32}NO_7$ $[M+H]^+$: 506.2179, found: 506.2178.

*4.1.7.47. 5-Hydroxy-3′-(3-((ethyl)(2-Methoxybenzyl) amino)propoxy)-6,7-dimethoxyflavone (**18b**).* Light yellow oil, 75.8% yield, 97.9% HPLC purity. ^{1}H NMR (400MHz, $CDCl_3$) δ 12.70 (s, 1H,

OH), 7.45 (dt, *J* = 1.2, 8.0 Hz, 1H, Ar-H), 7.41 (d, *J* = 7.6 Hz, 1H, Ar-H), 7.41-7.37 (m, 1H, Ar-H), 7.37-7.33 (m, 1H, Ar-H), 7.20 (t, *J* = 7.6 Hz, 1H, Ar-H), 7.05 (dd, *J* = 1.2, 7.6 Hz, 1H, Ar-H), 6.89 (t, *J* = 7.6 Hz, Ar-H), 6.84 (d, *J* = 8.0 Hz, Ar-H), 6.66 (s, 1H, =CH), 6.57 (s, 1H, Ar-H), 4.09 (t, *J* = 6.4 Hz, 2H, OCH_2), 3.97 (s, 3H, OCH_3), 3.94 (s, 3H, OCH_3), 3.81 (s, 3H, OCH_3), 3.63 (s, 2H, CH_2Ph), 2.70-2.66 (m, 2H, CH_2N), 2.60-2.56 (m, 2H, CH_2N), 2.03-1.98 (m, 2H, CH_2), 1.08 (t, *J* = 6.4 Hz, 3H, NCH_3); ^{13}C NMR (100MHz, $CDCl_3$) δ 182.6, 163.8, 159.5, 158.8, 157.6, 153.2, 152.9, 132.6, 132.4, 130.0, 127.7, 127.6, 120.2, 118.3, 117.7, 112.4, 110.1, 106.2, 105.6, 90.6, 66.4, 60.8, 56.3, 55.1, 51.4, 49.6, 47.7, 26.9, 11.8; HR-ESI-MS: Calcd. for $C_{30}H_{34}NO_7$ $[M+H]^+$: 520.2335, found: 520.2322.

4.1.7.48. 5-Hydroxy-3′-(3-((2-Methoxybenzyl)(methyl)amino)butoxy)-6,7-dimethoxyflavone ***(18c)****.* Light yellow oil, 74.4% yield, 98.0% HPLC purity. ^1H NMR (400MHz, $CDCl_3$) δ 12.69 (s, 1H, OH), 7.45 (dt, *J* = 1.6, 8.0 Hz, 1H, Ar-H), 7.42 (d, *J* = 7.6 Hz, 1H, Ar-H), 7.41-7.38 (m, 1H, Ar-H), 7.35 (d, *J* = 6.8 Hz, 1H, Ar-H), 7.23 (t, *J* = 7.6 Hz, 1H, Ar-H), 7.06 (dd, *J* = 1.6, 7.6 Hz, 1H, Ar-H), 6.92 (t, *J* = 7.2 Hz, Ar-H), 6.87 (d, *J* = 8.0 Hz, Ar-H), 6.66 (s, 1H, =CH), 6.59 (s, 1H, Ar-H), 4.06 (t, *J* = 6.0 Hz, 2H, OCH_2), 3.99 (s, 3H, OCH_3), 3.93 (s, 3H, OCH_3), 3.82 (s, 3H, OCH_3), 3.58 (s, 2H, CH_2Ph), 2.55-2.50 (m, 2H, CH_2N), 2.28 (s, 3H, NCH_3), 1.93-1.89 (m, 2H, CH_2), 1.80-1.76 (m, 2H, CH_2); ^{13}C NMR (100MHz, $CDCl_3$) δ 182.5, 163.6, 159.4, 158.8, 157.7, 153.1, 152.8, 132.5, 132.3, 130.6, 123.00, 128.1, 126.4, 120.1, 118.3, 117.6, 112.3, 110.3, 106.1, 105.5, 90.6, 67.9, 60.7, 57.0, 56.2, 55.4, 55.1, 42.2, 26.9, 23.6; HR-ESI-MS: Calcd. for $C_{30}H_{34}NO_7$ $[M+H]^+$: 520.2335, found: 520.2330.

4.1.7.49. 5-Hydroxy-3′-(3-((ethyl)(2-Methoxybenzyl) amino)butoxy)-6,7-dimethoxyflavone ***(18d)****.* Light yellow oil, 72.6% yield, 97.8% HPLC purity. ^1H NMR (400MHz, $CDCl_3$) δ 12.69 (s, 1H, OH), 7.45-7.38 (m, 4H, Ar-H), 7.21 (t, *J* = 7.2 Hz, 1H, Ar-H), 7.04 (dd, *J* = 1.2, 8.0 Hz, 1H, Ar-H), 6.92 (t, *J* = 7.6 Hz, Ar-H), 6.85 (d, *J* = 8.0 Hz, Ar-H), 6.66 (s, 1H, =CH), 6.57 (s, 1H, Ar-H), 4.02 (t, *J* = 6.4 Hz, 2H, OCH_2), 3.98 (s, 3H, OCH_3), 3.93 (s, 3H, OCH_3), 3.82 (s, 3H, OCH_3), 3.63 (s, 2H, CH_2Ph), 2.58-2.54 (m, 4H, CH_2N), 1.86-1.82 (m, 2H, CH_2), 1.73-1.68 (m, 2H, CH_2), 1.08 (t, *J* = 6.4

Hz, 3H, CH_3); ^{13}C NMR (100MHz, $CDCl_3$) δ 182.6, 163.7, 159.4, 158.8, 157.6, 153.1, 152.8, 132.5, 132.3, 130.1, 130.0, 127.7, 127.5, 120.2, 118.3, 117.6, 112.3, 110.1, 106.1, 105.6, 90.6, 68.0, 60.7, 56.2, 55.2, 52.8, 51.2, 47.5, 27.0, 23.4, 11.7; HR-ESI-MS: Calcd. for $C_{31}H_{36}NO_7$ $[M+H]^+$: 534.2492, found: 534.2486.

*4.1.7.50. 5-Hydroxy-3'-(3-((2-Methoxybenzyl)(methyl)amino)hexyloxy)-6,7-dimethoxyflavone (**18e**).* Light yellow oil, 73.7% yield, 98.3% HPLC purity. ^{1}H NMR (400MHz, $CDCl_3$) δ 12.68 (s, 1H, OH), 7.46-7.38 (m, 4H, Ar-H), 7.26 (t, *J* = 6.4 Hz, 1H, Ar-H), 7.07 (dd, *J* = 1.6, 7.6 Hz, 1H, Ar-H), 6.95 (t, *J* = 7.2 Hz, Ar-H), 6.88 (d, *J* = 8.0 Hz, Ar-H), 6.67 (s, 1H, =CH), 6.58 (s, 1H, Ar-H), 4.03 (t, *J* = 6.4 Hz, 2H, OCH_2), 3.98 (s, 3H, OCH_3), 3.93 (s, 3H, OCH_3), 3.84 (s, 3H, OCH_3), 3.67 (s, 2H, CH_2Ph), 2.56-2.52 (m, 2H, CH_2N), 2.32 (s, 3H, NCH_3), 1.84-1.80 (m, 2H, CH_2), 1.70-1.66 (m, 2H, CH_2), 1.53-1.49 (m, 2H, CH_2), 1.45-1.40 (m, 2H, CH_2); ^{13}C NMR (100MHz, $CDCl_3$) δ 182.5, 163.6, 159.4, 158.7, 157.7, 153.1, 152.7, 132.4, 132.2, 131.0, 129.9, 128.5, 125.0, 120.2, 118.2, 117.5, 112.2, 110.3, 106.0, 105.5, 90.5, 67.9, 60.6, 57.2, 56.2, 55.2, 54.9, 41.8, 29.0, 27.0, 26.6, 25.8; HR-ESI-MS: Calcd. for $C_{32}H_{38}NO_7$ $[M+H]^+$: 548.2648, found: 548.2646.

*4.1.7.51. 5-Hydroxy-3'-(3-((ethyl)(2-Methoxybenzyl) amino)hexyloxy)-6,7-dimethoxyflavone (**18f**).* Light yellow oil, 80.3% yield, 98.5% HPLC purity. ^{1}H NMR (400MHz, $CDCl_3$) δ 12.69 (s, 1H, OH), 7.46-7.40 (m, 4H, Ar-H), 7.23 (t, *J* = 7.2 Hz, 1H, Ar-H), 7.06 (dd, *J* = 1.2, 8.0 Hz, 1H, Ar-H), 6.94 (t, *J* = 7.2 Hz, Ar-H), 6.86 (d, *J* = 8.0 Hz, Ar-H), 6.67 (s, 1H, =CH), 6.58 (s, 1H, Ar-H), 4.02 (t, *J* = 6.4 Hz, 2H, OCH_2), 3.98 (s, 3H, OCH_3), 3.93 (s, 3H, OCH_3), 3.83 (s, 3H, OCH_3), 3.65 (s, 2H, CH_2Ph), 2.56-2.52 (m, 4H, CH_2N), 1.85-1.80 (m, 2H, CH_2), 1.63-1.59 (m, 2H, CH_2), 1.52-1.48 (m, 2H, CH_2), 1.43-1.39 (m, 2H, CH_2), 1.12-1.08 (m, 3H, CH_3); ^{13}C NMR (100MHz, $CDCl_3$) δ 182.5, 163.6, 159.4, 158.7, 157.5, 153.1, 152.8, 132.4, 132.3, 130.3, 123.0, 127.9, 126.5, 120.2, 118.2, 117.5, 112.2, 110.1, 106.1, 105.5, 90.5, 68.0, 60.7, 56.2, 55.2, 53.0, 51.0, 47.4, 29.0, 27.1, 26.4, 25.8, 11.3; HR-ESI-MS: Calcd. for $C_{33}H_{40}NO_7$ $[M+H]^+$: 562.2805, found: 562.2800.

4.2. Biological evaluation.

4.2.1. Antioxidant Activity Assay

The antioxidant activity was determined by the oxygen radical absorbance capacity fluorescein (ORAC-FL) method with slight modification [18,24]. All the assays were conducted with 75mM phosphate buffer (pH 7.4), and the final reaction mixture was 200 μL. Antioxidant (20 μL) and fluorescein (120 μL, 150nM final concentration) were placed in the wells of a black 96-well plate. The mixture was pre-incubated for 15 min at 37 °C, and then AAPH solution (60 μL, 12 mM final concentration) was added rapidly using an autosampler. The plate was immediately placed in a Varioskan Flash Multimode Reader (Thermo Scientific) and the fluorescence recorded every minute for 90 min with excitation at 485 nm and emission at 535 nm. The plate was automatically shaken prior to each reading. *Trolox* was used as standard (1–8 μM, final concentration). A blank (FL + AAPH) using phosphate buffer instead of antioxidant and trolox calibration were carried out in each assay. The samples were measured at different concentration (1-10 μM). All the reaction mixture was prepared in duplicate, and at least three independent assays were performed for each sample. Antioxidant curves (fluorescence versus time) were normalized to the curve of the blank in the same assay, and then the area under the fluorescence decay curve (AUC) was calculated. The net AUC of a sample was obtained by subtracting the AUC of the blank. ORAC-FL values were expressed as Trolox equivalents by using the standard curve calculated for each sample, where the ORAC-FL value of *Trolox* was taken as 1, indicating the antioxidant potency of the tested compounds.

4.2.2. Inhibition Experiments of AChE and BuChE

AChE and BuChE activities were measured by the spectrophotometric method of Ellman with slight modification using AChE from 5% rat cortex homogenate or purified AChE from *Electrophorus electricus* (Sigma Co.) and human erythrocytes (Sigma Co.) or BuChE from rat serum [18,37]. The brain homogenate was preincubated for 5 min with tetraisopropyl pyrophosphoramide (*iso*-OMPA, selective inhibitor of BuChE, 4.0 mmol/L) before use. For rat AChE or BuChE inhibition assays, a reaction mixture (100 μL) containing acetylthiocholine iodide (1mmol/L, 30 μL) (*J&K* Scientific) or butyrylthiocholine iodide (1mmol/L, 30 μL) (TCI Shanghai

Development), phosphate-buffered solution (0.1 mmol/L, pH=7.4, 40 μL), 5% homogenate or 25% serum (10 μL) and different concentrations of test compounds (20 μL) was incubated at 37°C for 15 min. Then 5,5'-dithiobis-2-nitrobenzoic acid (DTNB, 0.2%, 30 μL) (J&K Scientific) was added to produce the yellow anion of 5-thio-2-nitro-benzoic acid. Changes in absorbance were detected at 405 nm in a Varioskan Flash Multimode Reader (Thermo Scientific). For Electrophorus electricus AChE and human AChE inhibition assay, *Ee*AChE or *Hu*AChE (0.05 U/mL, final concentration) was used and the assay was carried out in a phosphate buffer (0.01 mmol/L, pH=8.0). Changes in absorbance were detected at 412 nm [18,41]. The other procedure was the same as above. Compounds inhibiting AChE or BuChE activity would reduce the color generation. Thus, IC_{50} values were calculated as the concentration of compound that produces 50% AChE or BuChE activity inhibition. Donepezil was applied as positive drug. All samples were assayed in triplicate.

4.2.3. Kinetic Characterization of AChE Inhibition

Kinetic characterization of AChE inhibition was performed based on a reported method using purified AChE from *Electrophorus electricus* (*Ee*AChE) [18]. The assay solution (100 μL) consists of 0.1 M phosphate buffer (pH 8.0), with the addition of 30 μL of 0.2% DTNB, 10 μL of 0.5 units/mL *Ee*AChE, and 20 μL of substrate (acetylthiocholine iodide). Three different concentrations of inhibitors were added to the assay solution and pre-incubated for 15 min at 37°C with the *Ee*AChE followed by the addition of substrate in different concentrations. Kinetic characterization of the hydrolysis of substrate catalyzed by *Ee*AChE was done spectrometrically at 412 nm. The parallel control experiments were performed without inhibitor in the assay. The plots were assessed by a weighted least square analysis that assumed the variance of v to be a constant percentage of v for the entire data set. Slopes of these reciprocal plots were then plotted against the concentration of **16d** in a weighted analysis, and K_i was determined as the intercept on the negative *x*-axis.

4.2.4. Molecular Docking

The crystal structure of AChE complexed with donepezil (code ID: 1EVE) was obtained from the Protein Data Bank after eliminating the original inhibitors and water molecules. The 3D Structure of

16d was built and performed geometry optimization by molecular mechanics. After addition of Gasteiger charges, removal of hydrogen atoms, addition of their atomic charges to skeleton atoms, and the assignment of proper atomic types, the further preparation of the inhibitor was accomplished. Autotors was then used to define the rotatable bonds in the ligands. Docking studies were performed using the AUTODOCK 4.2 program. By using Autodock Tools (ADT; version 1.5.6), polar hydrogen atoms were added to amino acid residues, and Gasteiger charges were assigned to all atoms of the enzyme. The resulting enzyme structure was used as an input for the AUTOGRID program. AUTOGRID performed a pre-calculated atomic affinity grid maps for each atom type in the ligand, plus an electrostatics map and a separate desolvation map presented in the substrate molecule. All maps were calculated with 0.375 Å spacing between grid points. The center of the grid box was placed at the center of donepezil with coordinates x = 2.023, y = 63.295, z = 67.062. The dimensions of the active site box were set at 50 × 50 × 50 Å. Flexible ligand docking was performed for the compounds. Each docked system was performed by 100 runs of the AUTODOCK search by the Lamarckian genetic algorithm (LGA). Other than the referred parameters above, the other parameters were accepted as default. A cluster analysis was performed on the docking results using a root mean square (RMS) tolerance of 1.0 and the lowest energy conformation of the highest populated cluster was selected for analysis. Graphic manipulations and visualizations were done by Autodock Tools or Discovery Studio 2.1 software.

4.2.5. Metal Binding Studies [18,27]

The metal binding studies were carried out in a Shimadzu UV-2450 spectrophotometer. To investigate the metal binding ability of compound, the UV absorption of the tested compound **15j** or **16d**, in the absence or presence of $CuCl_2$, $FeSO_4$, $ZnCl_2$, and $AlCl_3$, was recorded with wavelength ranging from 200 to 500 nm after incubating for 30 min at room temperature. The final volume of reaction mixture was 1 mL, and the final concentrations of tested compound and metals were 37.5 μM. Numerical subtraction of the spectra of the metal alone and the compound alone from the spectra of the mixture gave the difference UV-vis spectra due to complex formation. The molar

ration method was performed to determine the stoichiometry of the complex compound-metal by titrating the methanol solution of tested compound with ascending of $CuCl_2$. The final concentration of tested compound was 37.5 μM, and the final concentration of Cu^{2+} ranged from 7.5 to 93.75 μM. The UV spectra was recorded and treated by numerical subtraction of $CuCl_2$ and tested compound at corresponding concentrations, plotted versus the mole fraction of tested compound.

4.2.6. Determination of the Inhibitory Effect on the Self-induced Aβ_{1-42} Aggregation

In order to investigate the self-induced Aβ_{1-42} aggregation, a Thioflavin T-based flurometric assay was performed [18,26,42]. Briefly, Aβ_{1-42} (Sigma Co.) was dissolved in HFIP (1 mg/mL) and incubated for 24 h at room temperature, and solvent was evaporated. Then the HFIP pretreated Aβ_{1-42} was resolubilized in DMSO to a final stock concentration of 200 μM and was kept frozen at -80 °C until use. Solutions of test compounds were prepared in DMSO in 2.5 mM for storage and diluted with phosphate buffer solution (pH 7.4) before use. For the self-induced assay, Aβ_{1-42} (20 μL, 25 μM, final concentration) was incubated with 20 μL of test compounds at different concentrations ranging from 10-50 μM in 50 mM phosphate buffer solution (pH 7.4) at 37 °C for 24 h. To minimize evaporation effect the wells were sealed by a transparent heat-resistant plastic film. After incubation, 160 μL of 5 μM thioflavin T in 50 mM glycine-NaOH buffer (pH 8.5) was added. Each assay was run in triplicate. Fluorescence was measured on a Varioskan Flash Multimode Reader (Thermo Scientific) with excitation and emission wavelengths at 446 nm and 490 nm, respectively. The fluorescence intensities were compared and the percent inhibition due to the presence of the inhibitor was calculated by the following formula: $100\text{-}IF_i/IF_c*100$), where IF_i and IF_c were the fluorescence intensities obtained for Aβ_{1-42} in the presence and in the absence of inhibitors, respectively.

4.2.7. Inhibition of HuAChE-induced Aβ_{1-40} Aggregation

The thioflavin-T (ThT) fluorescence method was used as previously described [18]. HFIP pretreated Aβ_{1-40} (Sigma Co.) and tested compounds were dissolved in DMSO to obtain 2.3 mM and 1 mM solutions respectively. For the AChE-induced assay, Aliquots of 2 μL of Aβ_{1-40} were incubated for

24 h at room temperature in 0.215 mM sodium phosphate buffer (pH 8.0) at a final concentration of 230 μM. For co-incubations experiments, 16 μL of *Hu*AChE (final concentration of 2.3 μM, A$\beta_{1\text{-}40}$/AChE molar ration of 100:1) and AChE in the presence of 2 μL of the tested inhibitor (final concentration 100 μM) in 0.215 M sodium phosphate buffer (pH 8.0) solutions were added. Blanks containing A$\beta_{1\text{-}40}$ alone, human AChE alone, and A$\beta_{1\text{-}40}$ plus tested inhibitors in 0.215 sodium phosphate buffer (pH 8.0) were prepared. After incubation, 180 μL of 5 μM thioflavin T in 50 mM glycine-NaOH buffer (pH 8.5) was added. Each assay was run in triplicate. The detection method was the same as above. The percent inhibition of the AChE-induced aggregation due to the presence of the tested compound was calculated by the following formula: 100-IF_i/IF_c*100), where IF_i and IF_c were the fluorescence intensities obtained for Aβ plus AChE in the presence and in the absence of inhibitors, respectively, minus the fluorescence intensities due to the respectively blanks.

4.2.8. Effect of Test Compounds on Metal-induced A$\beta_{1\text{-}42}$ Aggregation and Disaggregation Experiments by ThT Method

Solutions of Cu^{2+} were prepared from standards to concentration of 75 μM using the HEPES buffer (20 mM, pH 6.6, 150 mM NaCl). For the inhibition of copper-induced A$\beta_{1\text{-}42}$ aggregation assay [18,35], the A$\beta_{1\text{-}42}$ stock solution was diluted in HEPES buffer (20 mM, pH 6.6, 150 mM NaCl). The mixture of the peptide (20 μL, 25 μM, final concentration) and Cu^{2+} (20 μL, 25 μM, final concentration), with or without the tested compound at different concentrations (20 μL, 10-35 μM, final concentration) was incubated at 37 °C for 24 h. After incubation, 190 μL of 5 μM thioflavin T in 50 mM glycine-NaOH buffer (pH 8.5) was added. Each assay was run in triplicate. The detection method was the same as that of self-induced A$\beta_{1\text{-}42}$ experiment.

For the disaggregation of copper-induced Aβ fibrils experiment, the A$\beta_{1\text{-}42}$ stock solution was diluted in HEPES buffer (20 mM, pH 6.6, 150mM NaCl). The mixture of the A$\beta_{1\text{-}42}$ (20 μL, 25 μM, final concentration) with Cu^{2+} (20 μL, 25 μM, final concentration) was incubated 37 °C for 24 h. The tested compound (20 μL, 25 μM, final concentration) was then added and incubated at 37 °C for another 24 h. To minimize evaporation effect the wells were sealed by a transparent

heat-resistant plastic film. After incubation, 190 μL of 5 μM thioflavin T in 50 mM glycine-NaOH buffer (pH 8.5) was added. Each assay was run in triplicate. The detection method was the same as above.

4.2.9. Transmission Electron Microscopy (TEM) Assay

Samples for TEM were prepared by following the previously reported method [35]. For the self-induced experiment, the Aβ stock solution was diluted with 50 mM phosphate buffer (pH 7.4). For the copper-induced experiment, the Aβ stock solution was diluted with HEPES buffer (20 mM, pH 6.6, 150 mM NaCl). The sample preparation was the same as for the ThT assay. Aliquots (10 μL) of the samples were placed on a carbon-coated copper/rhodium grid for 2 min at room temperature. Excess sample was removed using filter paper followed by washing twice with ddH_2O. Each grid was negatively stained with 2% phosphomolybdic acid solution for 2 min at room temperature. After the excess of staining solution was drained off by means of a filter paper, the specimen was transferred for examination using a Hitachi H-600 transmission electron microscope.

4.2.10. Hydrogen Peroxide Induced PC12 Cell Injury [37]

PC12 cells were propagated in phenol red free Dulbecco's modified Eagle's medium (DMEM from GIBCO) containing 10% (v/v) fetal calf serum (FCS, Hyclone), 100 U/ml penicillin, and 100 mg/ml streptomycin (Invitrogen). The cells were grown at 37°C in a humidified atmosphere of 5% CO_2. Neuronal PC12 cells were plated at a density of 10^5 cells/well on 96-well plates in 100μl of DMEM. The compounds **15j** and **16d** were dissolved with 2% DMSO first, and then diluted with phosphate-buffered saline (PBS). The cells were pre-incubated with compounds for 24 hours before H_2O_2 (100 μM) was added. The cells were treated with or without H_2O_2 for two hours, and then replaced with fresh DMEM medium. Assays for cell viability were performed 24 h after cultured at 37 °C in fresh medium. The cells were treated with 25 μl MTT (5 mg/ml in PBS) for 4 h at 37°C and then were lysed in a buffered solution containing *N*,*N*-dimethylformamide (pH 4.5, 50% (aq, v/v)) and sodium dodecyl sulfate (SDS, 20% (w/v)) overnight at room temperature in the dark. The absorbance (A590nm) was measured using Elx800 microplate reader (Bio-Tek). % inhibition =

$[1-(A_{sample}/A_{control})]\times100$.

4.2.11. Step-down Passive Avoidance Test

4.2.11.1 Materials and animals

Donepezil was purchased from Eisai China Inc. Scopolamine was purchase from J&K Scientific. Kunming mice at body weight of 18–22 g (six weeks old, either gender) were supplied by the Center of Experimental Animals of Sichuan Academy of Chinese Medicine Sciences (eligibility certification no. SCXK[chuan] 2013-19). Mice were maintained under standard conditions with a 12 h:12 h light–dark cycle, a temperature and humidity controlled environment with access to food and water ad libitum.

4.2.11.2 Assay method

A modification of step-down passive avoidance test was used to assess learning and memory in mice [18,43]. The apparatus consisted of a grid floor with a wooden block placed in the center. The block served as a shock free zone. The mice underwent two separate trials: a training trial and a test trial 24 h later. For training trial, mice were initially placed on the block and were given an electrical foot shock (0.5 mA, 2s) through the grid floor on stepping down. We used a total of 90 mice in the passive avoidance test with 10 mice were used per treatment. Compounds **16d** (0.66, 2.2, 6.6 and 19.8 mg/kg, *p.o.*) or donepezil (0.5 and 5.0 mg/kg, *p.o.*) as a positive control were orally given 1 h before each training trial. After 30 min, memory impairment was induced by administering scopolamine (3 mg/kg, *i.p.*). Twenty-four hours after the training trial, mice were placed on the block and the time for the animal to step down was measured as latency time for test trial. An upper cut-off time was set at 300 s.

4.2.11.3 Statistical analysis

All data are expressed as mean ± SEM. Differences between groups were examined for statistical significance using one-way ANOVA with Student's *t* test. A *P* value less than 0.05 denoted the presence of a statistically significant difference.

Supporting Information Available:

The metal-chelating properties of target compound **15j** and the ^{1}HNMR and ^{13}CNMR spectra of target compounds **15–18** are available as supplementary material.

Acknowledgments

This work was supported in part by the Chinese National Natural Science Foundation (20872099), the Research Fund for the Doctoral Program of Higher Education (20110181110079), the Sichuan Academic and Technical Leader Training Foundation (2012DTPY003) and the National Science and Technology Major Project on "Key New Drug Creation and Manufacturing Program"(2013ZX09301304-002).

References

[1] Alzheimer's Disease International, Policy brief: the global impact of dementia 2013-2050, http://www.alz.co.uk/research/G8-policy-brief.

[2] N. Herrmann, S.A. Chau, I. Kircanski, K.L. Lanctot, Current and emerging drug treatment options for Alzheimer's disease: a systematic review, Drugs 71 (2011) 2031-2065.

[3] Y. Huang, L. Mucke, Alzheimer mechanisms and therapeutic strategies, Cell 148 (2012) 1204-1222.

[4] T. Sobow, Combination treatments in Alzheimer's disease: risks and benefits, Expert Review of Neurotherapeutics 10 (2010) 693-702.

[5] A. Cavalli, M.L. Bolognesi, A. Minarini, M. Rosini, V. Tumiatti, M. Recanatini, C. Melchiorre, Multi-target-directed ligands to combat neurodegenerative diseases, Journal of Medicinal Chemistry 51 (2008) 347-372.

[6] R. Morphy, Z. Rankovic, Designing multiple ligands - medicinal chemistry strategies and challenges, Current Pharmaceutical Design 15 (2009) 587-600.

[7] A. Cavalli, M.L. Bolognesi, S. Capsoni, V. Andrisano, M. Bartolini, E. Margotti, A. Cattaneo,

M. Recanatini, C. Melchiorre, A small molecule targeting the multifactorial nature of Alzheimer's disease, Angew. Chem. Int. Ed. Engl. 46 (2007) 3689-3692.

[8] P.C. Trippier, K. Jansen Labby, D.D. Hawker, J.J. Mataka, R.B. Silverman, Target- and mechanism-based therapeutics for neurodegenerative diseases: strength in numbers, Journal of Medicinal Chemistry 56 (2013) 3121-3147.

[9] R. Leon, A.G. Garcia, J. Marco-Contelles, Recent advances in the multitarget-directed ligands approach for the treatment of Alzheimer's disease, Medicinal Research Reviews 33 (2013) 139-189.

[10] E. Scarpini, P. Scheltens, H. Feldman, Treatment of Alzheimer's disease: current status and new perspectives, Lancet Neurology 2 (2003) 539-547.

[11] M. Citron, Alzheimer's disease: strategies for disease modification, Nature Reviews Drug Discovery 9 (2010) 387-398.

[12] L.L. Guo, Z.Z. Guan, Y. Huang, Y.L. Wang, J.S. Shi, The neurotoxicity of beta-amyloid peptide toward rat brain is associated with enhanced oxidative stress, inflammation and apoptosis, all of which can be attenuated by scutellarin, Experimental and Toxicologic Pathology 65 (2013) 579-584.

[13] J.T. Zhu, R.C. Choi, J. Li, H.Q. Xie, C.W. Bi, A.W. Cheung, T.T. Dong, Z.Y. Jiang, J.J. Chen, K.W. Tsim, Estrogenic and neuroprotective properties of scutellarin from Erigeron breviscapus: a drug against postmenopausal symptoms and Alzheimer's disease, Planta Medica 75 (2009) 1489-1493.

[14] H. Hong, G.Q. Liu, Protection against hydrogen peroxide-induced cytotoxicity in PC12 cells by scutellarin, Life Science 74 (2004) 2959-2973.

[15] L. Qian, M. Shen, H. Tang, Y. Tang, L. Zhang, Y. Fu, Q. Shi, N.G. Li, Synthesis and protective effect of scutellarein on focal cerebral ischemia/reperfusion in rats, Molecules 17 (2012) 10667-10674.

[16] X. Chen, L. Cui, X. Duan, B. Ma, D. Zhong, Pharmacokinetics and metabolism of the

flavonoid scutellarin in humans after a single oral administration, Drug Metabolism and Disposition 34 (2006) 1345-1352.

[17] C. Gao, X. Chen, D. Zhong, Absorption and disposition of scutellarin in rats: a pharmacokinetic explanation for the high exposure of its isomeric metabolite, Drug Metabolism and Disposition 39 (2011) 2034-2044.

[18] X. Qiang, Z. Sang, W. Yuan, Y. Li, Q. Liu, P. Bai, Y. Shi, W. Ang, Z. Tan, Y. Deng, Design, synthesis and evaluation of genistein-O-alkylbenzylamines as potential multifunctional agents for the treatment of Alzheimer's disease, European Journal of Medicinal Chemistry 76 (2014) 314-331.

[19] G.S. Mason, R. Hans, N.H. Max, 4',5,6,7-Oxygenated flavones and flavanones, Journal of Pharmaceutical Sciences 2 (1964) 192-195.

[20] C. Fruit, A. Turck, N. Ple, L. Mojovic, G. Queguiner, A new route to septorin via controlled metalations of pyrazines. Diazines XXX, Tetrahedron 57 (2001) 9429-9435.

[21] H. Tokunaru, K. Hiroki, T. Masao, M. Miisuo, N. Mtisuru, Studies of the selective O-alkylation and dealkylation of flavonoids. VII. Partial dealkylation of 5,6,7-trioxygenated flavones and synthesis of pectolinarigenin and its analogues, Yakugaku Zasshi 105 (1985) 2232-2239.

[22] M. Rosini, E. Simoni, A. Milelli, A. Minarini, C. Melchiorre, Oxidative stress in Alzheimer's disease: are we connecting the dots? Journal of Medicinal Chemistry 57 (2014) 2821-2831.

[23] D. Pratico, S. Sung, Lipid peroxidation and oxidative imbalance: early functional events in Alzheimer's disease, Journal of Alzheimer's Disease 6 (2004) 171-175.

[24] A. Davalos, C. Gomez-Cordoves, B. Bartolome, Extending applicability of the oxygen radical absorbance capacity (ORAC-fluorescein) assay, Journal of Agricultural and Food Chemistry 52 (2004) 48-54.

[25] G.L. Ellman, K.D. Courtney, V. Andres, Jr., R.M. Feather-Stone, A new and rapid colorimetric determination of acetylcholinesterase activity, Biochemical Pharmacology 7 (1961) 88-95.

[26] M. Rosini, E. Simoni, M. Bartolini, A. Cavalli, L. Ceccarini, N. Pascu, D.W. McClymont, A. Tarozzi, M.L. Bolognesi, A. Minarini, V. Tumiatti, V. Andrisano, I.R. Mellor, C. Melchiorre, Inhibition of acetylcholinesterase, beta-amyloid aggregation, and NMDA receptors in Alzheimer's disease: a promising direction for the multi-target-directed ligands gold rush, Journal of Medicinal Chemistry 51 (2008) 4381-4384.

[27] Y. He, P.F. Yao, S.B. Chen, Z.H. Huang, S.L. Huang, J.H. Tan, D. Li, L.Q. Gu, Z.S. Huang, Synthesis and evaluation of 7,8-dehydrorutaecarpine derivatives as potential multifunctional agents for the treatment of Alzheimer's disease, European Journal of Medicinal Chemistry 63 (2013) 299-312.

[28] L. Pezzementi, K. Johnson, I. Tsigelny, J. Cotney, E. Manning, A. Barker, S. Merritt, Amino acids defining the acyl pocket of an invertebrate cholinesterase, Comparative biochemistry and physiology. Part B, Biochemistry & Molecular Biology 136 (2003) 813-832.

[29] W. Xing, Y. Fu, Z. Shi, D. Lu, H. Zhang, Y. Hu, Discovery of novel 2,6-disubstituted pyridazinone derivatives as acetylcholinesterase inhibitors, European Journal of Medicinal Chemistry 63 (2013) 95-103.

[30] R. Squitti, C. Salustri, Agents complexing copper as a therapeutic strategy for the treatment of Alzheimer's disease, Current Alzheimer Research 6 (2009) 476-487.

[31] X. Huang, M.P. Cuajungco, C.S. Atwood, M.A. Hartshorn, J.D. Tyndall, G.R. Hanson, K.C. Stokes, M. Leopold, G. Multhaup, L.E. Goldstein, R.C. Scarpa, A.J. Saunders, J. Lim, R.D. Moir, C. Glabe, E.F. Bowden, C.L. Masters, D.P. Fairlie, R.E. Tanzi, A.I. Bush, Cu(II) potentiation of alzheimer abeta neurotoxicity. Correlation with cell-free hydrogen peroxide production and metal reduction, Journal of Biological Chemistry 274 (1999) 37111-37116.

[32] P. Camps, X. Formosa, C. Galdeano, D. Munoz-Torrero, L. Ramirez, E. Gomez, N. Isambert, R. Lavilla, A. Badia, M.V. Clos, M. Bartolini, F. Mancini, V. Andrisano, M.P. Arce, M.I. Rodriguez-Franco, O. Huertas, T. Dafni, F.J. Luque, Pyrano[3,2-c]quinoline-6-chlorotacrine hybrids as a novel family of acetylcholinesterase- and beta-amyloid-directed anti-Alzheimer

compounds, Journal of Medicinal Chemistry 52 (2009) 5365-5379.

[33] M.L. Bolognesi, V. Andrisano, M. Bartolini, R. Banzi, C. Melchiorre, Propidium-based polyamine ligands as potent inhibitors of acetylcholinesterase and acetylcholinesterase-induced amyloid-beta aggregation, Journal of Medicinal Chemistry 48 (2005) 24-27.

[34] A. Alvarez, C. Opazo, R. Alarcon, J. Garrido, N.C. Inestrosa, Acetylcholinesterase promotes the aggregation of amyloid-beta-peptide fragments by forming a complex with the growing fibrils, Journal of Molecular Biology 272 (1997) 348-361.

[35] S.S. Hindo, A.M. Mancino, J.J. Braymer, Y. Liu, S. Vivekanandan, A. Ramamoorthy, M.H. Lim, Small molecule modulators of copper-induced Abeta aggregation, Journal of the American Chemical Society 131 (2009) 16663-16665.

[36] M.I. Fernandez-Bachiller, C. Perez, N.E. Campillo, J.A. Paez, G.C. Gonzalez-Munoz, P. Usan, E. Garcia-Palomero, M.G. Lopez, M. Villarroya, A.G. Garcia, A. Martinez, M.I. Rodriguez-Franco, Tacrine-melatonin hybrids as multifunctional agents for Alzheimer's disease, with cholinergic, antioxidant, and neuroprotective properties, ChemMedChem 4 (2009) 828-841.

[37] W. Yuan, Z.P. Sang, X.M. Qiang, Z.H. Tan, Y. Deng, Synthesis of pterostilbene and resveratrol carbamate derivatives as potential dual cholinesterase inhibitors and neuroprotective agents, Research on Chemical Intermediates 40 (2014) 787-800**.**

[38] M.A. Abd-El-Fattah, N.F. Abdelakader, H.F. Zaki, Pyrrolidine dithiocarbamate protects against scopolamine-induced cognitive impairment in rats, European Journal of Pharmacology, 723 (2014) 330-338.

[39] S.H. Kwon, H.K. Lee, J.A. Kim, S.I. Hong, H.C. Kim, T.H. Jo, Y.I. Park, C.K. Lee, Y.B. Kim, S.Y. Lee, C.G. Jang, Neuroprotective effects of chlorogenic acid on scopolamine-induced amnesia via anti-acetylcholinesterase and anti-oxidative activities in mice, European Journal of Pharmacology, 649 (2010) 210-217.

[40] E.J. Kim, I.H. Jung, T.K. Van Le, J.J. Jeong, N.J. Kim, D.H. Kim, Ginsenosides Rg5 and Rh3

protect scopolamine-induced memory deficits in mice, Journal of Ethnopharmacology, 146 (2013) 294-299.

[41] H. Zheng, M.B. Youdim, M. Fridkin, Selective acetylcholinesterase inhibitor activated by acetylcholinesterase releases an active chelator with neurorescuing and anti-amyloid activities, ACS Chemical Neuroscience, 1 (2010) 737-746.

[42] M. Bartolini, C. Bertucci, M.L. Bolognesi, A. Cavalli, C. Melchiorre, V. Andrisano, Insight into the kinetic of amyloid beta (1-42) peptide self-aggregation: elucidation of inhibitors' mechanism of action, ChemBioChem 8 (2007) 2152-2161.

[43] R. Gupta, L.K. Gupta, P.K. Mediratta, S.K. Bhattacharya, Effect of resveratrol on scopolamine-induced cognitive impairment in mice, Pharmacological Reports 64 (2012) 438-444.

Table, Scheme, and Figures Legends

Table 1. Oxygen radical absorbance capacity (ORAC, Trolox equivalents) and AChE and BuChE inhibitory activities by scutellarein-*O*-alkylamines, scutellarein, rivastigmine and donepezil.

Table 2. Inhibition of *Hu*AChE, self-induced A$\beta_{1\text{-}42}$ aggregation, Cu^{2+}-induced A$\beta_{1\text{-}42}$ aggregation, *Hu*AChE-induced A$\beta_{1\text{-}40}$ aggregation and disaggregating Cu^{2+}-induced A$\beta_{1\text{-}42}$ aggregation by selected compounds and reference compounds.

Table 1.

Compd	R	Position	n	NR_1R_2	ORAC[b]	IC_{50} ± SD[a] (μM)			Selectivity Index[f]
						*Rat*AChE[c]	*Rat*BuChE[d]	*Ee*AChE[e]	
15a	CH_3	4'	3	**A**	0.42	2.62±0.06	135.7±0.87	11.53±0.06	51.8
15b	CH_3	4'	3	**B**	0.40	2.04±0.07	81.3±0.26	7.30±0.04	39.9
15c	CH_3	4'	3	**C**	0.18	1.76±0.01	107.6±0.91	8.60±0.05	61.1
15d	CH_3	4'	3	**D**	0.27	0.17±0.01	74.2±0.33	0.72±0.01	436.5
15e	CH_3	4'	3	**E**	0.33	1.80±0.07	>500	8.70±0.05	>277.8
15f	CH_3	4'	3	**F**	0.24	8.30±0.16	>500	34.67±0.23	>60.2
15g	CH_3	4'	4	**A**	0.45	1.43±0.11	85.9±0.68	6.20±0.02	60.1
15h	CH_3	4'	4	**B**	0.15	0.80±0.02	40.8± 0.19	3.07±0.02	51.0
15i	CH_3	4'	4	**C**	0.30	0.57±0.01	96.2±0.96	2.27±0.04	168.8
15j	CH_3	4'	4	**D**	0.21	0.12±0.01	68.2±0.56	0.62±0.02	568.3
15k	CH_3	4'	4	**E**	0.18	2.56±0.07	130.8±1.02	8.53±0.03	51.1
15l	CH_3	4'	4	**F**	0.54	1.07±0.03	146.1±1.32	5.27±0.03	136.5
15m	CH_3	4'	6	**A**	0.27	0.99±0.02	84.6±0.39	5.40±0.03	85.5
15n	CH_3	4'	6	**B**	0.32	0.34±0.01	>500	2.83±0.03	>1470.6
15o	CH_3	4'	6	**C**	0.44	0.45±0.01	96.1±0.66	2.23±0.02	213.6
15p	CH_3	4'	6	**D**	0.24	0.21±0.01	61.2±0.34	1.50±0.01	291.4
15q	CH_3	4'	6	**E**	0.18	8.07±0.23	>500	26.5±0.14	>62.0
16a	H	4'	3	**C**	0.51	5.00±0.09	>500	31.07±0.20	>100.0
16b	H	4'	3	**D**	0.47	2.13±0.02	>500	12.00±0.04	>234.7
16c	H	4'	4	**C**	0.54	3.43±0.04	>500	14.40±0.02	>145.8
16d	H	4'	4	**D**	0.84	0.62±0.01	62.0±0.72	0.85±0.02	100.0
16e	H	4'	6	**C**	0.33	5.07±0.06	>500	22.63±0.17	>98.6
16f	H	4'	6	**D**	0.50	1.19±0.02	>500	2.91±0.04	>420.2
17a	CH_3	3'	2	**A**	0.36	9.20±0.13	87.9±0.34	35.67±0.31	9.6
17b	CH_3	3'	2	**B**	0.41	3.37±0.07	79.6±0.28	3.80±0.01	23.6
17c	CH_3	3'	2	**C**	0.18	3.22±0.23	31.4±0.17	2.49±0.04	9.8
17d	CH_3	3'	2	**E**	0.48	1.18±0.02	>500	2.91±0.04	>423.7
17e	CH_3	3'	2	**F**	0.27	8.20±0.18	>500	22.47±0.11	>61.0
17f	CH_3	3'	3	**A**	0.39	5.17±0.07	117.3±1.12	25.00±0.21	22.7

17g	CH_3	3’	3	**B**	0.80	5.40±0.15	101.2±0.78	20.43±0.12	18.7
17h	CH_3	3’	3	**C**	0.36	0.38±0.01	75.4±0.21	1.59±0.02	198.4
17i	CH_3	3’	3	**D**	0.20	0.33±0.02	77.2±0.35	1.78±0.01	233.9
17j	CH_3	3’	3	**E**	0.24	3.12±0.05	148.7±1.35	1.59±0.02	47.7
17k	CH_3	3’	3	**F**	0.41	7.47±0.16	>500	35.17±0.45	>66.9
17l	CH_3	3’	4	**A**	0.38	4.53±0.09	90.7±0.63	18.43±0.09	20.0
17m	CH_3	3’	4	**B**	0.15	2.35±0.04	63.4±0.42	8.30±0.05	27.0
17n	CH_3	3’	4	**C**	0.12	2.61±0.03	85.0±0.25	12.23±0.04	32.6
17o	CH_3	3’	4	**D**	0.18	0.80±0.01	78.3±0.33	2.37±0.02	97.9
17p	CH_3	3’	4	**E**	0.23	4.03±0.33	108.8±0.79	25.27±0.08	27.0
17q	CH_3	3’	4	**F**	0.27	0.25±0.01	>500	1.15±0.01	>2000
17r	CH_3	3’	6	**A**	0.23	2.13±0.02	78.7±0.15	6.13±0.02	36.9
17s	CH_3	3’	6	**B**	0.30	2.03±0.03	52.1±0.26	12.23±0.05	25.7
17t	CH_3	3’	6	**C**	0.23	0.96±0.01	60.7±0.18	4.50±0.03	63.2
17u	CH_3	3’	6	**D**	0.27	0.22±0.01	41.6±0.11	1.30±0.01	189.1
17v	CH_3	3’	6	**E**	0.23	7.33±0.08	>500	21.40±0.06	>68.2
18a	H	3’	3	**C**	0.77	8.10±0.19	354.0±2.23	28.57±0.03	43.7
18b	H	3’	3	**D**	0.34	1.58±0.03	240.0±1.47	4.50±0.03	151.9
18c	H	3’	4	**C**	0.42	7.73±0.11	>500	31.03±0.11	>64.7
18d	H	3’	4	**D**	0.69	2.40±0.03	>500	7.97±0.04	>208.3
18e	H	3’	6	**C**	0.27	1.59±0.05	404.0±2.71	5.80±0.02	254.1
18f	H	3’	6	**D**	0.68	1.27±0.01	484.0±3.11	0.77±0.01	381.1
Scutellarein					10.0	>500	>500	NT [g]	
Rivastigmine					NT [g]	21.0±0.24	13.7±0.12	NT [g]	0.65
Donepezil					NT [g]	0.015±0.002	20.7±0.36	0.11±0.003	1380

[a] Values are expressed as the mean ± standard deviation of the mean of 3 independent experiments in triplicate. [b] Results are expressed as μM of Trolox equivalent/μM of tested compound. [c] From 5% rat cortex homogenate. [d] BuChE from rat serum. [e] From *electrophorus electricusc.* [f] selectivity index = IC_{50} (*Rat*BuChE)/IC_{50} (*Rat*AChE). [g] NT = not tested.

Table 2.

Comp.	IC_{50} (μM) [g] *Hu*AChE [a]	% Inhibition of Aβ Aggregation [b, g]			Disaggregating (%) [f]
		Self-induced [c]	Cu^{2+}-induced [d]	*Hu*AChE -Induced [e]	
15d	0.20± 0.01	32.1± 2.8	44.7± 1.1	NT [h]	NT [h]
15g	0.95± 0.06	35.4± 1.6	48.2± 3.2	NT [h]	NT [h]
15h	1.36± 0.11	31.3± 2.7	43.1± 1.8	NT [h]	NT [h]
15i	0.50± 0.02	37.1± 1.3	46.2± 1.3	NT [h]	NT [h]
15j	0.08± 0.003	34.3± 2.2	46.8± 1.5	37.0± 2.6	41.3± 1.7
15p	0.43± 0.02	35.6± 1.8	49.2± 1.2	NT [h]	NT [h]
16b	0.90±0.02	66.5± 1.1	84.8± 1.1	NT [h]	NT [h]
16d	0.25± 0.03	43.5±0.8 (12.5μM) 69.1±1.8 (25.0μM) 87.2±2.6 (50.0μM)	46.5±3.5 (5μM) 64.6±1.2 (10μM) 85.7±2.5 (25μM)	62.2± 1.8	81.3± 3.4
16f	2.00± 0.08	71.4± 2.3	87.2± 1.7	NT [h]	NT [h]
Curcumin	NT [h]	43.1 ± 1.1	58.0 ± 2.3	NT [h]	56.5± 2.1
Donepezil	0.012± 0.002	< 5.0	< 5.0	18.8± 1.6	NT [h]

[a] From human erythrocytes. [b] For inhibition of Aβ aggregation, the thioflavin-T fluorescence method was used. [c] Inhibition of self-induced $A\beta_{1\text{-}42}$ aggregation, the concentration of tested compounds and $A\beta_{1\text{-}42}$ were 25μM. [d] Inhibition of Cu^{2+}-induced $A\beta_{1\text{-}42}$ aggregation produced by tested compounds at 25 μM. [e] Inhibition of human AChE-induced $A\beta_{1\text{-}40}$ aggregation. The concentration of tested compounds and $A\beta_{1\text{-}40}$ was 100 and 230 μM, respectively, and the $A\beta_{1\text{-}40}$/*Hu*AChE ratio was equal to 100/1. [f] Disaggregating Cu^{2+}-induced $A\beta_{1\text{-}42}$ aggregation. The concentration of tested inhibitors and $A\beta_{1\text{-}42}$ were 25μM. [g] Data are presented as the mean ± SEM of three independent experiments. [h] NT=not tested.

Scheme 1. Synthesis of scutellarein-*O*-alkylamines **15-18**. *Reagents and conditions:* (a) *p*-MOMO-PhCHO (**2**) or *m*-HO-PhCHO (**3**), KOH, EtOH, at room temperature (r.t.), for 3 days; (b) 10% HCl, ethanol, at 50°C, for 4 h; (c) KI, *conc.* H_2SO_4, DMSO, at 100°C, for 3–5 h; (d) anhydrous $AlCl_3$, CH_3CN, at 55–60°C, for 1 h; (e) $Br(CH_2)_nBr$ (**9**), K_2CO_3, CH_3CN, at 60–65 °C for 8–10 h; (f) R_1R_2NH (**14**), K_2CO_3, CH_3CN, at 60–65°C, for 12–15 h.

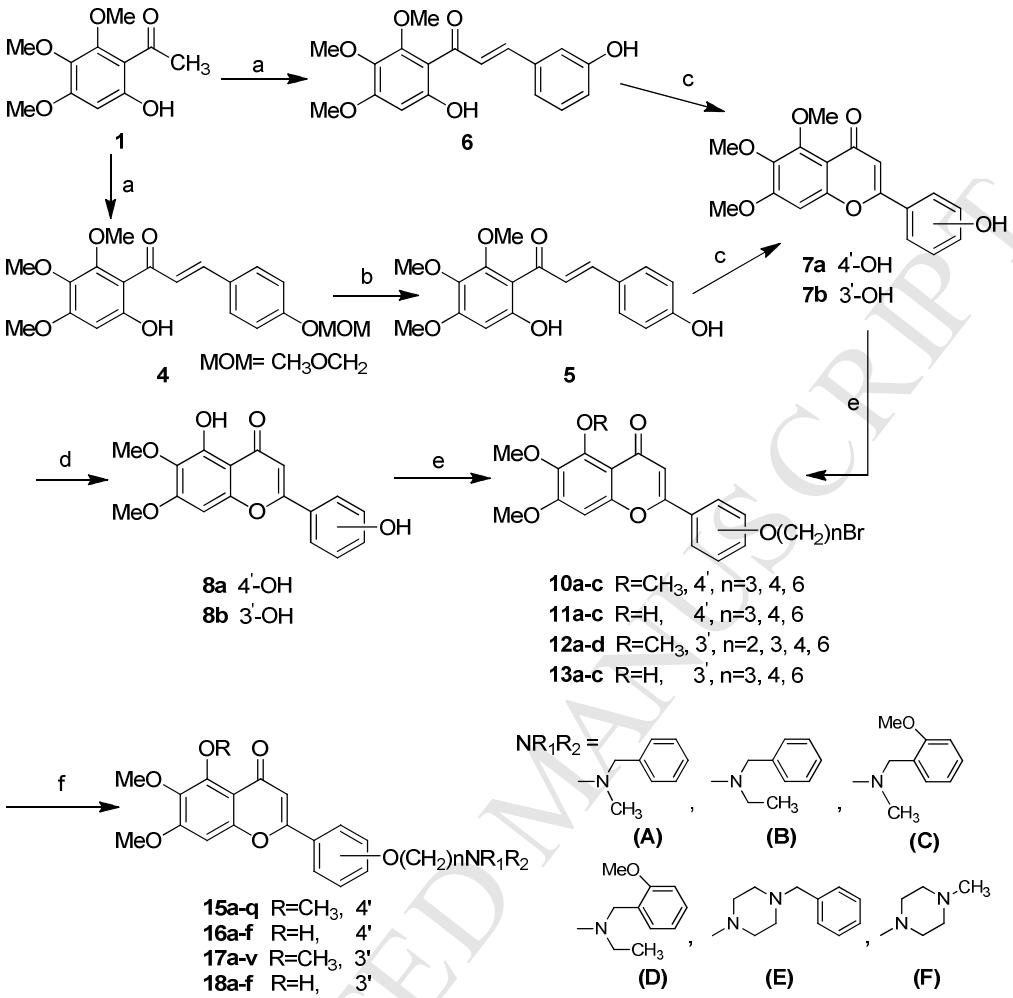

Scheme 1.

Figure 1. Design strategy for the scutellarein-*O*-alkylamine derivatives.

Figure 2. Effects of substituted at flavonoid nucleus 5 position on anti-AChE activities.

Figure 3. Kinetic study on the mechanism of *Ee*AChE inhibition by compound **16d**. Overlaid Lineweaver-Burk reciprocal plots of AChE initial velocity at increasing substrate concentration (0.1-0.4mM) in the absence of inhibitor and in the presence of **16d** are shown. Lines were derived from a weighted least-squares analysis of data points. The experimental data are the means ± SD of three independent experiments.

Figure 4. Docking models of the compounds with *Tc*AChE (PDB code: *1EVE*) complex. (**A**) **16d**-*Tc*AChE complex. (**B**) **15j**-*Tc*AChE complex. Compound (coloured by atom type) interacting with residues in the binding site of *Tc*AChE, highlighting the protein residues that participate in the main interactions with the inhibitor.

Figure 5. The UV spectrum of compound **16d** (37.5 μM, in methanol) alone or in the presence of $CuCl_2$, $FeSO_4$, $ZnCl_2$ and $AlCl_3$ (37.5 μM, in methanol).

Figure 6. Determination of the stoichiometry of complex-Cu^{2+} by using molar ratio method through titrating the methanol solution of compound **16d** with ascending amounts of $CuCl_2$. The final concentration of tested compound was 37.5 μM, and the final concentration of Cu^{2+} ranged from 7.5 to 93.75 μM.

Figure 7. Visualization of A*β* species from inhibition experiments: (top) scheme of the inhibition experiment; (bottom) TEM images of samples.

Figure 8. Visualization of A*β* species from disaggregation experiments: (top) scheme of the disaggregation experiments; (bottom) TEM images of samples.

Figure 9. Effects of **15j** and **16d** on cell viability in human SH-SY5Y cells. Data are mean values ± SEM of three independent experiments.

Figure 10. Protective effects of **15**j and **16d** on cell injury induced by hydrogen peroxide (100 μM)

in PC12 cells. $^{\#\#}P < 0.01$ *vs* control; $^{*}P < 0.05$ *vs* H_2O_2 group and $^{**}P < 0.01$ *vs* H_2O_2 group.

Figure 11. Effects of compound **16d** on scopolamine-induced memory deficit in the step-down passive avoidance test. Compounds **16d** (0.66, 2.2, 6.6 and 19.8 mg/kg, *p.o.*) or donepezil (0.5 and 5.0 mg/kg, *p.o.*) were orally given 1 h before treatment with scopolamine. After 30 min, the mice were treated with scopolamine (1 and 3 mg/kg, *i.p.*) and tested in the step-down passive avoidance. Values are expressed as the mean ± SEM (n=10). $^{\#\#}P < 0.01$ *vs* normal group. $^{*}P < 0.05$ and $^{**}P < 0.01$ *vs* scopolamine-treated control group.

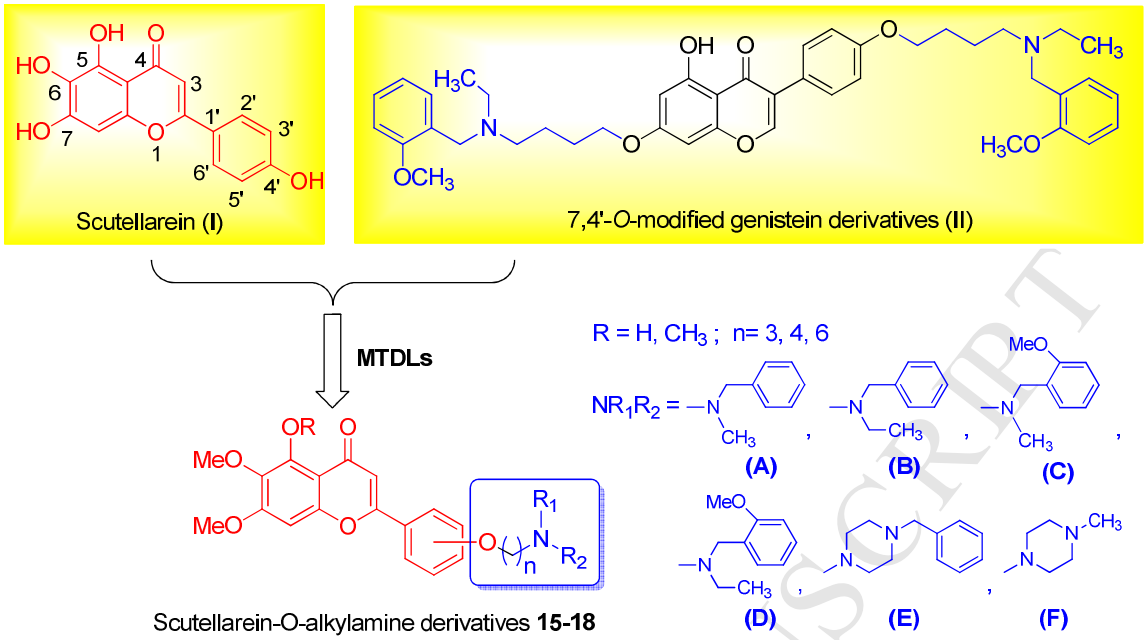

Figure 1

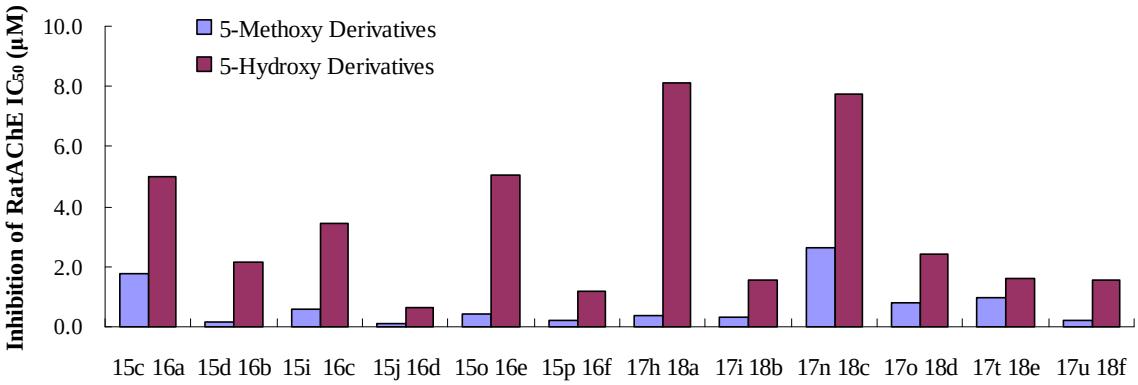

Figure 2

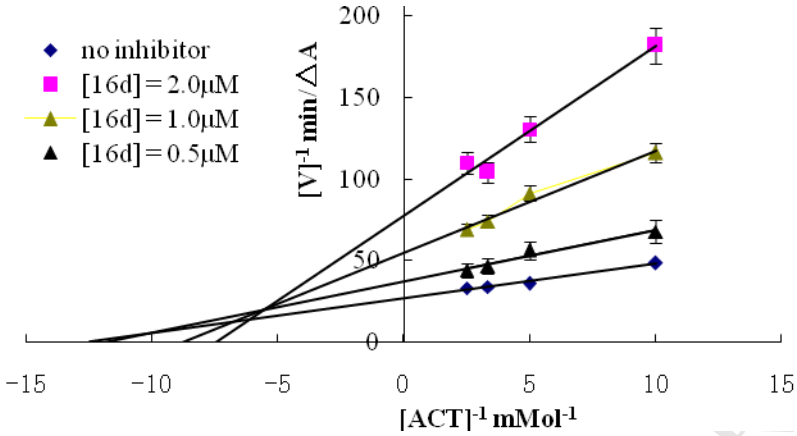

Figure 3

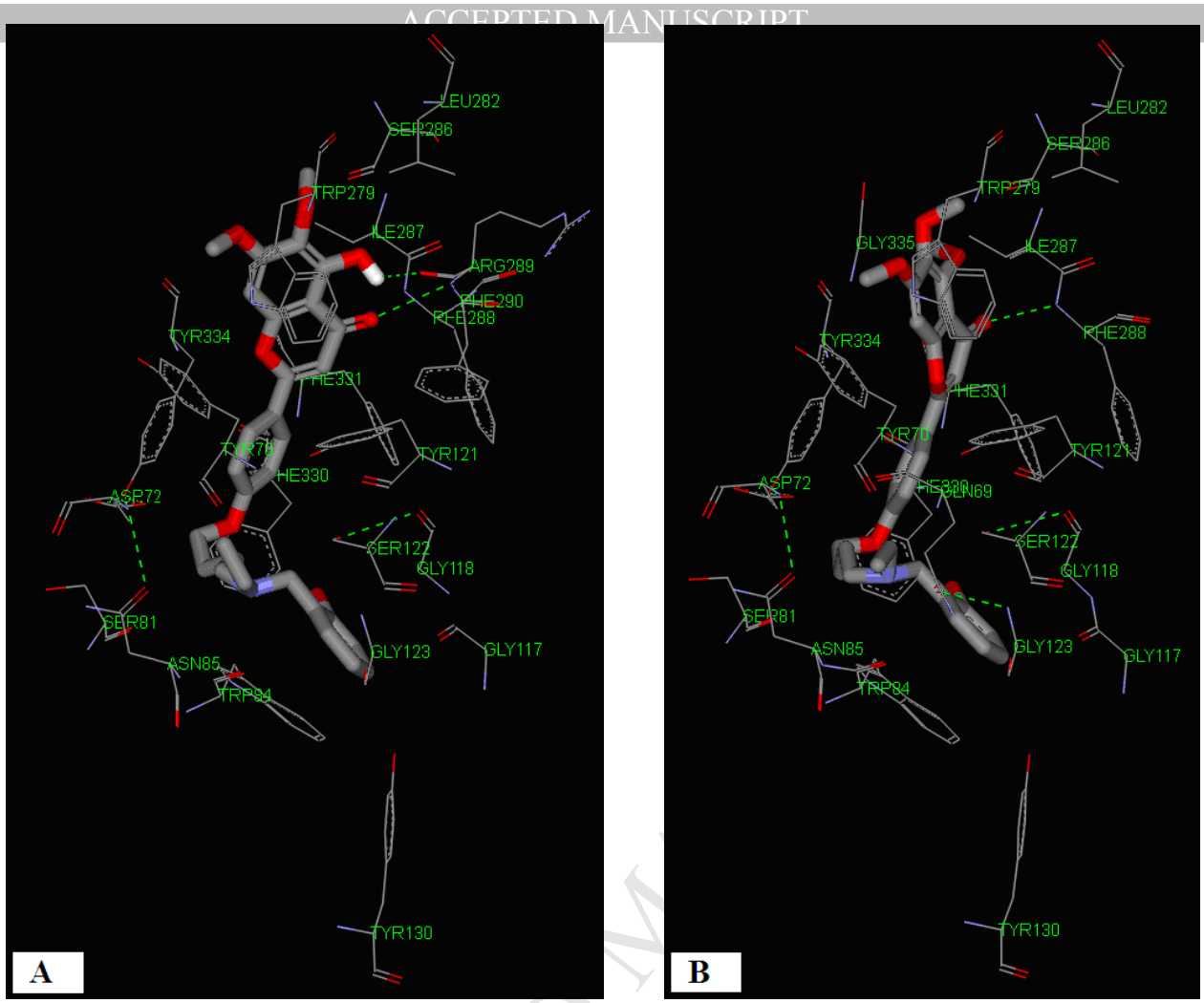

Figure 4

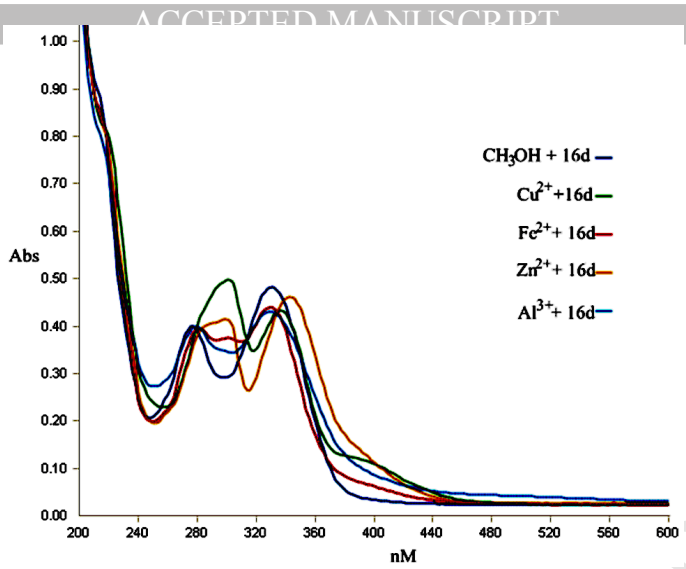

Figure 5

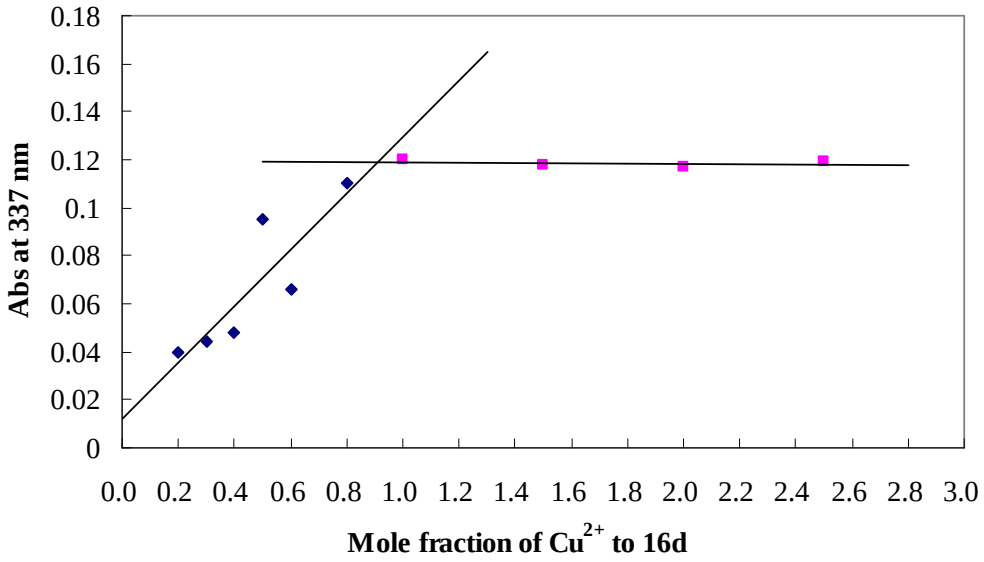

Figure 6

Inhibition experiment

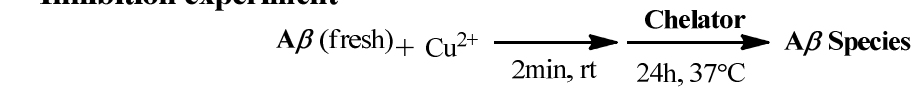

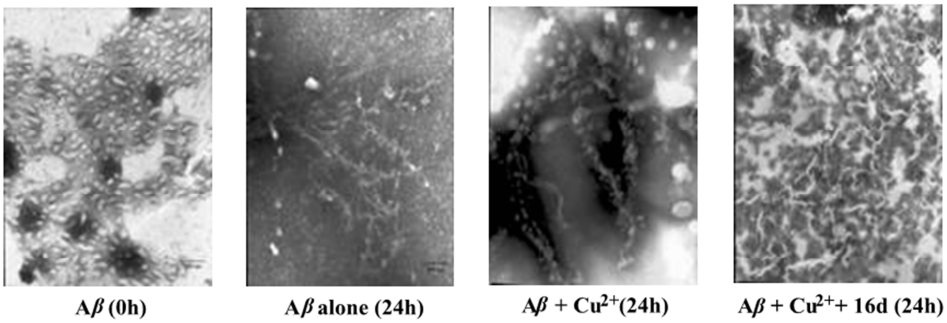

Figure 7

Disaggregation experiment

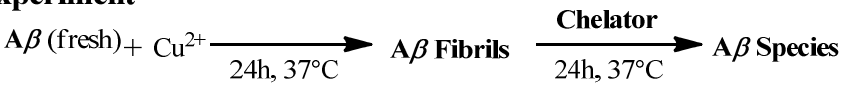

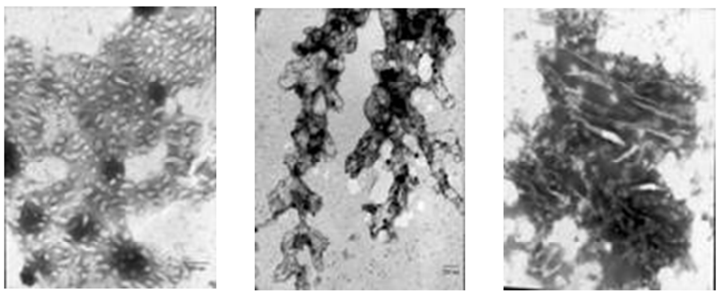

Figure 8

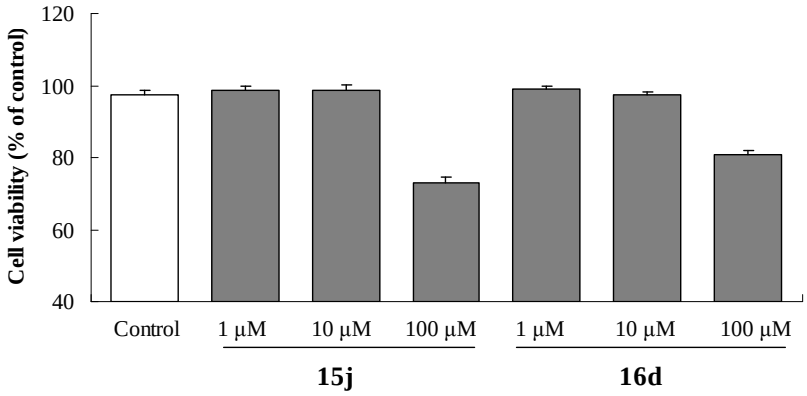

Figure 9

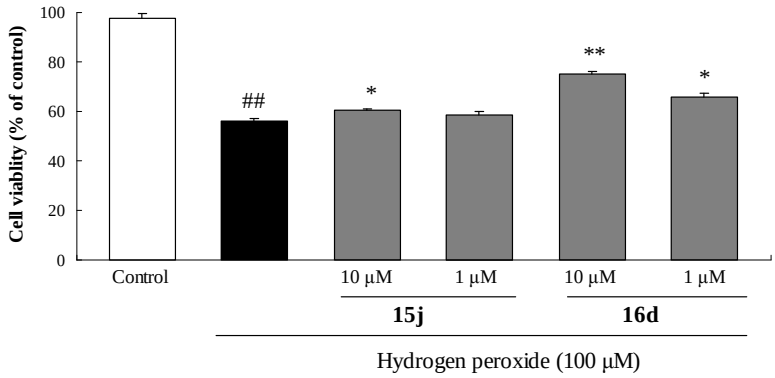

Figure 10

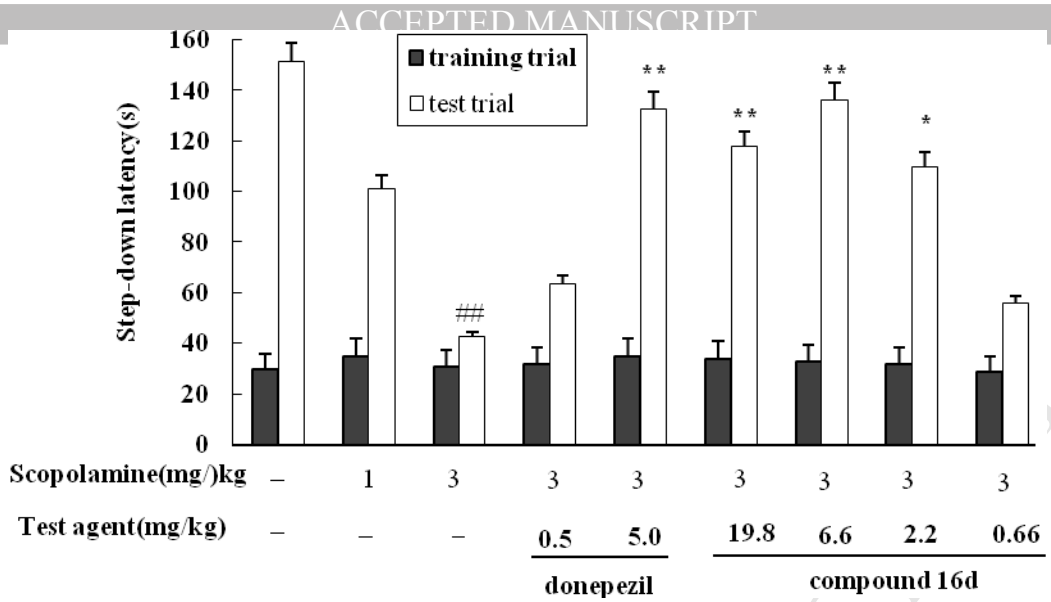

Figure 11

Highlights

- Novel scutellarein derivatives with carbon spacer-linked alkylamines were synthesized.
- Compound **16d** exhibited good acetylcholinesterase inhibitory and antioxidant activity.
- Compound **16d** exhibited excellent inhibitory effects on Aβ aggregation.
- Compound **16d** markedly disassembled the Cu^{2+}-induced Aβ aggregation.
- **16d** showed neuroprotective effects and reversed scopolamine-induced memory deficit in mice.

Supporting Information

Design, synthesis and evaluation of scutellarein-*O*-alkylamines as multifunctional agents for the treatment of Alzheimer's disease

Zhipei Sang[1,#], Xiaoming Qiang[1,#], Yan Li[1], Wen Yuan[1], Qiang Liu[1], Yikun Shi[3], Wei Ang[1], Youfu Luo[2], Zhenghuai Tan[3,] and Yong Deng[1,*]*

[1]Department of Medicinal Chemistry, Key Laboratory of Drug Targeting and Drug Delivery System of the Education Ministry, West China School of Pharmacy, Sichuan University, Chengdu, 610041, China

[2]State Key Laboratory of Biotherapy, West China Hospital, West China Medical School, Sichuan University, Chengdu, 610041, China

[3]Institute of Traditional Chinese Medicine Pharmacology and Toxicology, Sichuan Academy of Chinese Medicine Sciences, Chengdu, 610041, China

Table of Contents

SI 1. Metal-chelating properties of target compound 15j.

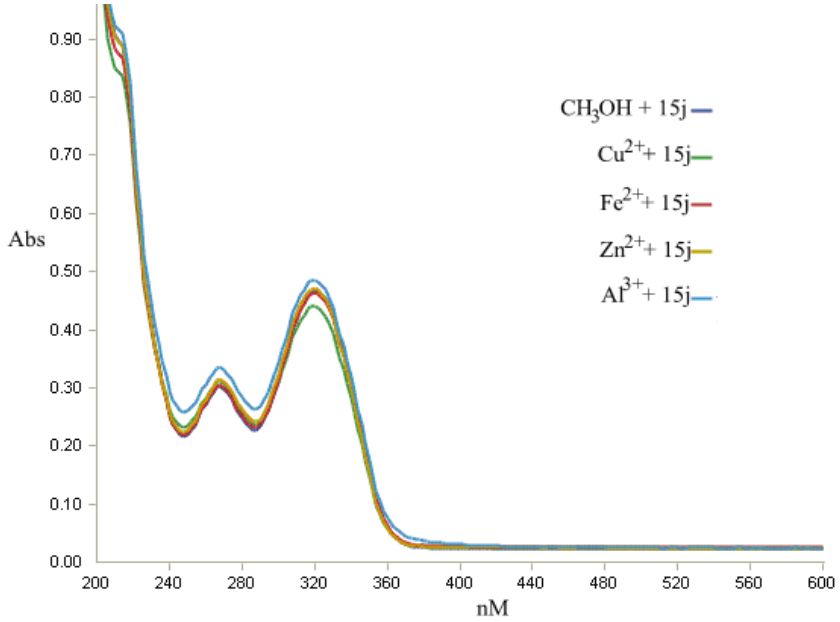

SI 2. The ^{1}HNMR and ^{13}CNMR spectra of target compound 15-18.

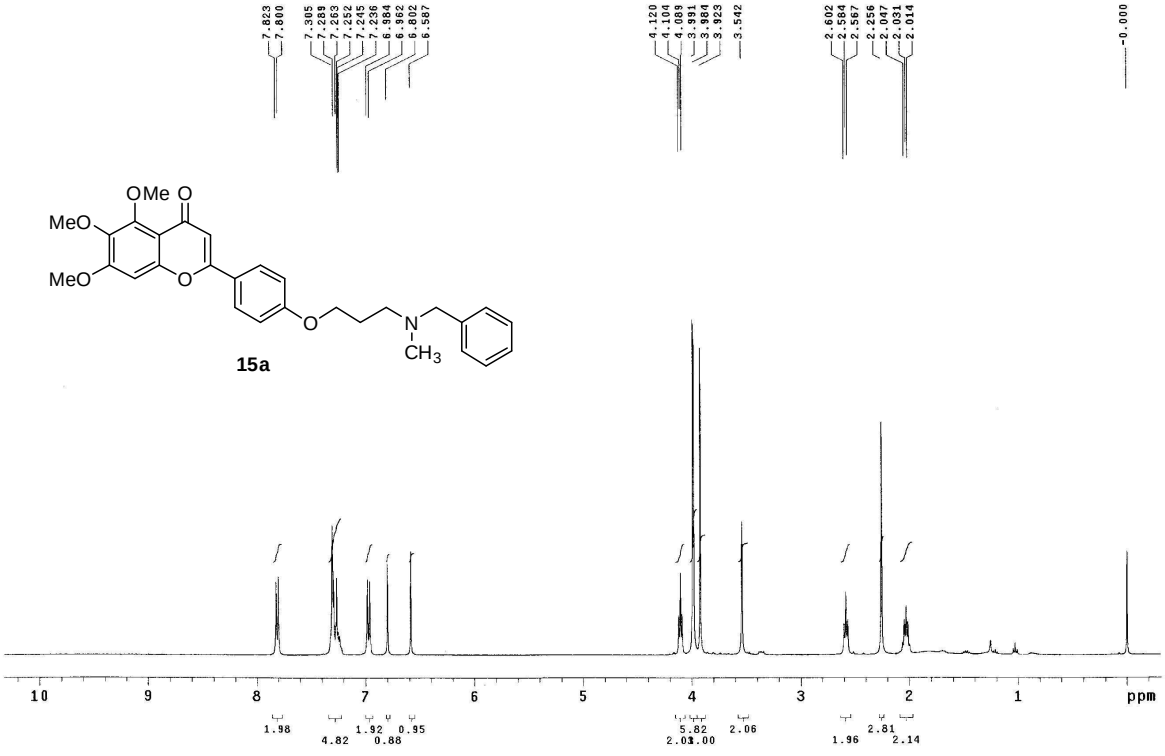

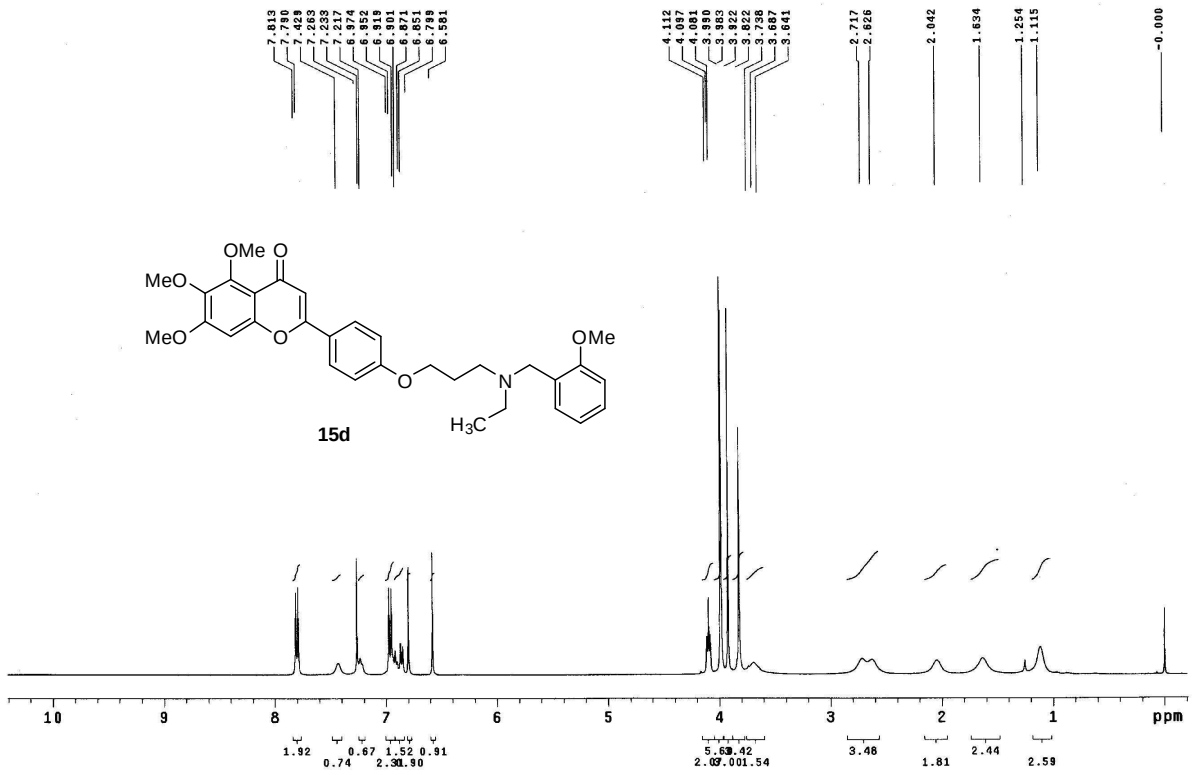
OMe O
MeO
MeO
O
O
N
OMe
H3C
15d
ppm

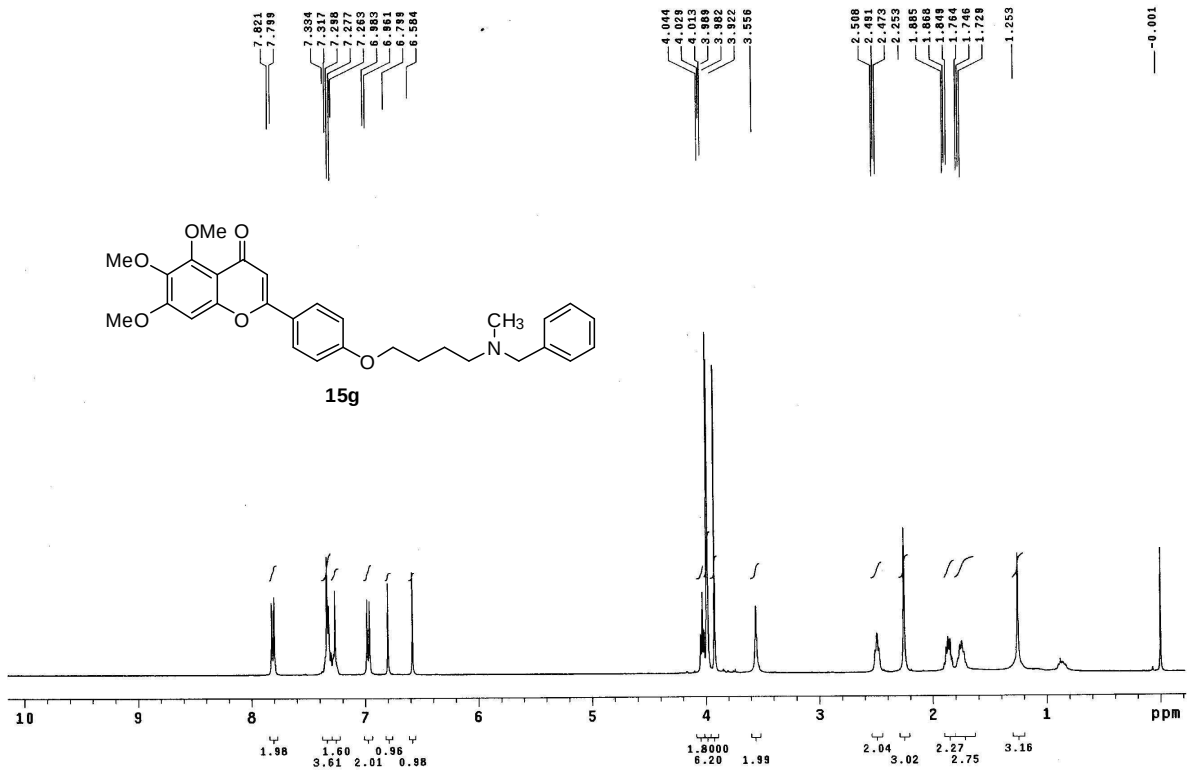
OMe O
MeO
MeO
O
O
N
CH3
15g
ppm

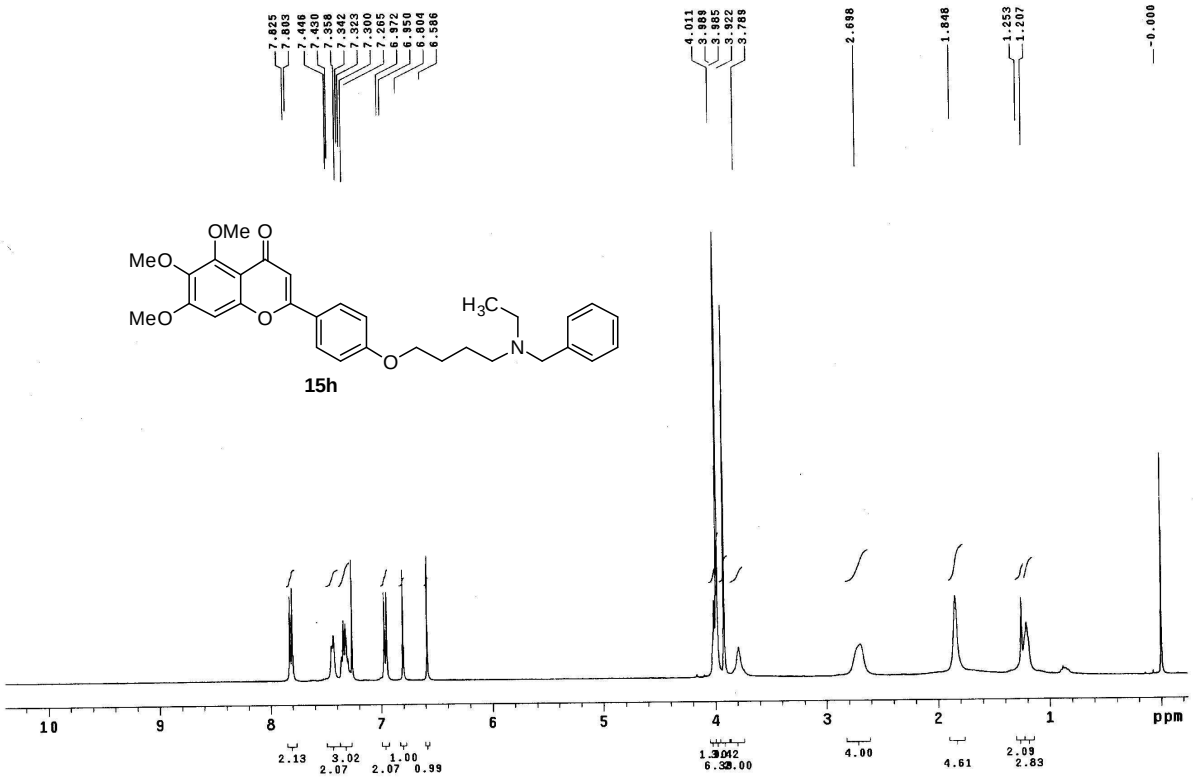
7.825
7.803
7.446
7.430
7.358
7.342
7.323
7.300
7.265
6.972
6.950
6.804
6.586
4.011
3.988
3.985
3.922
3.788
2.698
1.848
1.253
1.207
-0.000
OMe O
MeO
MeO
O
H3C
N
O
15h
10
9
8
7
6
5
4
3
2
1
ppm
2.13
3.02
2.07
1.00
2.07
0.99
4.00
4.61
2.09
2.83

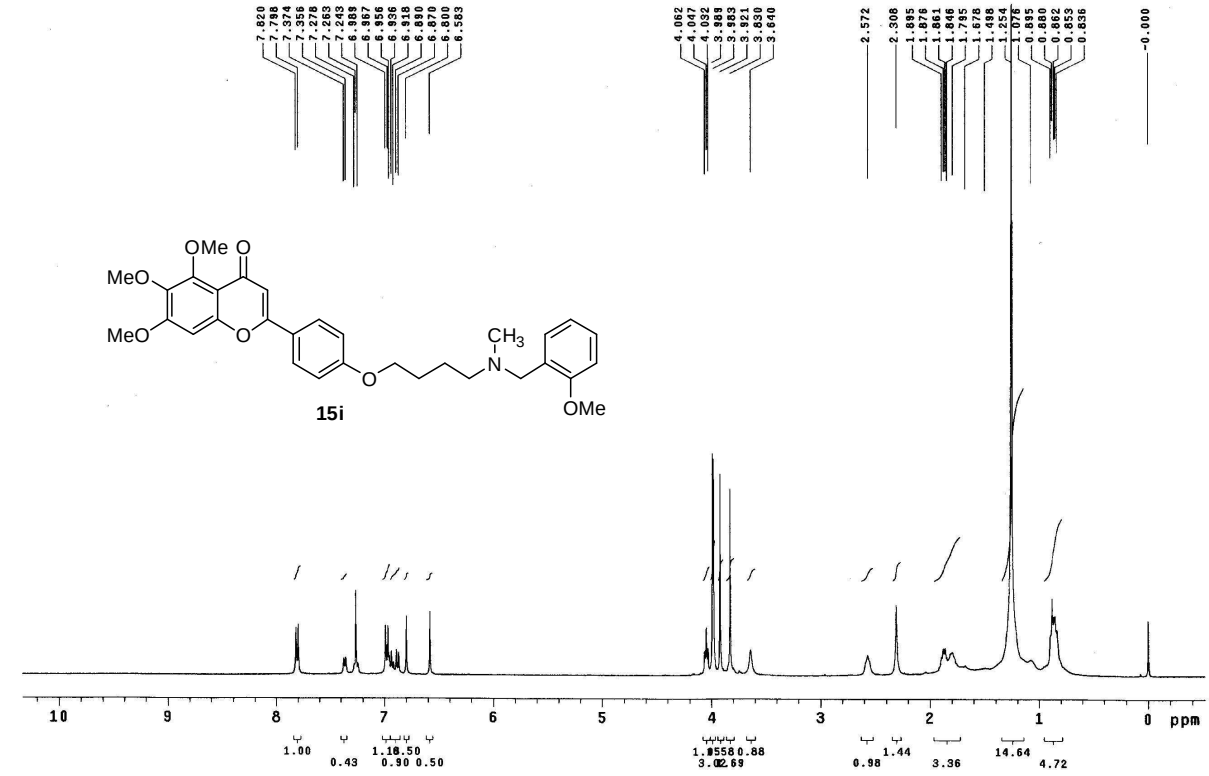
7.820
7.798
7.374
7.356
7.278
7.263
7.243
6.989
6.967
6.956
6.936
6.918
6.880
6.870
6.800
6.583
4.062
4.047
4.032
3.983
3.921
3.830
3.640
2.572
2.306
1.895
1.878
1.861
1.846
1.795
1.678
1.498
1.254
1.076
0.895
0.880
0.862
0.853
0.836
-0.000
OMe O
MeO
MeO
O
CH3
N
O
OMe
15i
10
9
8
7
6
5
4
3
2
1
0
ppm
1.00
0.43
1.10
0.90
0.50
0.88
0.98
1.44
3.36
14.64
4.72

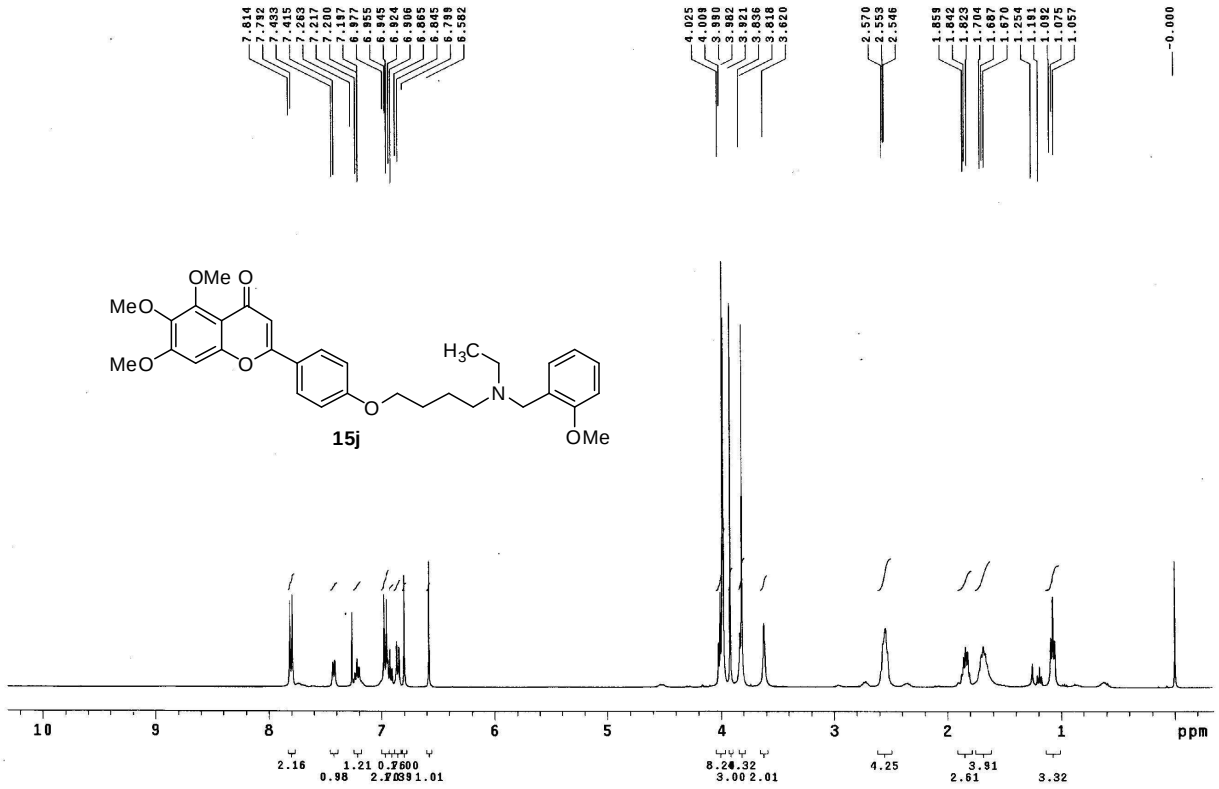
7.814
7.792
7.433
7.415
7.263
7.217
7.200
7.197
6.977
6.955
6.945
6.924
6.906
6.865
6.845
6.799
6.582
4.025
4.008
3.990
3.982
3.821
3.836
3.818
3.620
2.570
2.553
2.546
1.859
1.842
1.823
1.704
1.687
1.670
1.254
1.191
1.092
1.075
1.057
-0.000
OMe O
MeO
MeO
O
H3C
N
O
OMe
15j
10
9
8
7
6
5
4
3
2
1
ppm
2.16
1.21
0.98
8.24
4.32
3.00
2.01
4.25
3.91
2.61
3.32

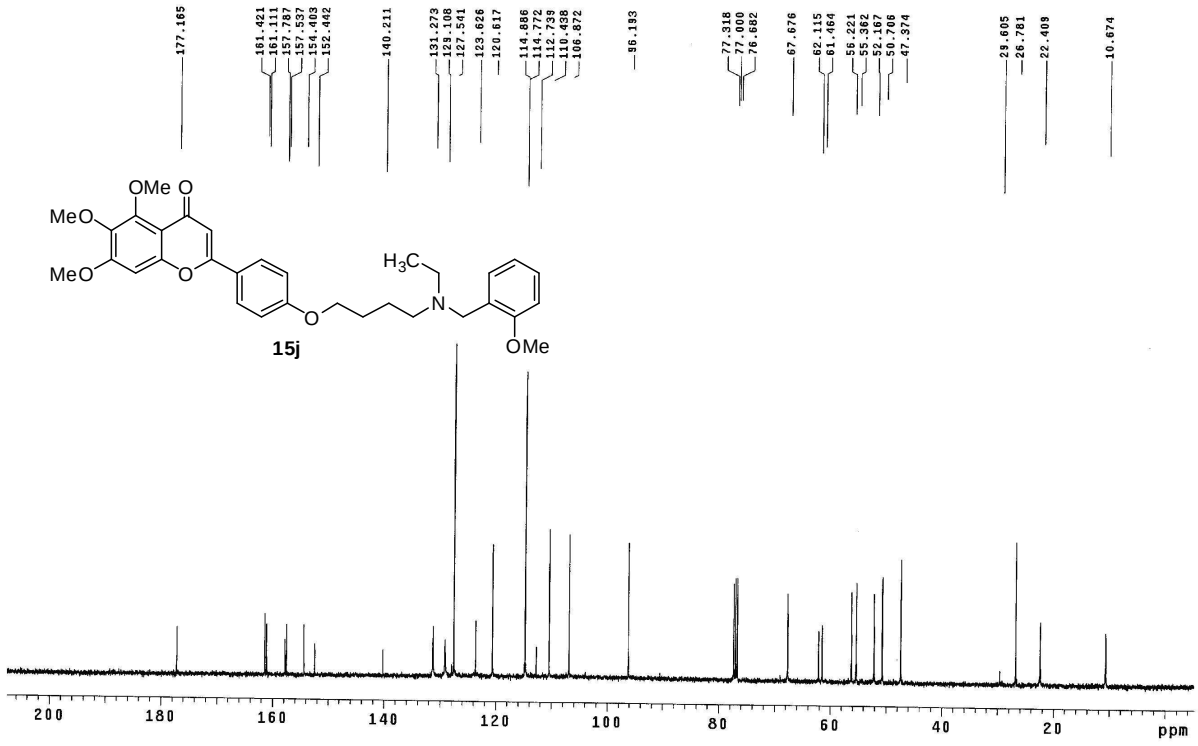
177.165
161.421
161.111
157.787
157.537
154.493
152.492
140.211
131.273
129.108
127.541
123.626
120.617
114.886
114.772
112.738
110.438
106.872
96.193
77.318
77.000
76.682
67.676
62.115
61.464
56.221
55.362
52.167
50.706
47.374
29.605
26.781
22.409
10.674
OMe O
MeO
MeO
O
H3C
N
O
OMe
15j
200
180
160
140
120
100
80
60
40
20
ppm

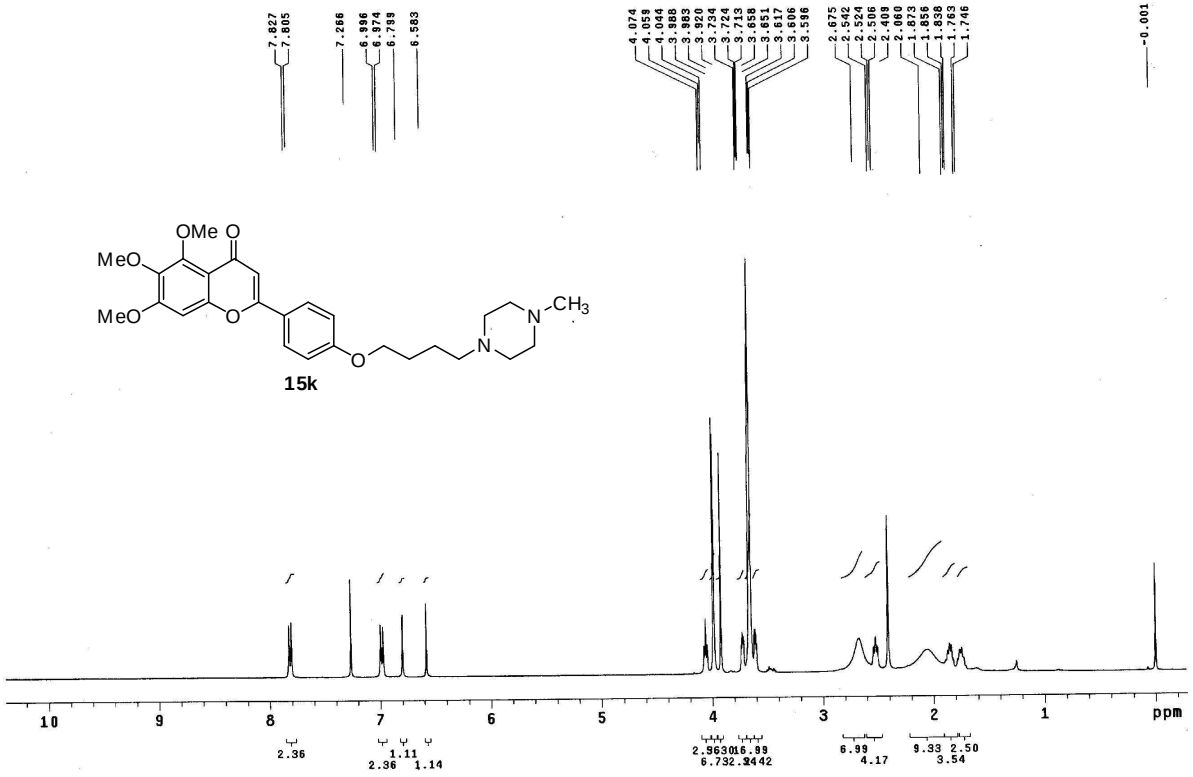
7.827
7.805
7.266
6.996
6.974
6.799
6.583
4.074
4.059
4.044
3.988
3.983
3.920
3.734
3.724
3.713
3.658
3.651
3.617
3.606
3.596
2.675
2.542
2.534
2.506
2.409
2.060
1.873
1.856
1.838
1.763
1.746
-0.001
OMe O
MeO
MeO
O
N
CH3
N
O
15k
10
9
8
7
6
5
4
3
2
1
ppm
2.36
1.11
2.36
1.14
2.96
3.01
6.99
6.73
2.44
2
6.99
4.17
9.33
2.50
3.54

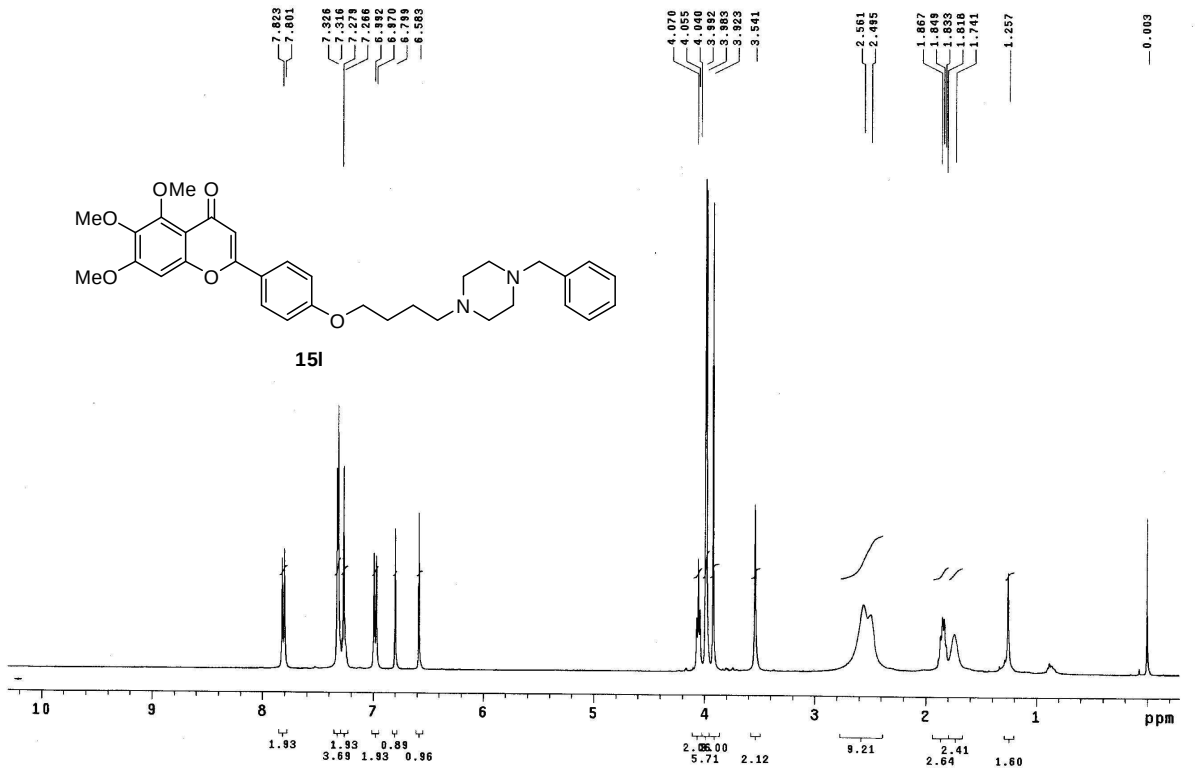
7.823
7.801
7.326
7.316
7.279
7.266
6.892
6.870
6.799
6.583
4.070
4.055
4.040
3.992
3.983
3.923
3.541
2.561
2.495
1.867
1.849
1.833
1.818
1.741
1.257
0.003
OMe O
MeO
MeO
O
N
N
O
15l
10
9
8
7
6
5
4
3
2
1
ppm
1.93
1.93
3.69
1.93
0.89
0.96
2.00
5.71
2.12
9.21
2.41
2.64
1.60

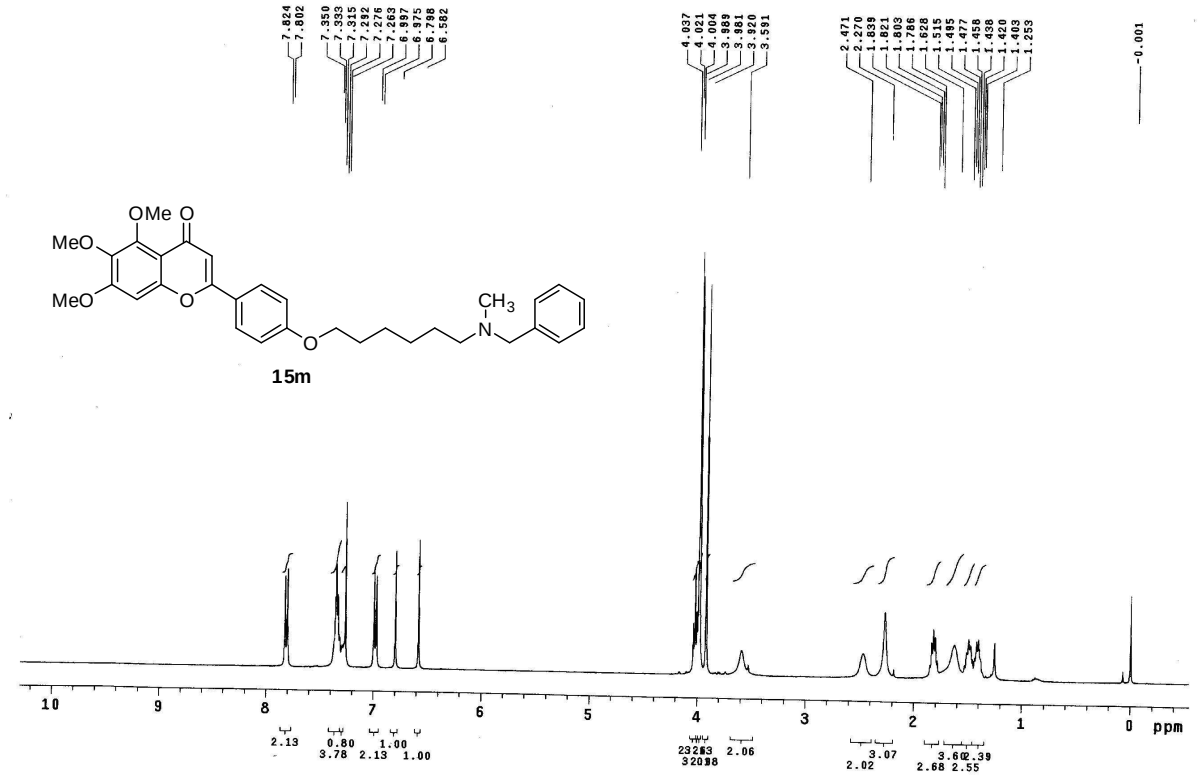
7.824
7.802
7.350
7.333
7.315
7.292
7.276
7.263
6.997
6.975
6.798
6.582
4.037
4.021
4.004
3.889
3.881
3.920
3.591
2.471
2.270
1.839
1.821
1.803
1.786
1.628
1.515
1.495
1.477
1.458
1.438
1.420
1.408
1.253
-0.001
OMe O
MeO
MeO
O
O
CH3
N
10
9
8
7
6
5
4
3
2
1
0 ppm
2.13
0.80
3.78
2.13
1.00
1.00
2.06
3.07
2.02
2.68
2.55

15m

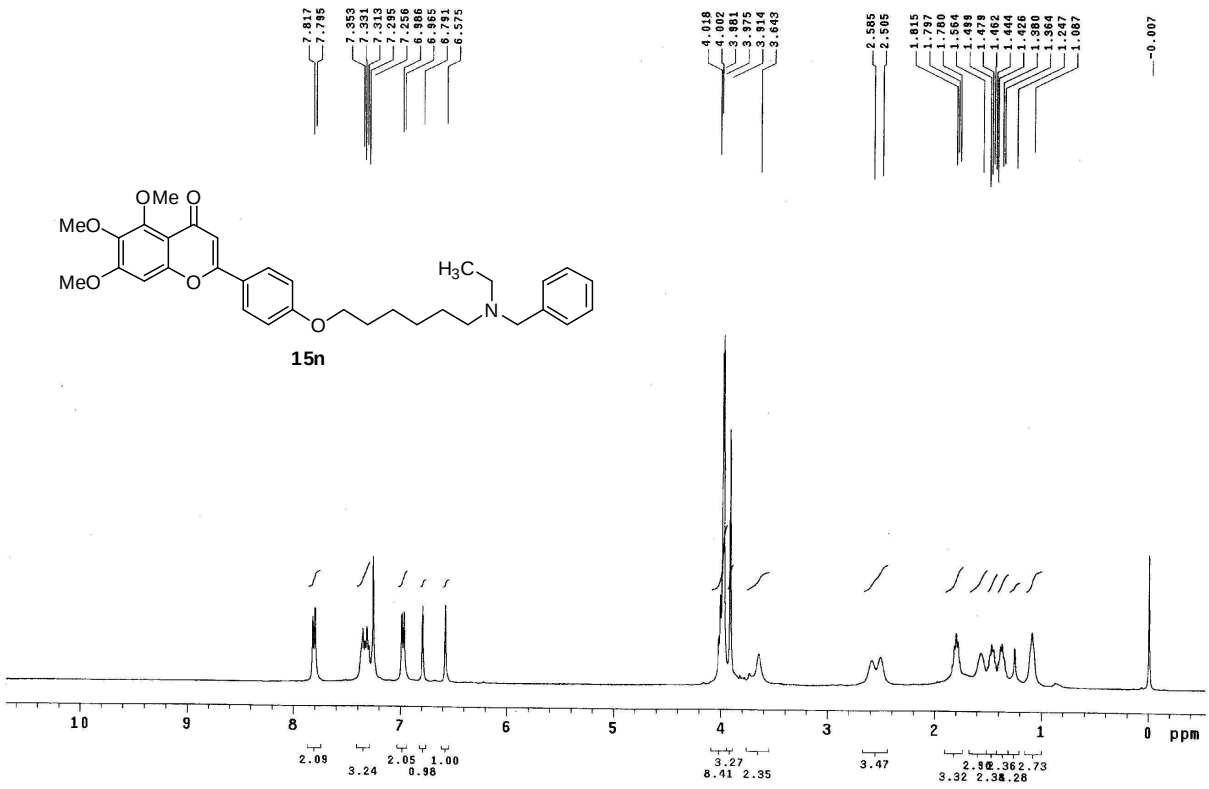
7.817
7.795
7.353
7.331
7.313
7.295
7.256
6.986
6.965
6.791
6.575
4.018
4.002
3.981
3.975
3.914
3.643
2.585
2.505
1.815
1.797
1.780
1.564
1.499
1.479
1.462
1.444
1.426
1.380
1.364
1.247
1.087
-0.007
OMe O
MeO
MeO
O
O
H3C
N
10
9
8
7
6
5
4
3
2
1
0 ppm
2.09
3.24
2.05
0.98
1.00
3.27
8.41
2.35
3.47
3.32
2.73
1.28

15n

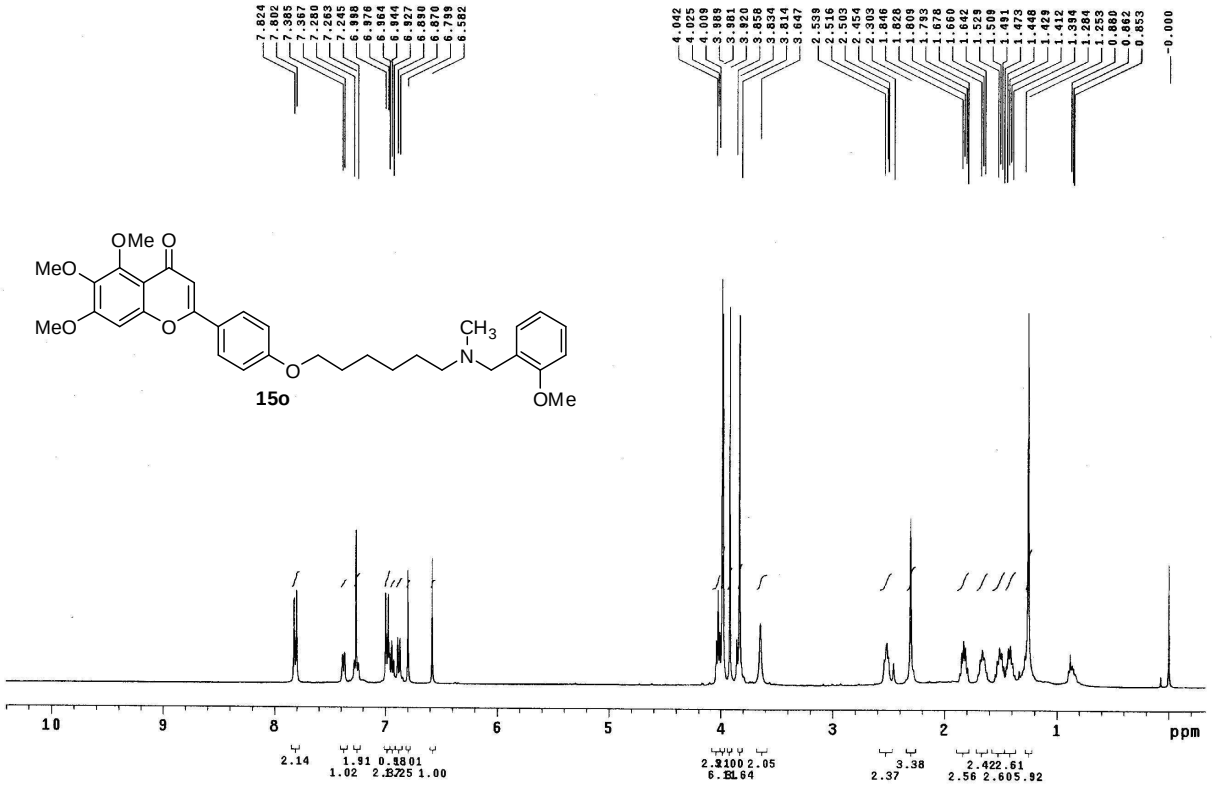
OMe O
MeO
MeO
O
O
CH3
N
OMe
15o
ppm

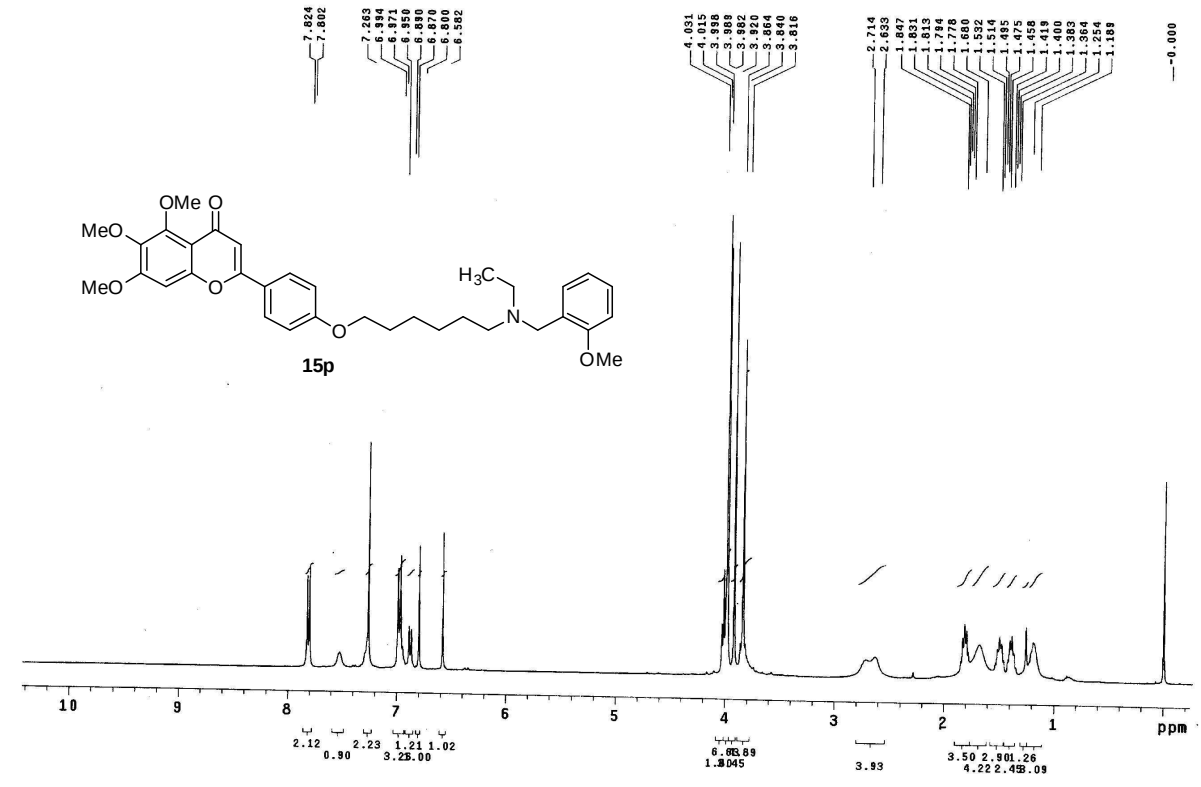
OMe O
MeO
MeO
O
O
H3C
N
OMe
15p
ppm

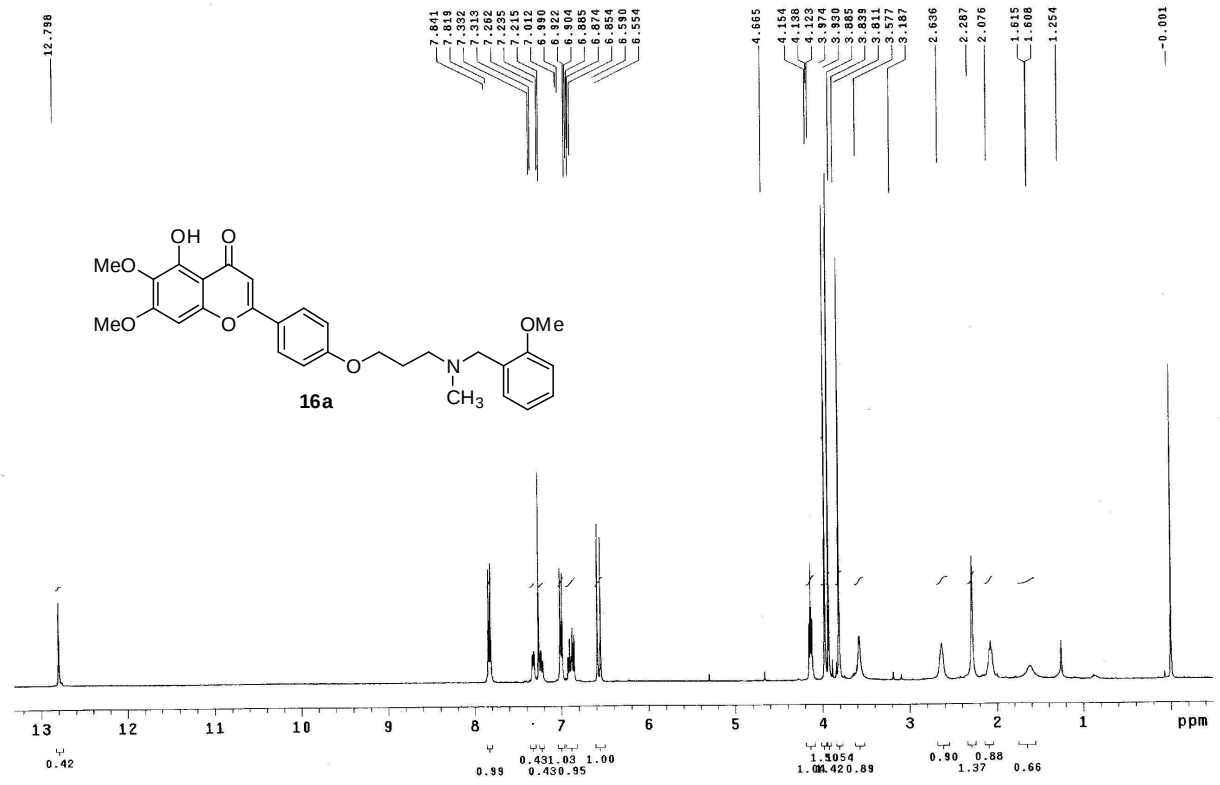
12.798
7.841
7.819
7.332
7.313
7.262
7.235
7.215
7.102
6.940
6.922
6.904
6.885
6.874
6.854
6.590
6.554
4.665
4.154
4.138
4.123
3.974
3.960
3.885
3.839
3.811
3.577
3.187
2.636
2.287
2.076
1.615
1.608
1.254
-0.001
OH
O
MeO
MeO
O
O
OMe
N
CH3
16a
13
12
11
10
9
8
7
6
5
4
3
2
1
ppm
0.42
0.99
0.431.03
0.430.95
1.00
1.00
1.054
1.420.89
0.90
0.88
1.37
0.66

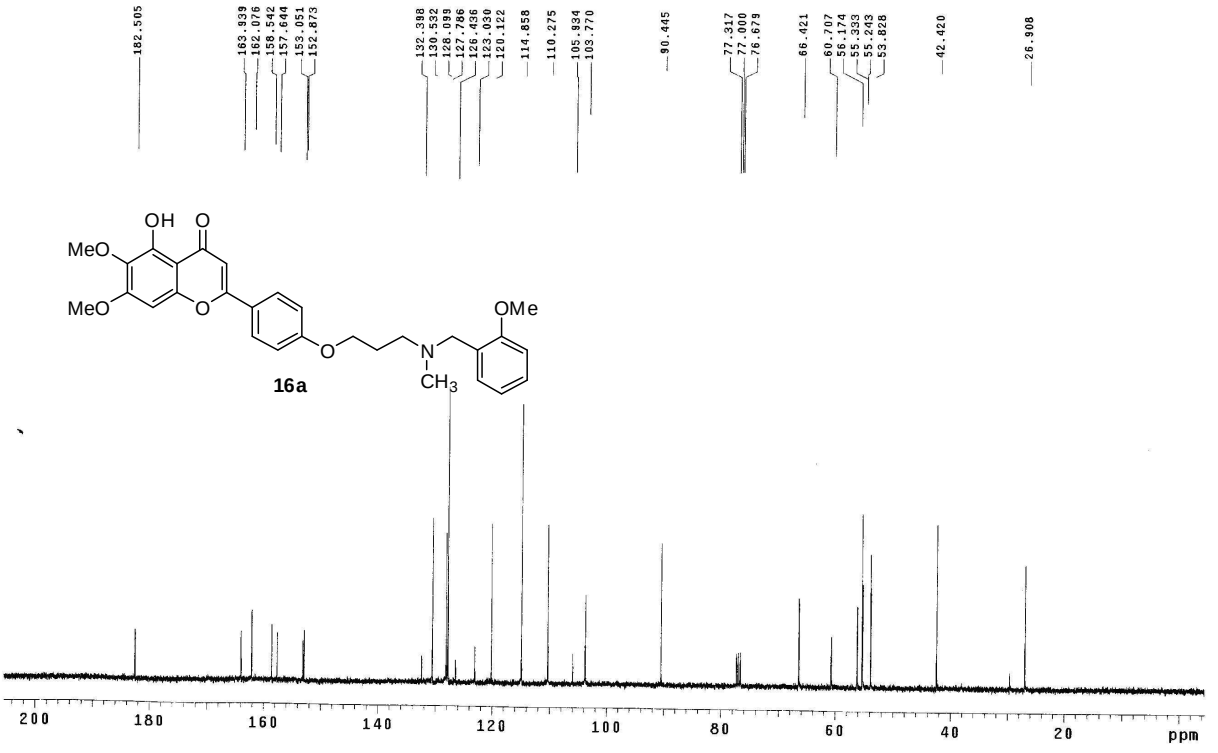
182.505
163.339
162.076
158.542
157.644
153.051
152.873
132.398
130.532
128.099
127.786
126.436
123.030
120.122
114.858
110.275
105.934
103.770
90.445
77.317
77.000
76.679
66.421
60.707
56.174
55.333
55.243
53.828
42.420
26.908
OH
O
MeO
MeO
O
O
OMe
N
CH3
16a
200
180
160
140
120
100
80
60
40
20
ppm

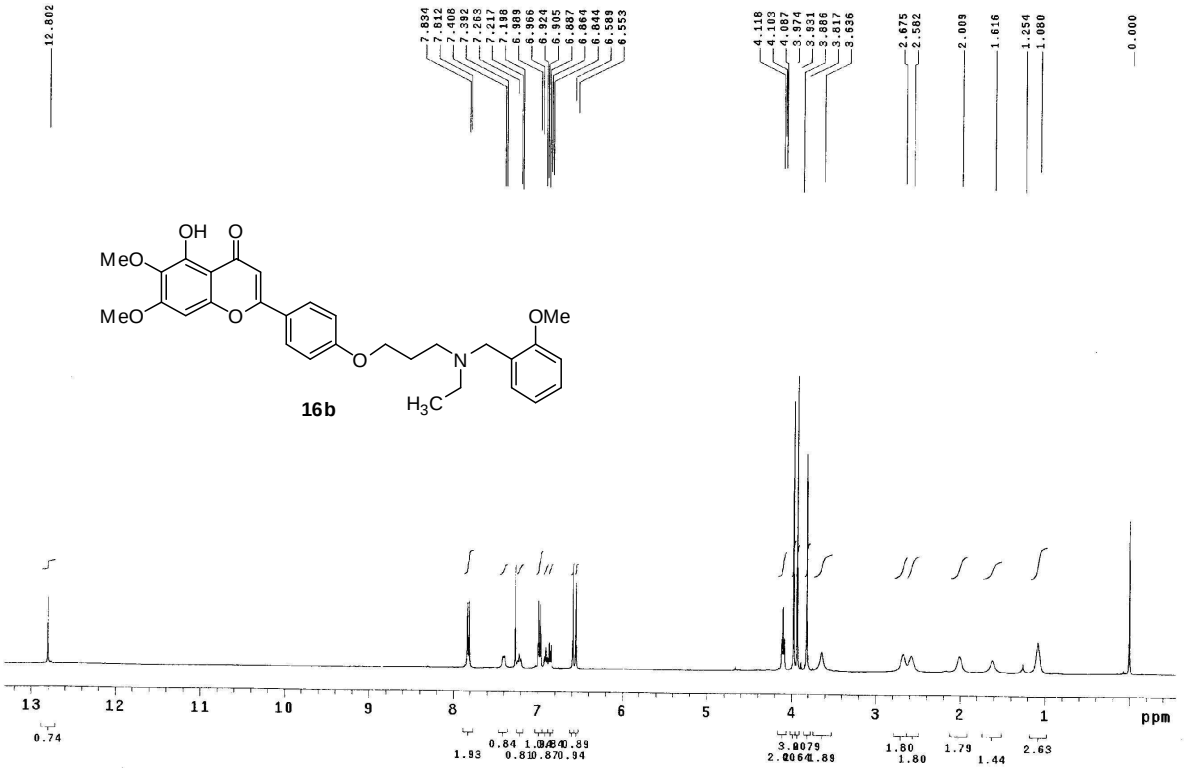
12.802
7.834
7.812
7.408
7.392
7.263
7.217
7.198
7.089
6.926
6.905
6.887
6.864
6.844
6.589
6.553
4.118
4.103
4.087
3.974
3.831
3.686
3.617
3.636
2.675
2.582
2.009
1.616
1.254
1.080
0.000
OH
O
MeO
MeO
O
OMe
N
H3C
16b
ppm

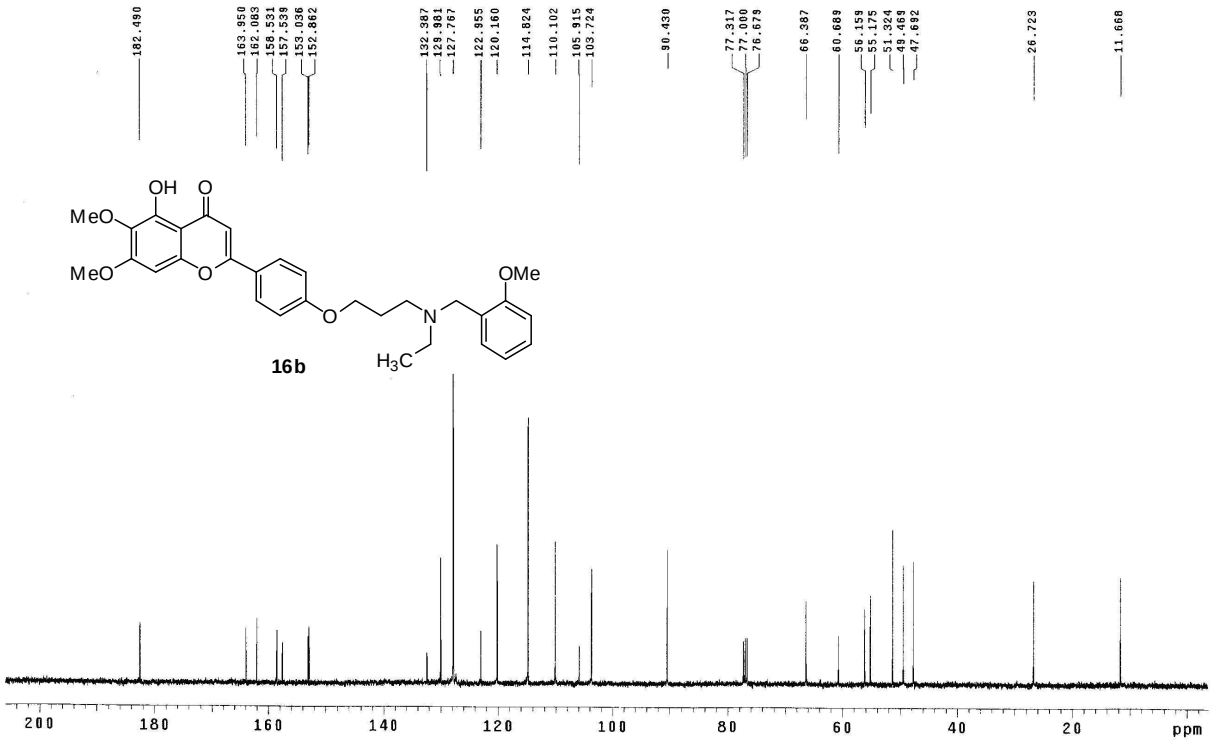
182.490
163.950
162.085
158.531
157.539
153.036
152.862
132.387
129.961
127.767
122.955
120.160
114.824
110.102
105.915
103.724
90.430
77.317
77.000
76.679
66.387
60.689
56.159
55.175
51.324
49.469
47.692
26.723
11.668
OH
O
MeO
MeO
O
OMe
N
H3C
16b
ppm

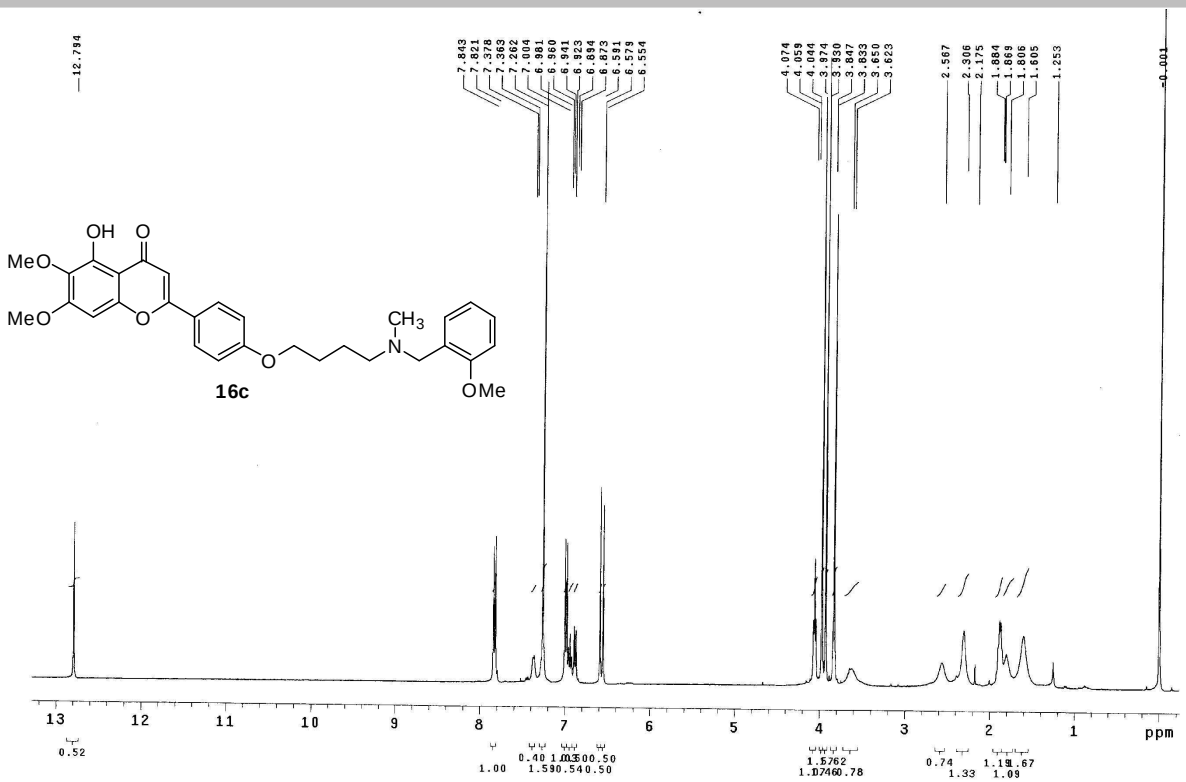
12.794
7.843
7.821
7.378
7.358
7.282
7.004
6.981
6.960
6.941
6.923
6.894
6.873
6.591
6.579
6.554
4.074
4.059
4.044
3.974
3.850
3.847
3.833
3.650
3.623
2.567
2.306
2.175
1.884
1.869
1.806
1.605
1.253
0.001
OH
O
MeO
MeO
O
O
CH3
N
OMe
16c
13
12
11
10
9
8
7
6
5
4
3
2
1
ppm
0.52
1.00
0.40
1.59
0.54
0.50
1.57
1.07
0.78
0.74
1.33
1.08

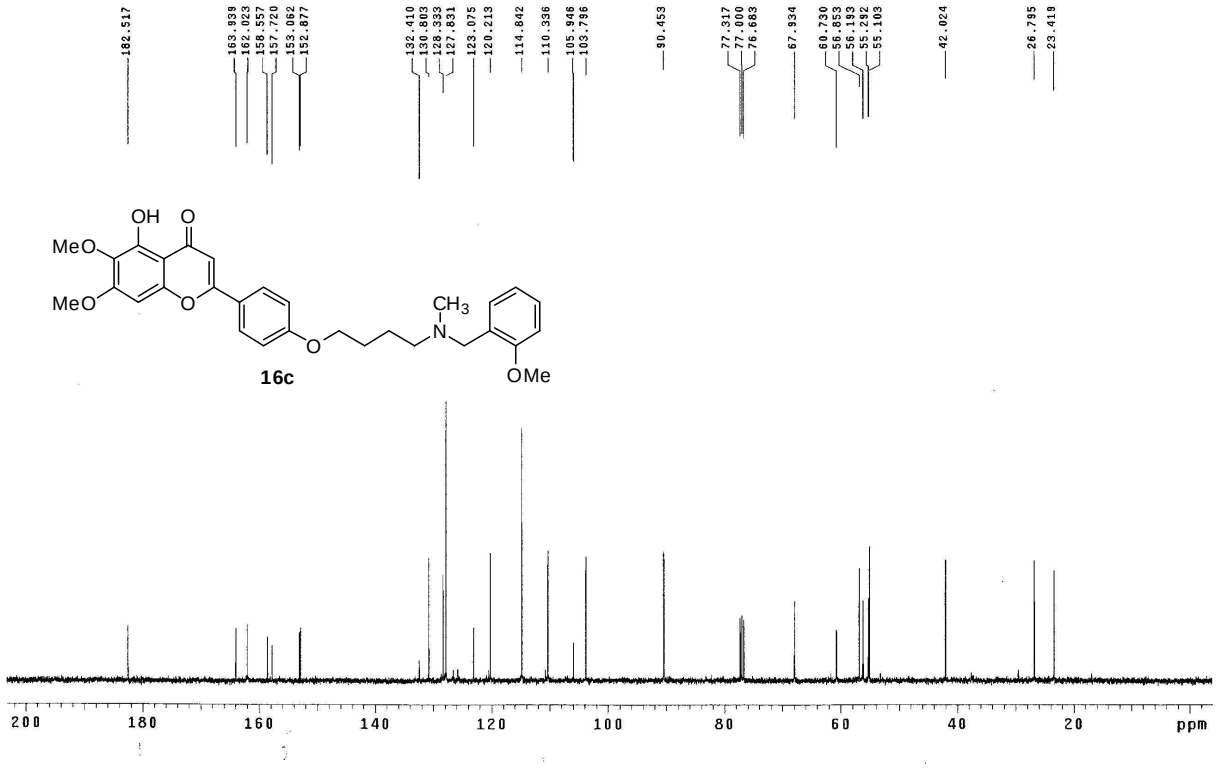
182.517
163.938
162.023
158.557
157.720
153.062
152.877
132.410
130.803
128.333
127.831
123.075
120.213
114.842
110.336
105.946
103.796
90.453
77.317
77.000
76.683
67.934
60.730
56.053
56.193
55.242
55.103
42.024
26.795
23.419
OH
O
MeO
MeO
O
O
CH3
N
OMe
16c
200
180
160
140
120
100
80
60
40
20
ppm

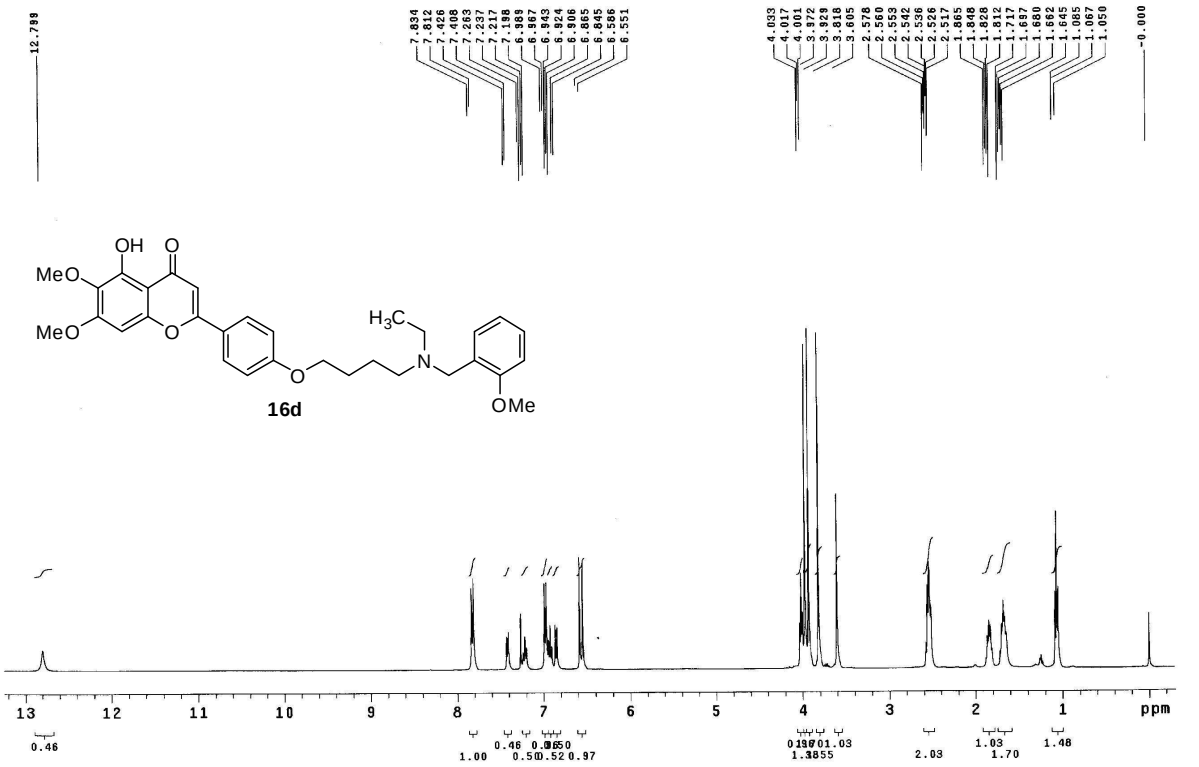
OH
O
MeO
MeO
O
O
H3C
N
OMe
16d

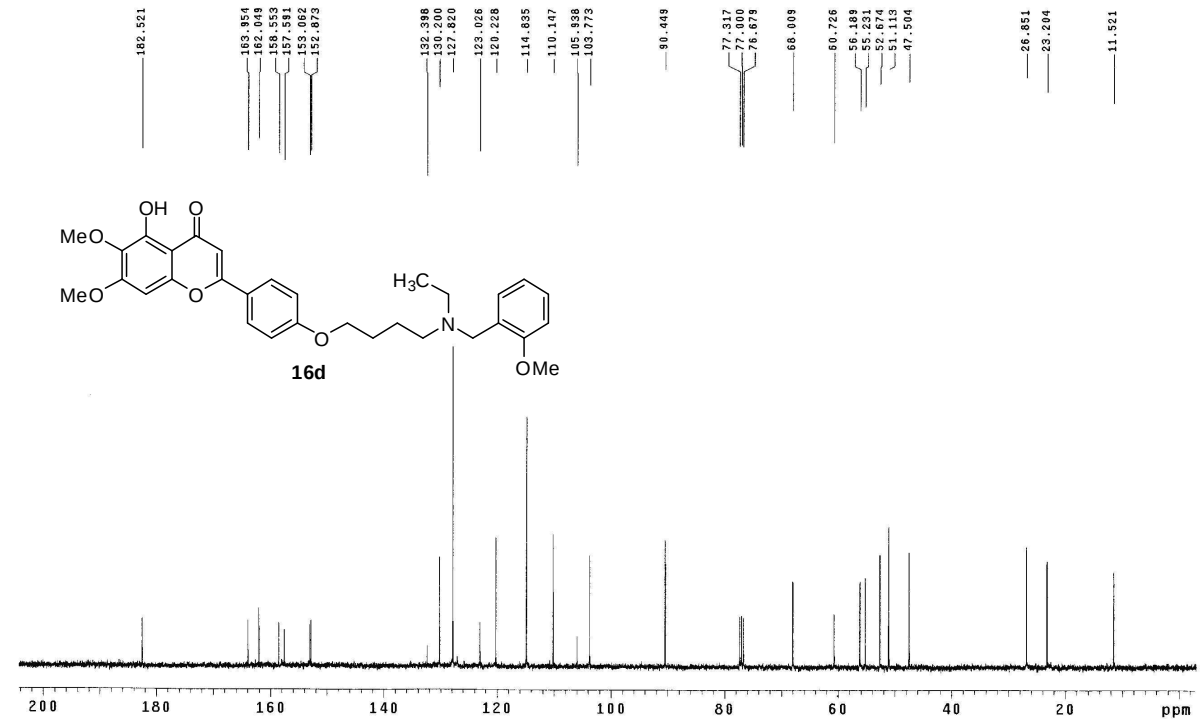
OH
O
MeO
MeO
O
O
H3C
N
OMe
16d

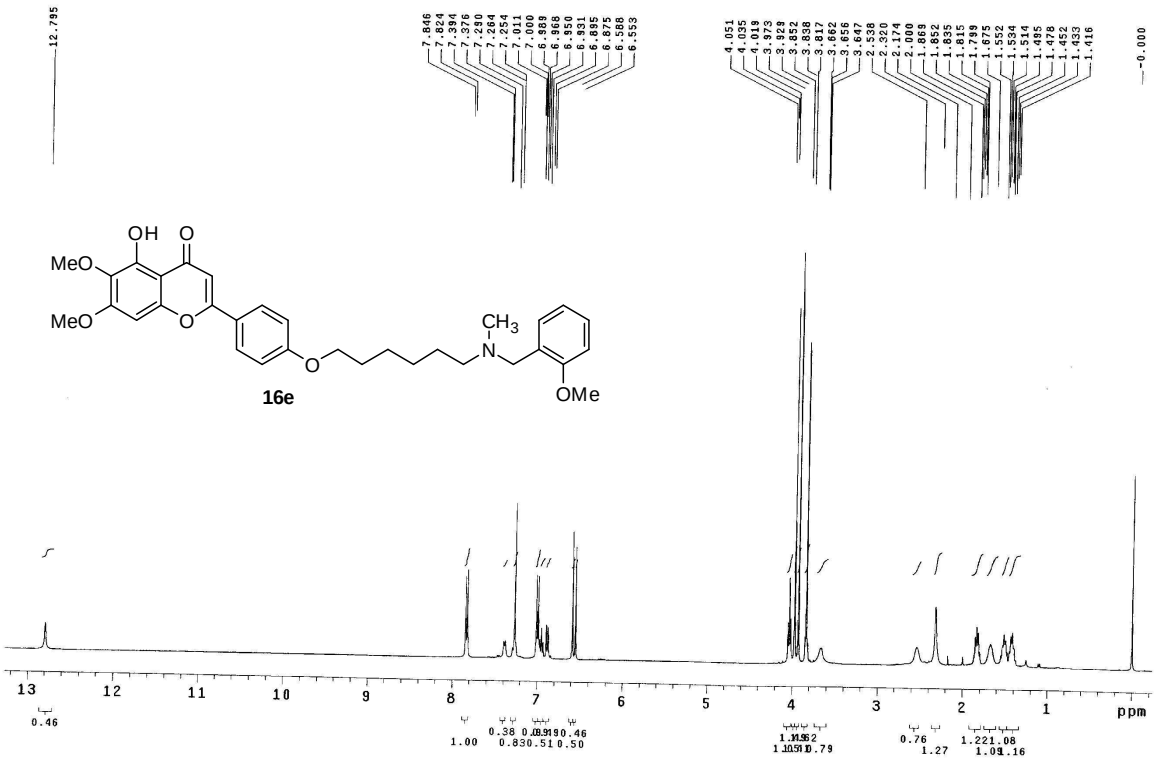
12.795
7.846
7.824
7.394
7.376
7.230
7.264
7.254
7.011
7.000
6.969
6.956
6.931
6.895
6.875
6.588
6.553
4.051
4.035
4.019
3.973
3.829
3.812
3.808
3.817
3.662
3.656
3.647
2.538
2.320
2.174
2.000
1.869
1.852
1.835
1.815
1.795
1.675
1.552
1.534
1.514
1.495
1.478
1.452
1.433
1.416
0.000
OH
O
MeO
MeO
O
CH3
N
O
OMe
16e
13
12
11
10
9
8
7
6
5
4
3
2
1
ppm
0.46
1.00
0.38
0.83
0.51
0.50
0.76
1.27
1.22
1.08
1.09
1.16

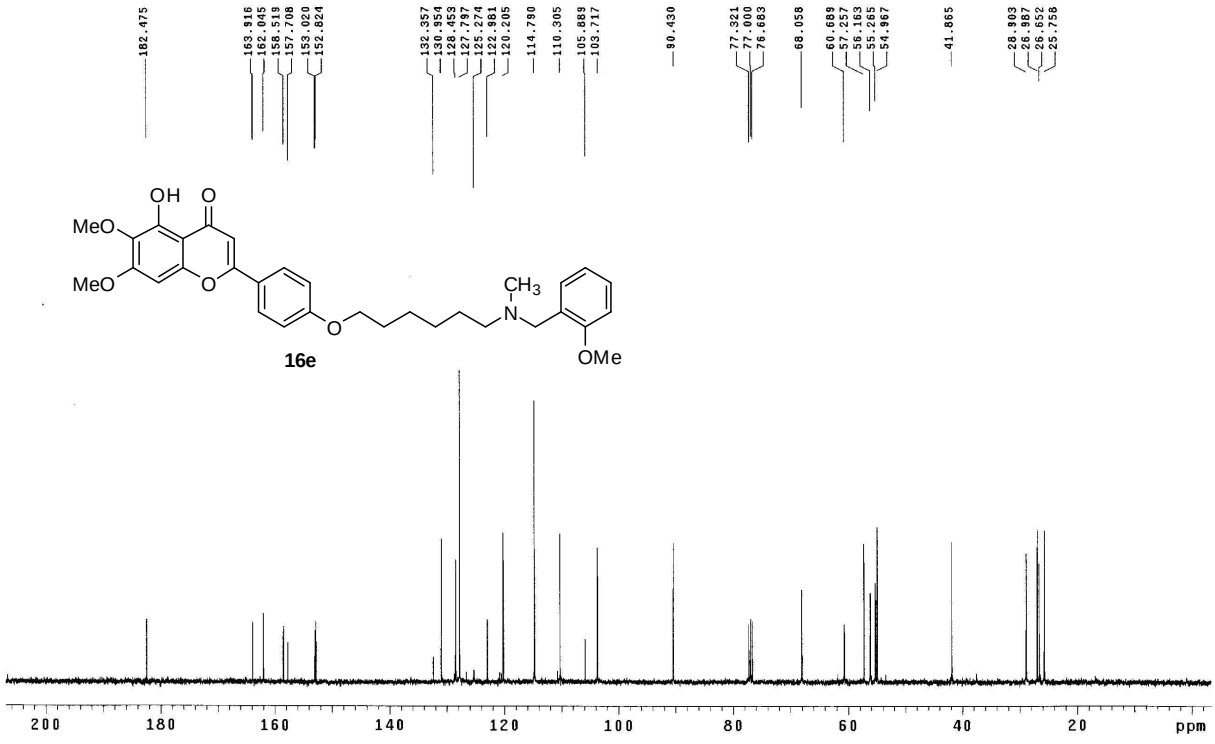
182.475
163.916
162.045
158.519
157.706
153.020
152.824
132.357
130.354
128.453
127.777
122.681
120.205
114.790
110.305
105.889
103.717
90.430
77.321
77.000
76.683
68.058
60.689
57.257
56.163
55.665
54.967
41.865
28.903
26.387
26.552
25.758
OH
O
MeO
MeO
O
CH3
N
O
OMe
16e
200
180
160
140
120
100
80
60
40
20
ppm

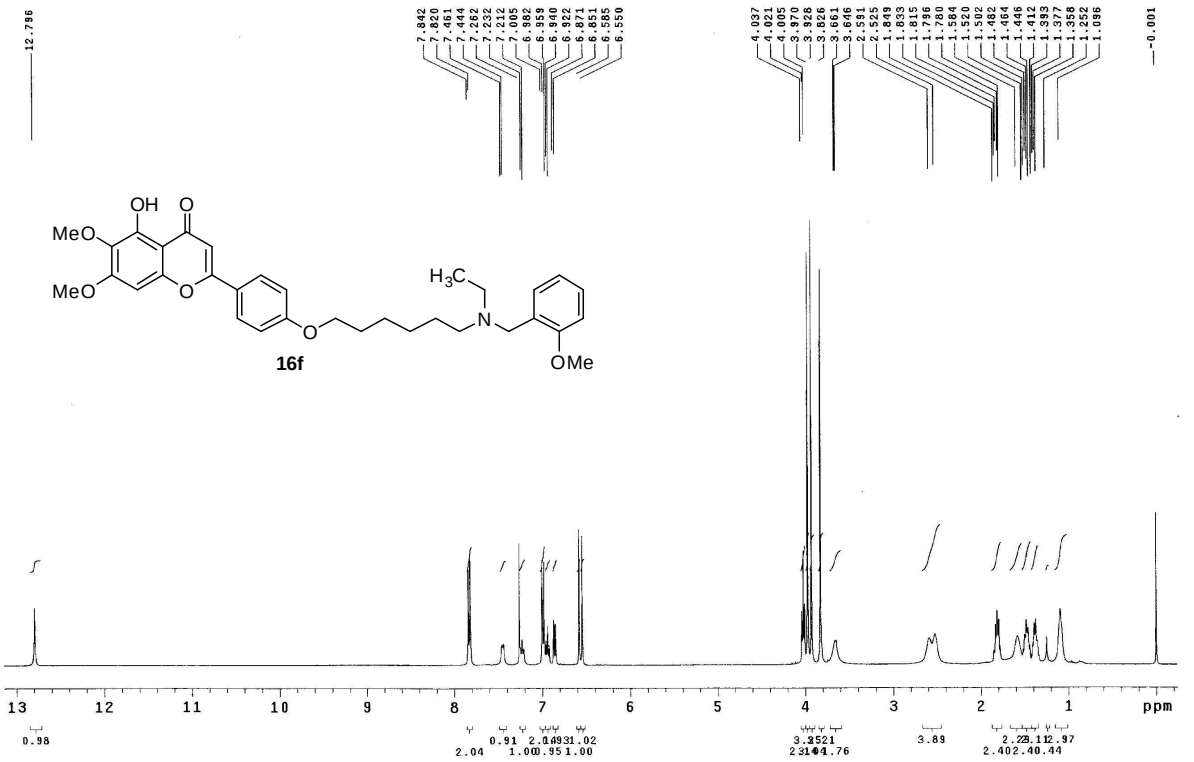
12.796
7.842
7.820
7.461
7.444
7.252
7.232
7.212
7.005
6.982
6.959
6.940
6.922
6.871
6.851
6.585
6.550
4.037
4.021
4.005
3.970
3.928
3.826
3.661
3.646
2.591
2.525
1.849
1.833
1.815
1.796
1.780
1.584
1.520
1.502
1.482
1.464
1.446
1.412
1.393
1.377
1.358
1.252
1.096
-0.001
OH
O
MeO
MeO
O
O
H3C
N
OMe
16f
13
12
11
10
9
8
7
6
5
4
3
2
1
ppm
0.98
2.04
0.91
1.00
2.04
0.95
31.02
1.00
3.89
2.40
2.40
12.97
2.44

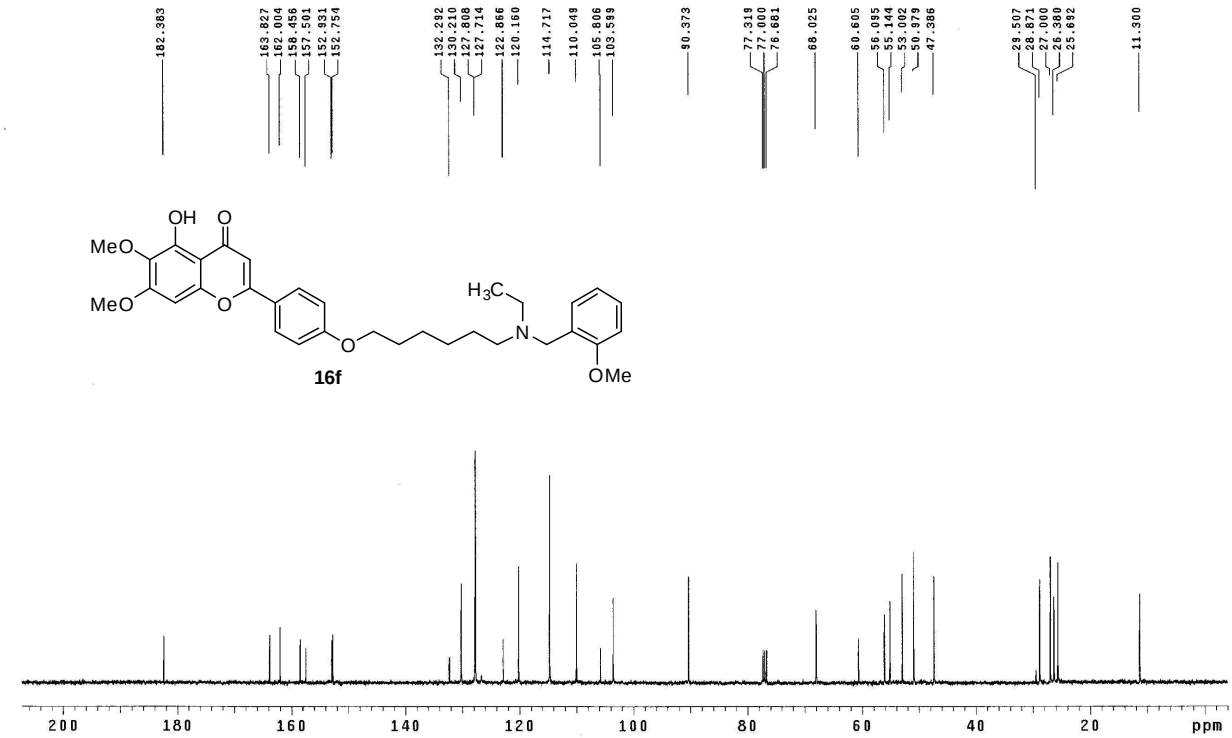
182.383
163.827
162.004
158.456
157.501
152.931
152.754
132.292
130.210
127.808
127.714
122.866
120.160
114.717
110.049
105.806
103.539
90.373
77.319
77.000
76.681
68.025
60.605
56.095
55.144
53.002
50.879
47.386
29.507
29.371
27.000
26.380
25.692
11.300
OH
O
MeO
MeO
O
O
H3C
N
OMe
16f
200
180
160
140
120
100
80
60
40
20
ppm

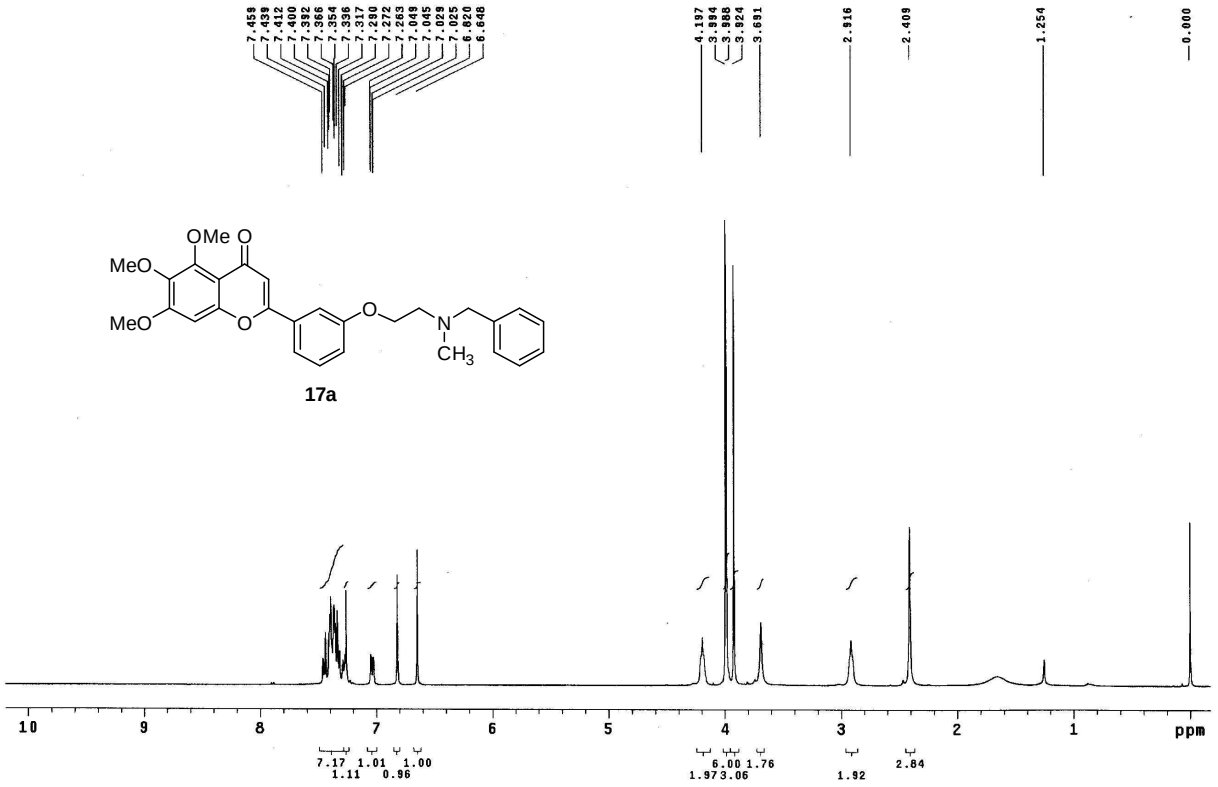
7.458
7.439
7.412
7.400
7.392
7.366
7.354
7.336
7.317
7.290
7.272
7.263
7.049
7.045
7.029
7.025
6.820
6.648
4.197
3.994
3.988
3.924
3.681
2.916
2.409
1.254
0.000
OMe O
MeO
MeO
O
O
N
CH3
10
9
8
7
6
5
4
3
2
1
ppm
7.17 1.01 1.00
1.11 0.96
6.00 1.76
1.97 3.06
1.92
2.84

17a

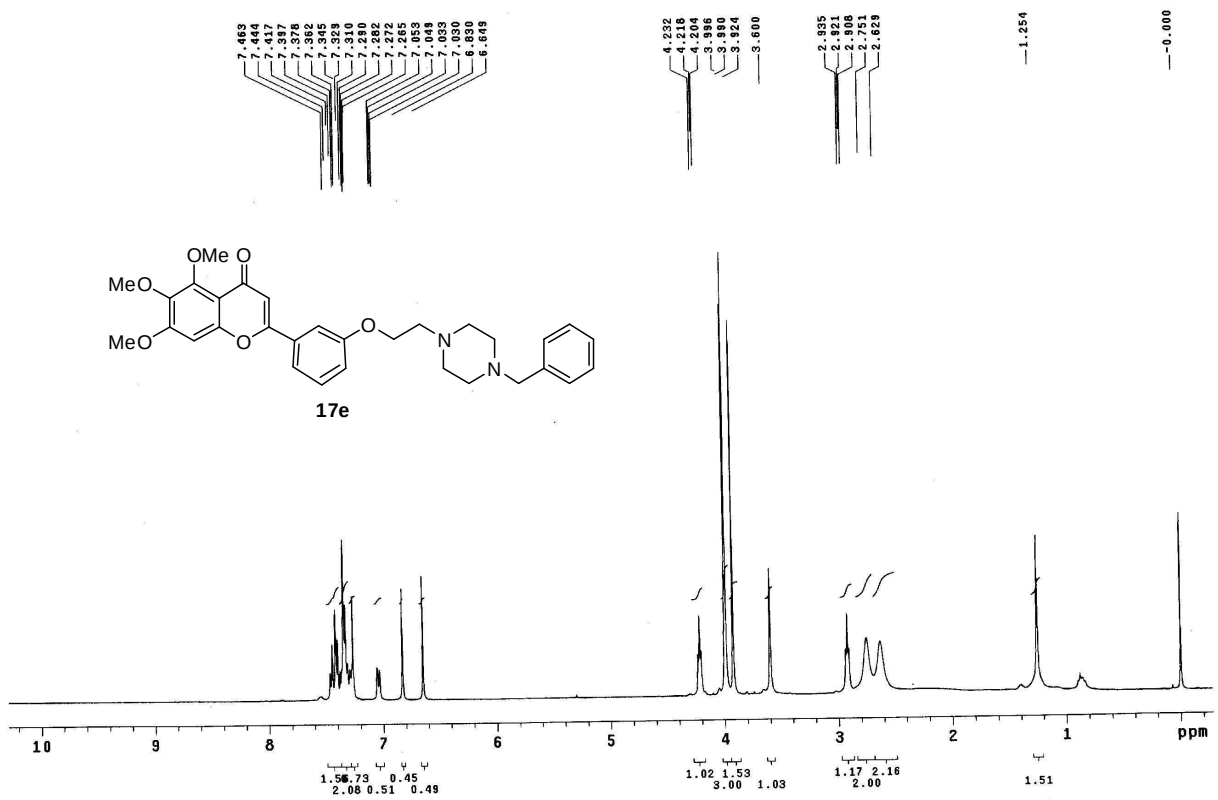
7.463
7.444
7.417
7.397
7.378
7.362
7.345
7.323
7.310
7.280
7.282
7.272
7.265
7.053
7.049
7.033
7.030
6.830
6.649
4.232
4.218
4.204
3.996
3.990
3.924
3.600
2.935
2.921
2.908
2.751
2.629
1.254
0.000
OMe O
MeO
MeO
O
O
N
N
10
9
8
7
6
5
4
3
2
1
ppm
1.56 6.73 0.45
2.08 0.51 0.49
1.02 1.53
3.00 1.03
1.17 2.16
2.00
1.51

17e

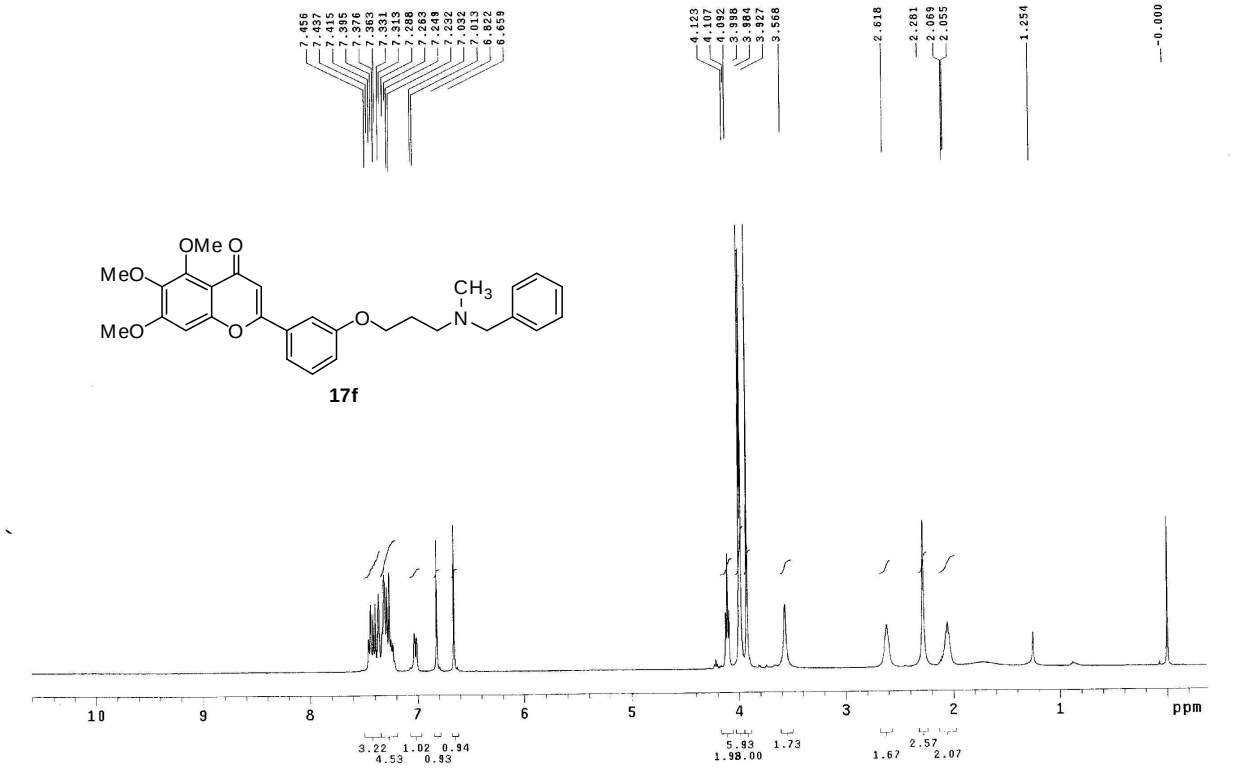
7.456
7.437
7.415
7.395
7.376
7.363
7.331
7.313
7.288
7.263
7.249
7.232
7.032
7.013
6.822
6.659
4.123
4.107
4.092
3.998
3.984
3.927
3.568
2.618
2.281
2.069
2.055
1.254
-0.000
OMe O
MeO
MeO
O
CH3
N
O
10
9
8
7
6
5
4
3
2
1
ppm
3.22 1.02 0.94
4.53 0.93
5.93 1.73
1.98 8.00
1.67 2.57
2.07

17f

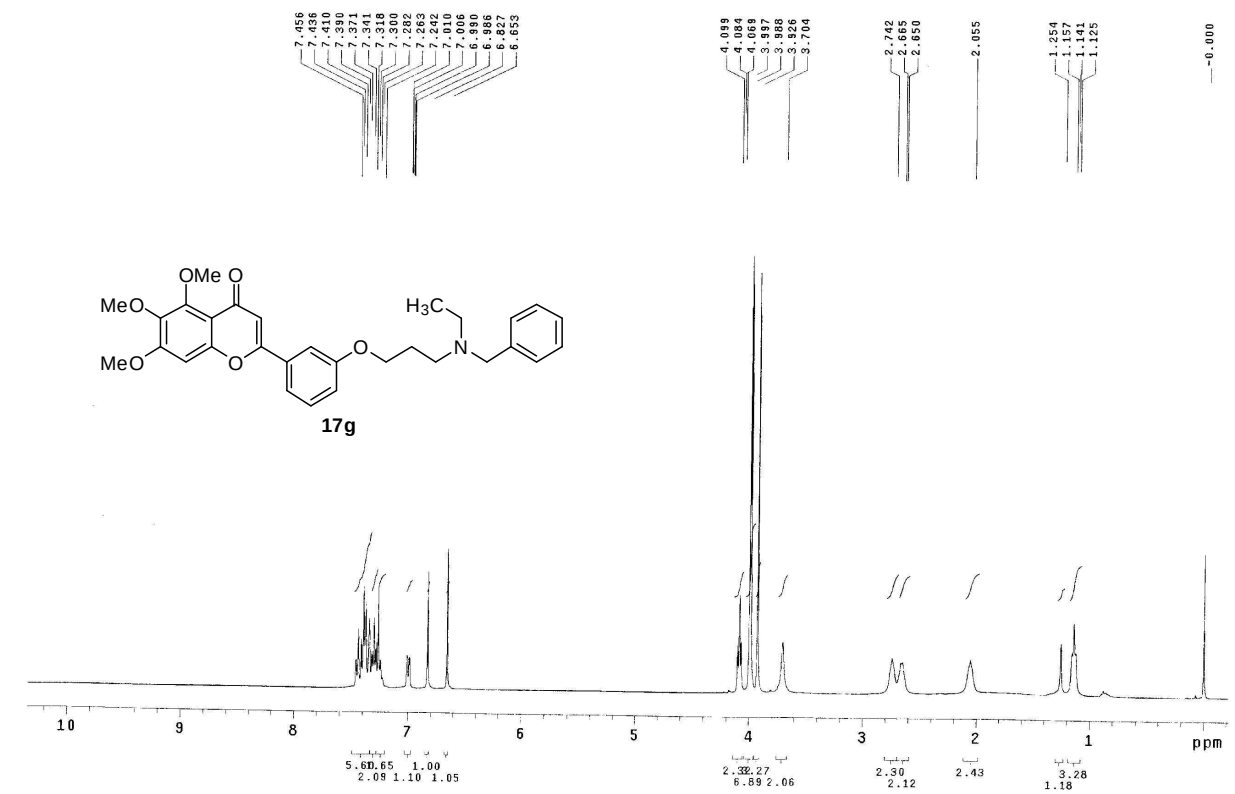
7.456
7.436
7.410
7.390
7.371
7.341
7.318
7.300
7.282
7.263
7.242
7.010
7.006
6.990
6.986
6.827
6.653
4.099
4.084
4.069
3.997
3.888
3.826
3.704
2.742
2.665
2.650
2.055
1.254
1.157
1.141
1.125
-0.000
OMe O
MeO
MeO
O
H3C
N
O
10
9
8
7
6
5
4
3
2
1
ppm
5.60 0.65 1.00
2.09 1.10 1.05
2.32 2.27
6.89 2.06
2.30
2.12
2.43
3.28
1.18

17g

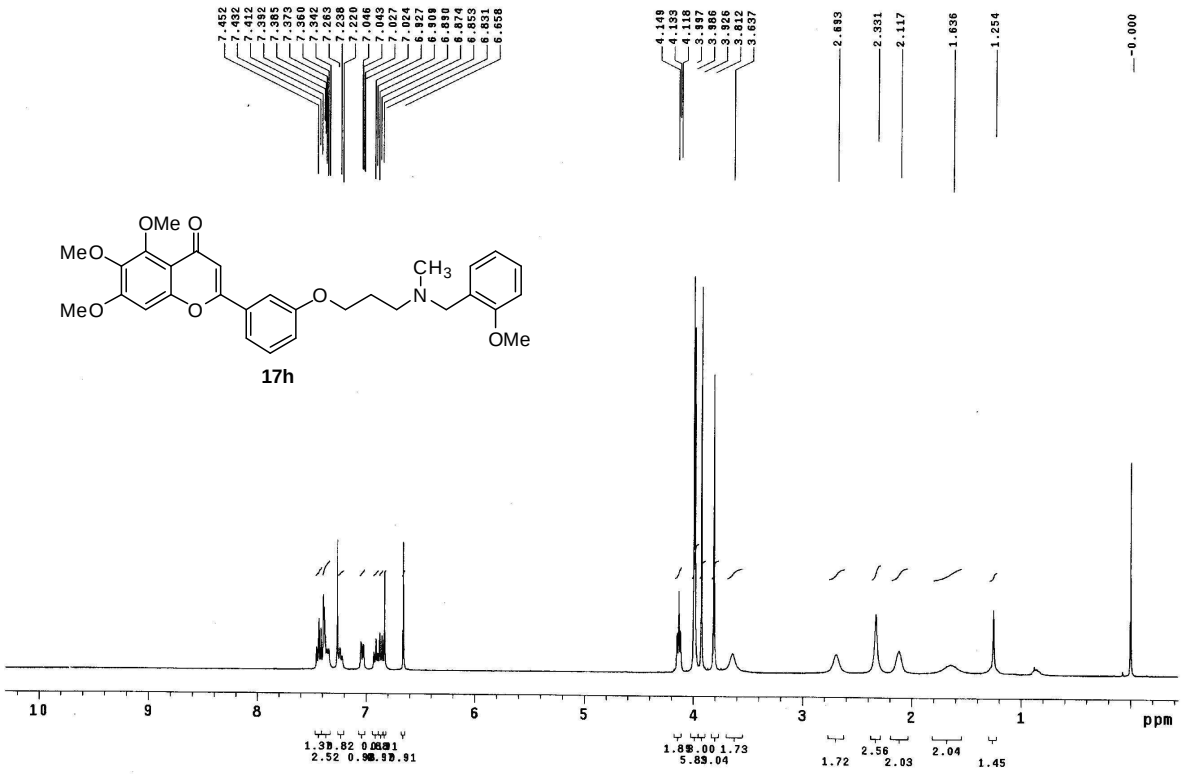
7.452
7.432
7.412
7.382
7.365
7.373
7.360
7.342
7.283
7.238
7.220
7.046
7.043
7.027
7.024
6.927
6.909
6.890
6.874
6.853
6.831
6.658
4.149
4.133
4.118
3.997
3.986
3.926
3.812
3.637
2.693
2.331
2.117
1.636
1.254
-0.000
OMe O
MeO
MeO
O
O
CH3
N
OMe
10
9
8
7
6
5
4
3
2
1
ppm
1.72
2.56
2.03
2.04
1.45

17h

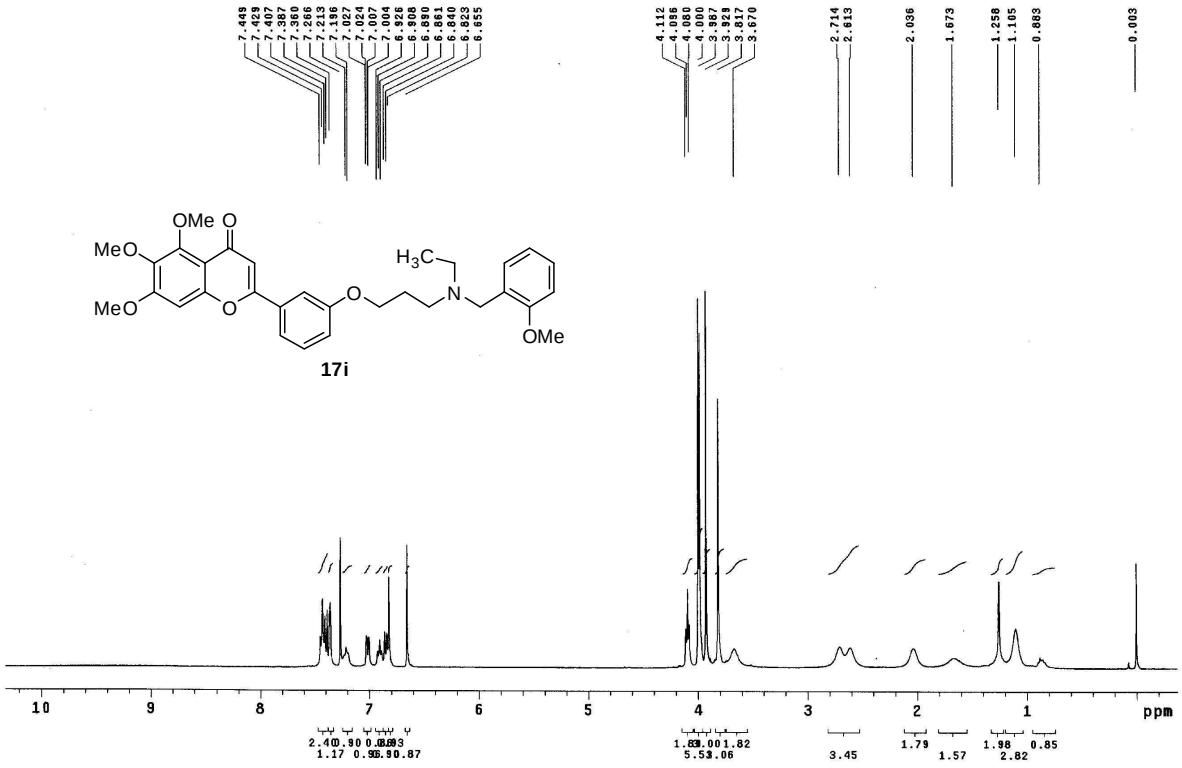
7.449
7.429
7.407
7.387
7.360
7.266
7.213
7.196
7.027
7.024
7.007
7.004
6.926
6.908
6.890
6.861
6.840
6.823
6.655
4.112
4.086
4.086
4.000
3.987
3.929
3.817
3.670
2.714
2.613
2.036
1.673
1.258
1.165
0.883
0.003
OMe O
MeO
MeO
O
O
H3C
N
OMe
10
9
8
7
6
5
4
3
2
1
ppm
3.45
1.79
1.57
1.98
0.85
2.82

17i

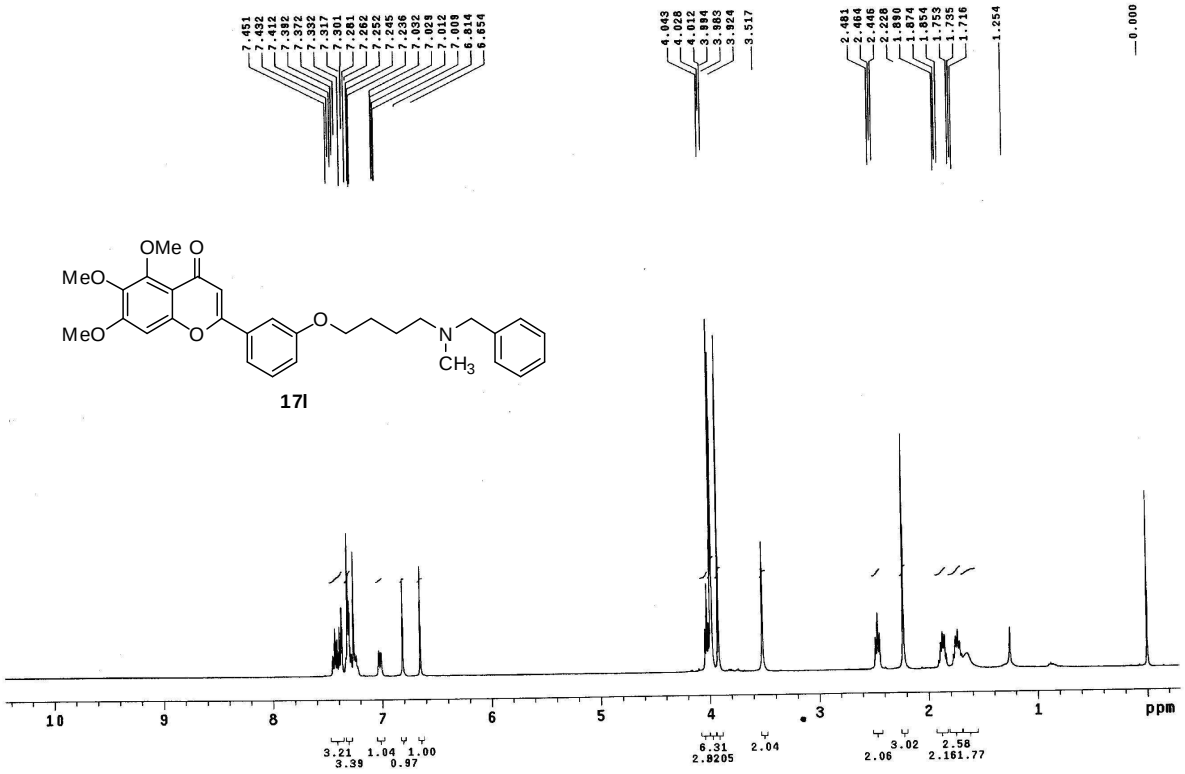
7.451
7.432
7.412
7.392
7.372
7.332
7.317
7.301
7.281
7.262
7.252
7.245
7.236
7.032
7.028
7.013
7.008
6.814
6.654
4.043
4.028
4.012
3.984
3.983
3.924
3.517
2.481
2.464
2.446
2.228
1.890
1.874
1.854
1.753
1.735
1.716
1.254
0.000
OMe O
MeO
MeO
O
O
N
CH3
10
9
8
7
6
5
4
3
2
1
ppm
3.21
3.39
1.04
1.00
0.97
6.31
2.8205
2.04
3.02
2.06
2.58
2.161.77

17l

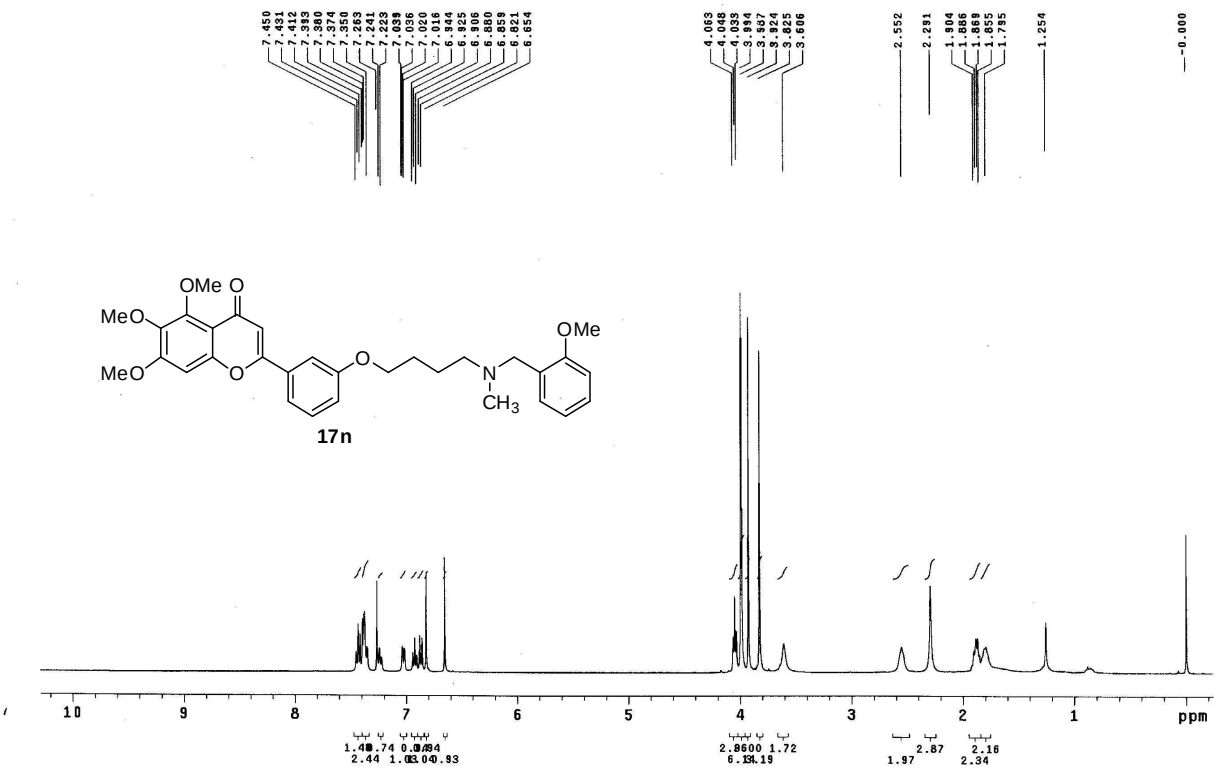
7.450
7.431
7.412
7.393
7.380
7.374
7.350
7.263
7.241
7.223
7.039
7.035
7.020
7.016
6.944
6.925
6.906
6.880
6.859
6.821
6.654
4.063
4.048
4.033
3.994
3.987
3.974
3.825
3.606
2.552
2.281
1.904
1.886
1.869
1.855
1.795
1.254
0.000
OMe O
MeO
MeO
O
O
N
CH3
OMe
10
9
8
7
6
5
4
3
2
1
ppm
1.40
2.44
0.74
1.00
0.84
0.93
2.8600
6.19
1.72
4.19
1.97
2.87
2.16
2.34

17n

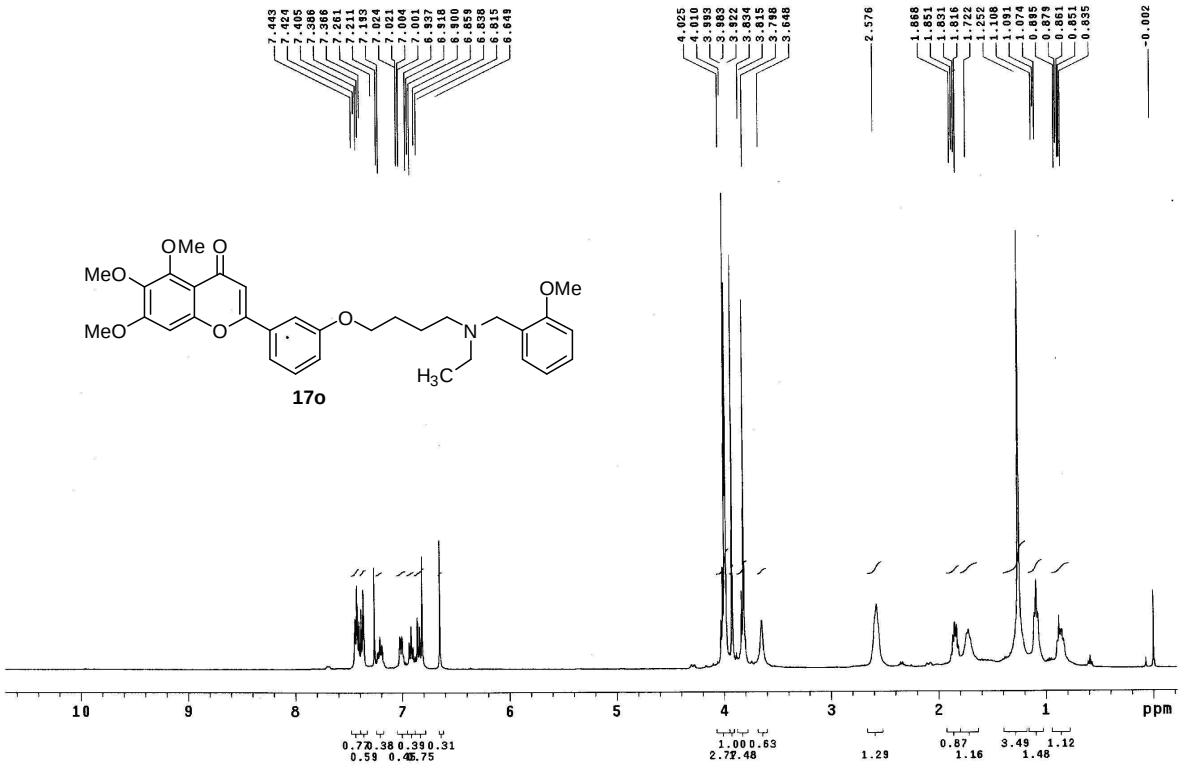
OMe O
MeO
MeO
O
O
OMe
N
H3C
17o
7.443
7.424
7.405
7.386
7.366
7.261
7.211
7.193
7.024
7.021
7.004
7.001
6.937
6.916
6.900
6.855
6.838
6.815
6.649
4.025
4.010
3.993
3.982
3.922
3.834
3.815
3.748
3.648
2.576
1.868
1.851
1.831
1.816
1.722
1.252
1.108
1.091
1.074
0.885
0.879
0.861
0.851
0.835
-0.002
10
9
8
7
6
5
4
3
2
1
ppm
0.77 0.38 0.39 0.31
0.59 0.45 0.75
1.00 0.63
2.72 2.48
1.29
0.87
1.16
3.49 1.12
1.48

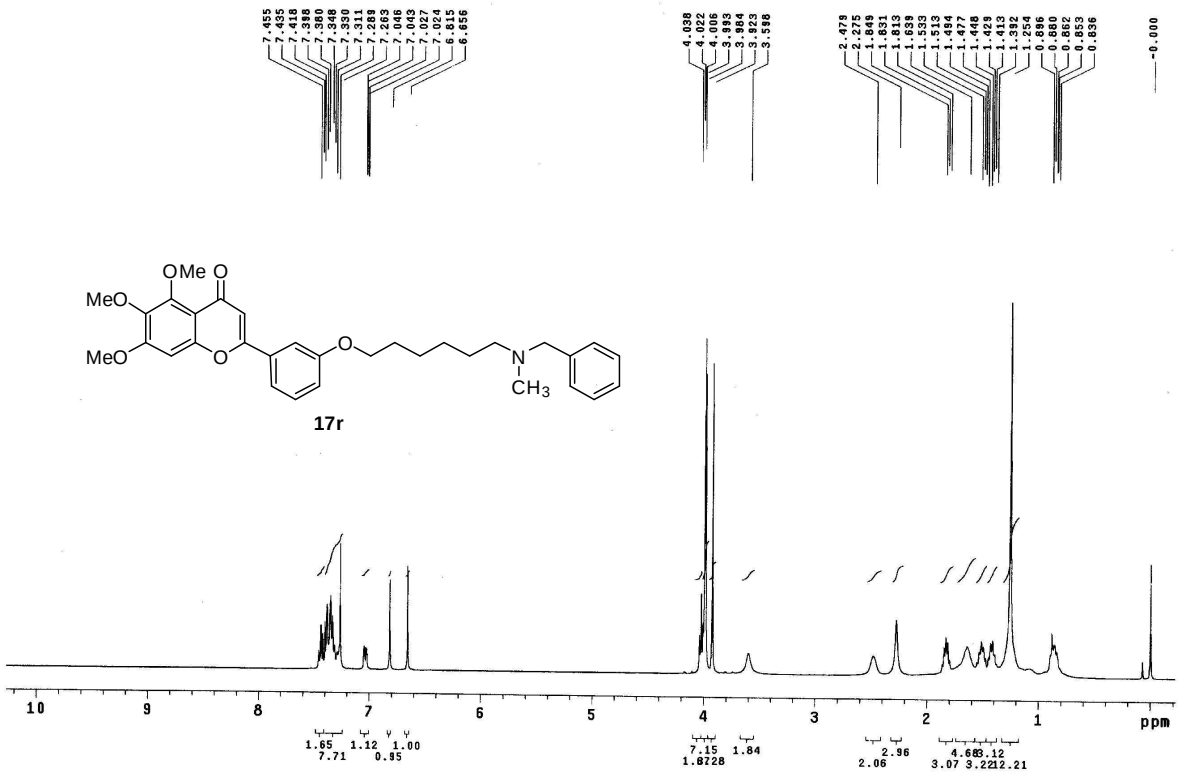
OMe O
MeO
MeO
O
O
N
CH3
17r
7.455
7.435
7.418
7.398
7.380
7.348
7.330
7.311
7.288
7.263
7.046
7.043
7.027
7.024
6.815
6.656
4.038
4.022
4.006
3.993
3.984
3.823
3.598
2.479
2.275
1.849
1.831
1.813
1.639
1.533
1.513
1.494
1.477
1.448
1.429
1.413
1.382
1.254
0.886
0.880
0.862
0.853
0.836
-0.000
10
9
8
7
6
5
4
3
2
1
ppm
1.65 1.12 1.00
7.71 0.95
7.15 1.84
1.8728
2.96
2.06
4.68 3.12
3.07 3.22 2.21

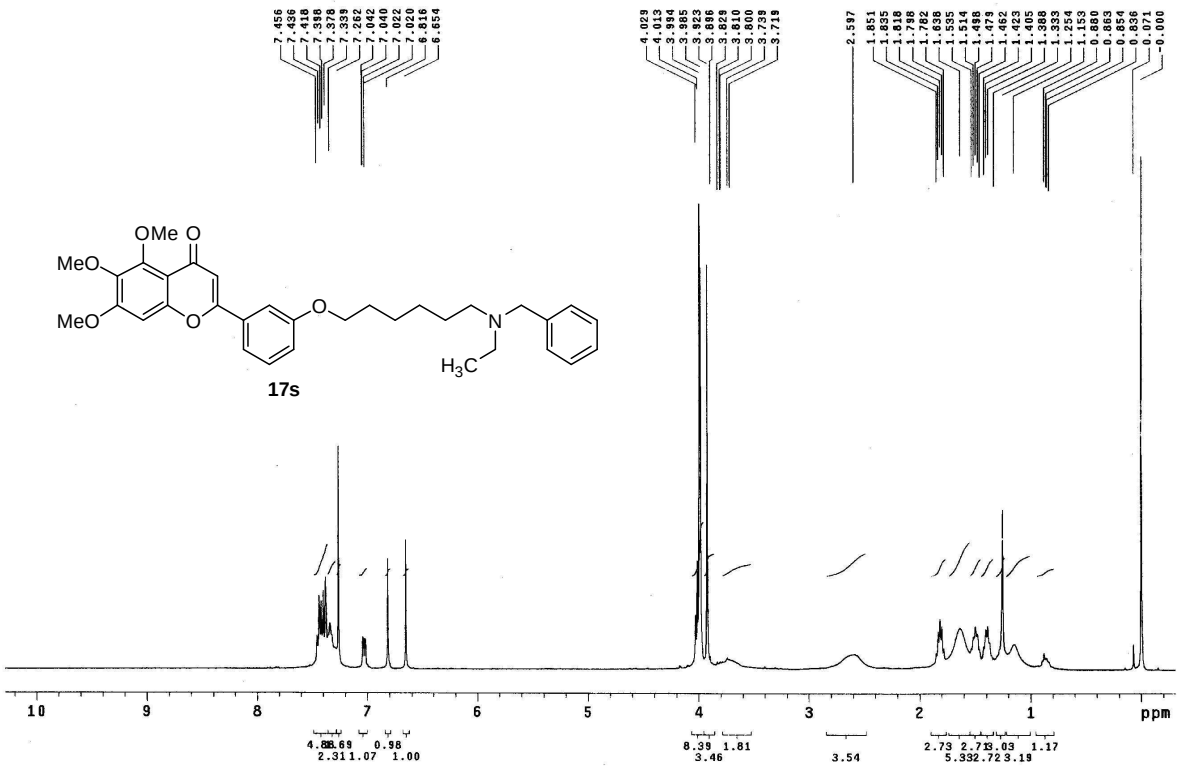
OMe O
MeO
MeO
O
O
N
H3C
17s
7.456
7.436
7.418
7.398
7.378
7.339
7.262
7.042
7.040
7.022
7.020
6.816
6.654
4.029
4.013
3.994
3.985
3.923
3.896
3.829
3.810
3.800
3.738
3.719
2.597
1.851
1.835
1.818
1.798
1.782
1.636
1.535
1.514
1.498
1.479
1.462
1.423
1.405
1.388
1.333
1.254
1.153
0.880
0.863
0.856
0.836
0.071
-0.000
10
9
8
7
6
5
4
3
2
1
ppm
4.68 0.98
2.31 1.07 1.00
8.39 1.81
3.46
3.54
2.73 2.71 3.03 1.17
5.33 2.72 3.19

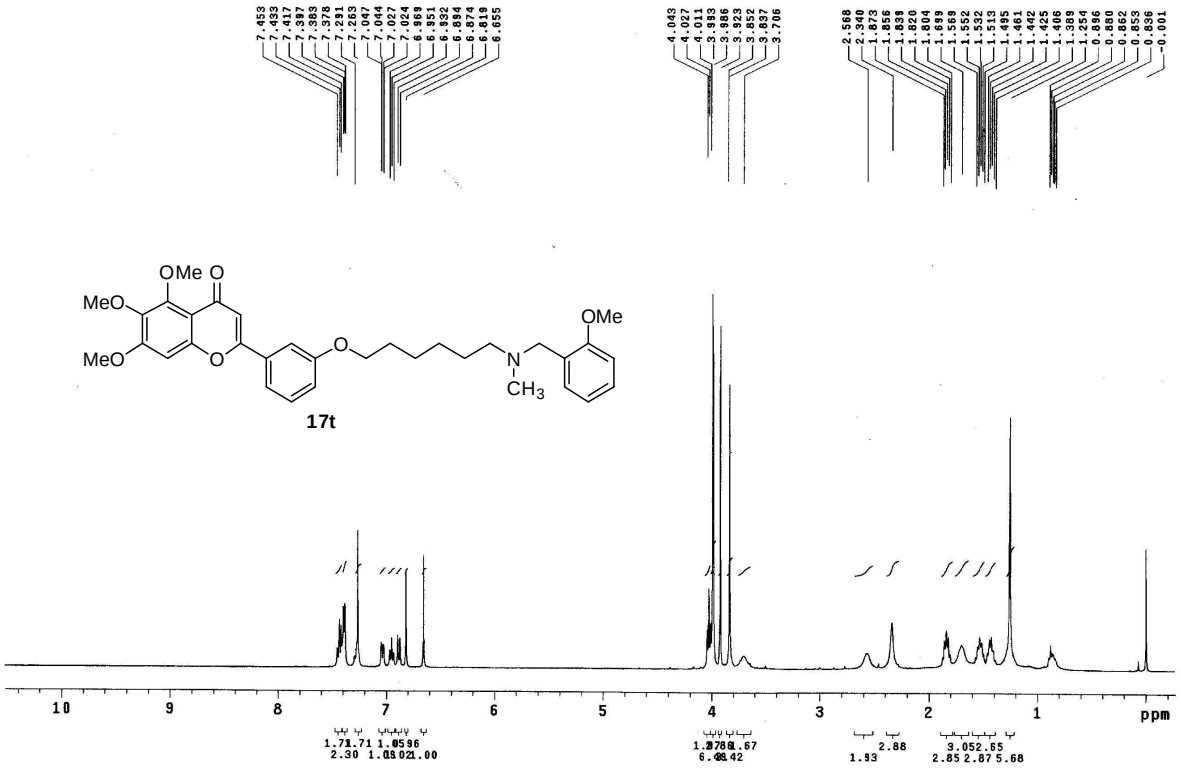
OMe O
MeO
MeO
O
O
OMe
N
CH3
17t
7.453
7.433
7.417
7.397
7.383
7.378
7.373
7.251
7.245
7.047
7.044
7.027
7.024
6.969
6.951
6.932
6.884
6.874
6.819
6.655
4.043
4.027
4.011
3.993
3.986
3.923
3.852
3.837
3.706
2.568
2.340
1.873
1.856
1.838
1.820
1.804
1.689
1.568
1.552
1.532
1.513
1.495
1.461
1.442
1.425
1.406
1.389
1.254
0.896
0.880
0.862
0.853
0.836
-0.001
10
9
8
7
6
5
4
3
2
1
ppm
1.71 1.05 96
2.30 1.00 1.00
1.67
6.42
2.88
1.93
3.05 2.55
2.85 2.87 5.68

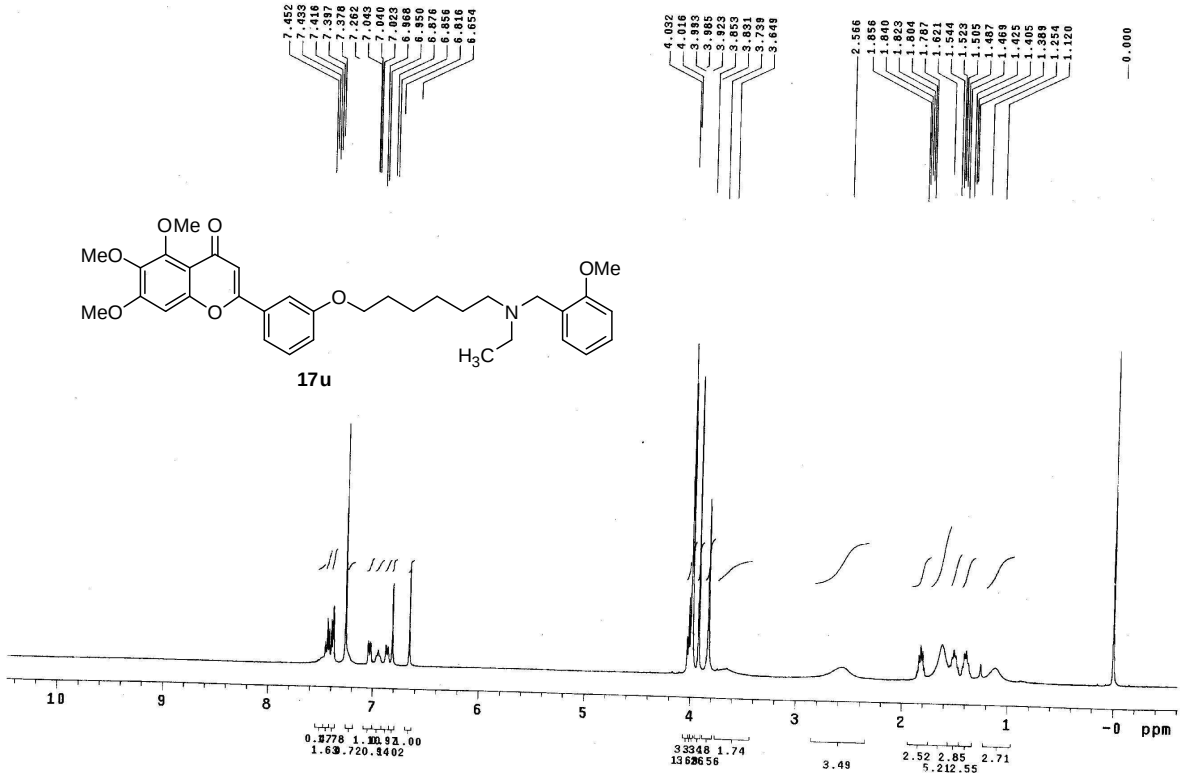
OMe O
MeO
MeO
O
O
N
OMe
H3C
17u
ppm

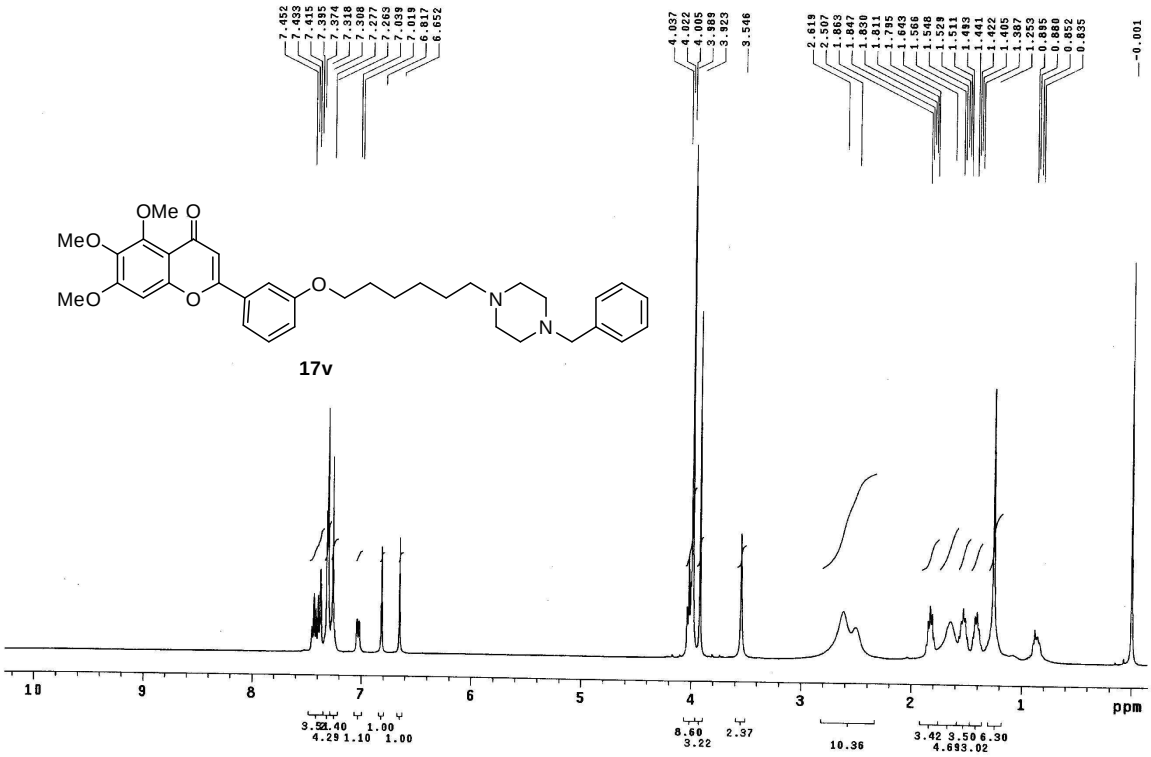
OMe O
MeO
MeO
O
O
N
N
17v
ppm

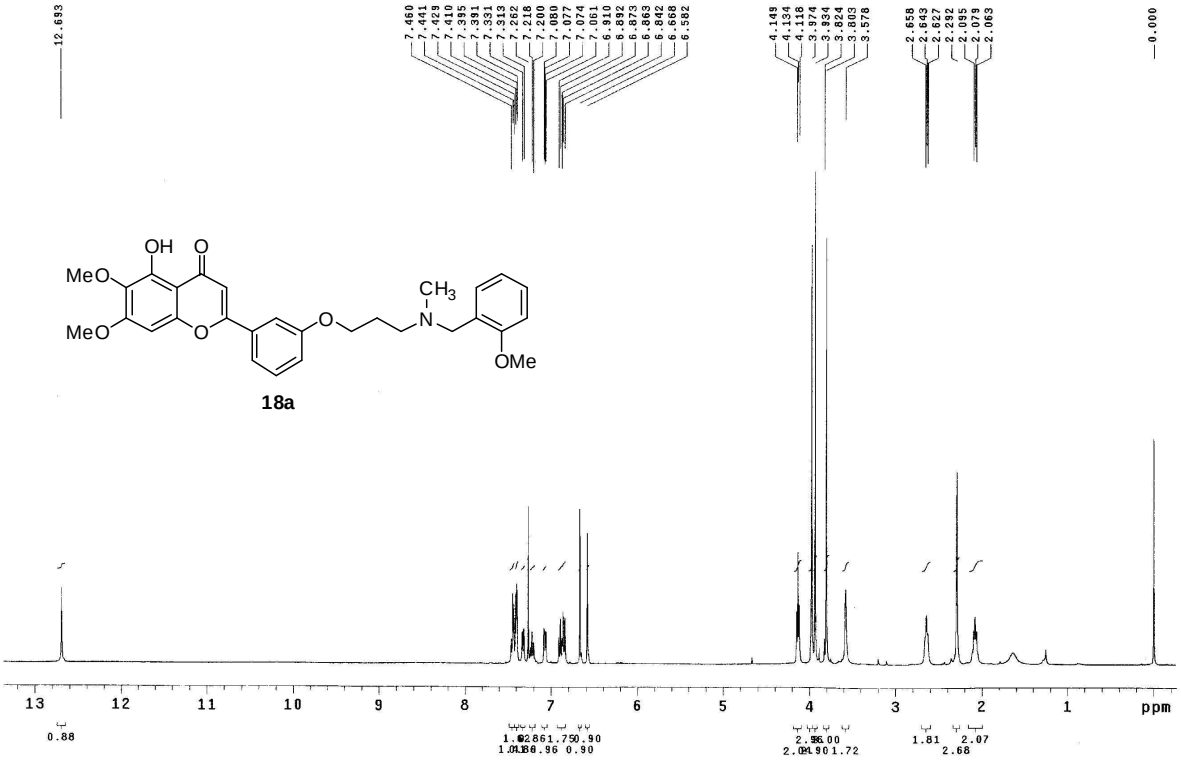
12.683
7.460
7.441
7.429
7.410
7.395
7.391
7.331
7.313
7.262
7.218
7.200
7.080
7.077
7.074
7.061
6.910
6.892
6.873
6.863
6.842
6.668
6.582
4.149
4.134
4.116
3.974
3.934
3.824
3.803
3.578
2.658
2.643
2.627
2.252
2.085
2.079
2.063
0.000
OH
O
MeO
MeO
O
O
CH3
N
OMe
13
12
11
10
9
8
7
6
5
4
3
2
1
ppm
0.88
1.81
2.07
2.68

18a

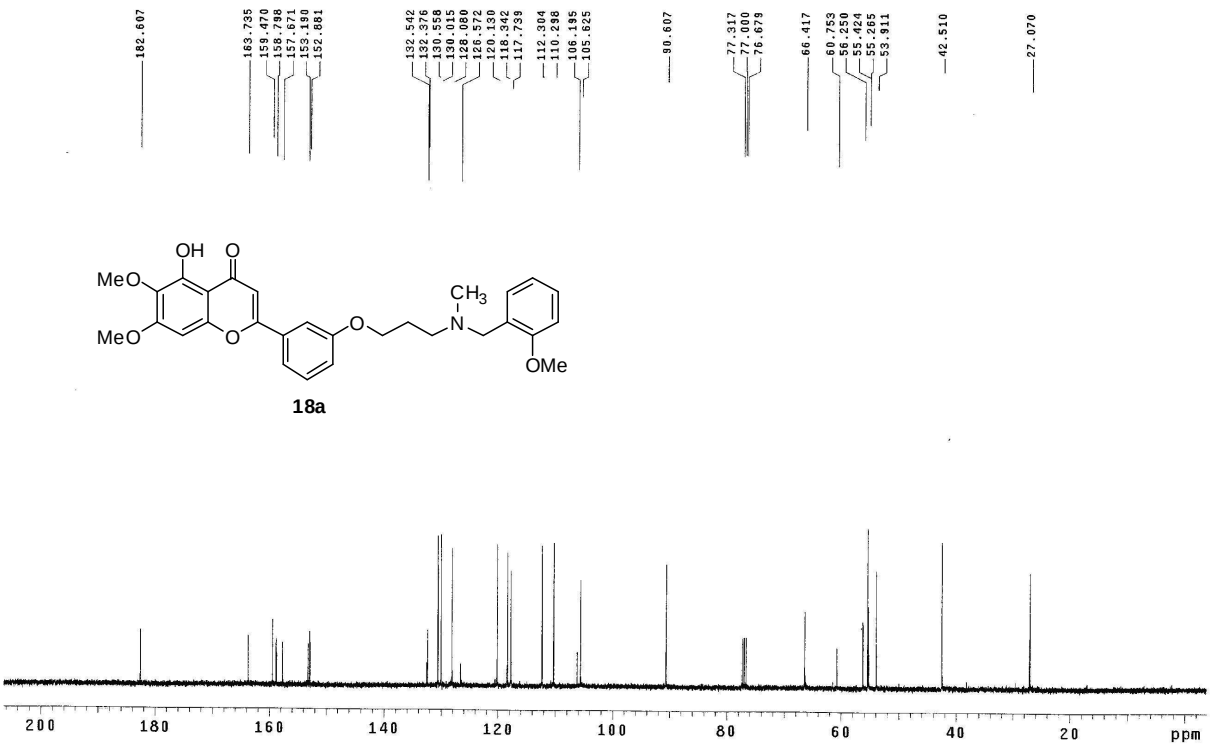
182.607
163.735
159.470
158.798
157.671
153.180
152.881
132.542
132.376
130.558
130.015
128.080
126.572
120.130
118.342
117.739
112.304
110.298
106.195
105.625
90.607
77.317
77.000
76.679
66.417
60.753
56.250
55.424
55.265
53.911
42.510
27.070
OH
O
MeO
MeO
O
O
CH3
N
OMe
200
180
160
140
120
100
80
60
40
20
ppm

18a

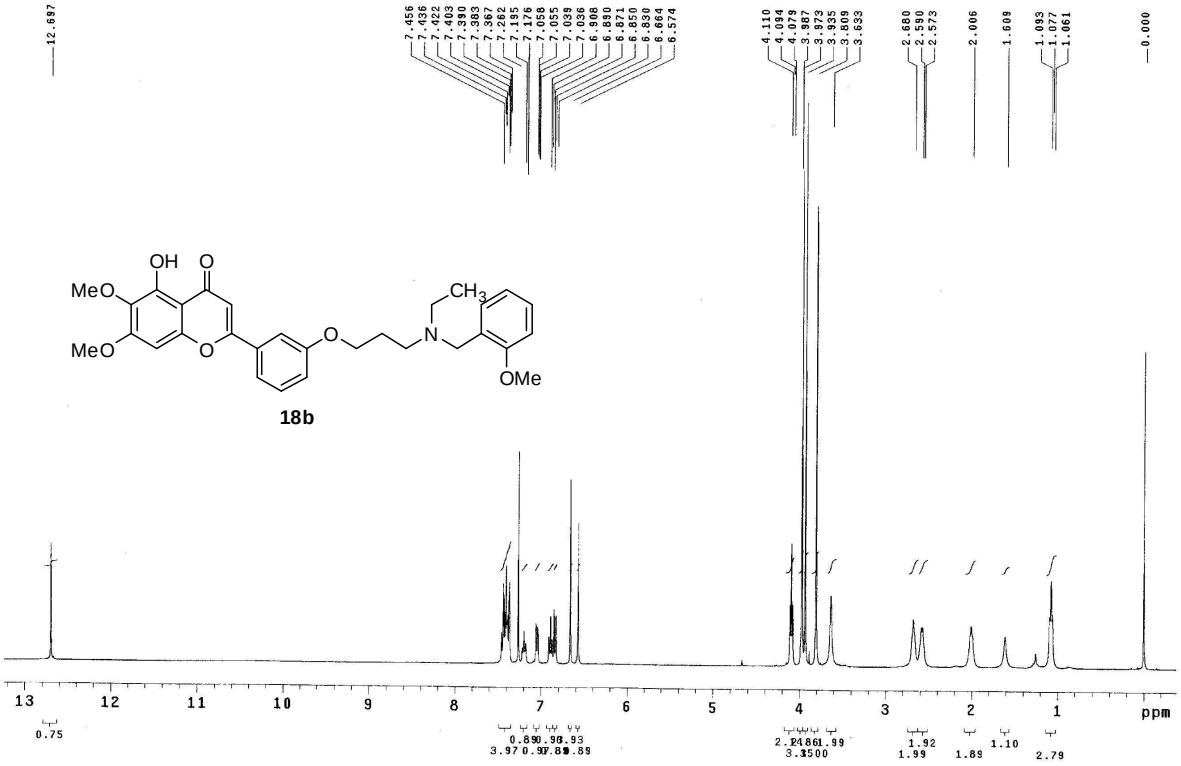
12.697
7.456
7.436
7.422
7.403
7.390
7.383
7.367
7.282
7.195
7.176
7.058
7.055
7.038
7.036
6.908
6.880
6.871
6.850
6.830
6.664
6.574
4.110
4.094
4.079
3.887
3.873
3.835
3.809
3.633
2.680
2.590
2.573
2.006
1.609
1.093
1.077
1.061
0.000
OH
O
MeO
MeO
O
O
N
CH3
OMe
18b
13
12
11
10
9
8
7
6
5
4
3
2
1
ppm
0.75
0.89
0.98
0.93
3.97
0.97
0.89
2.24
1.86
1.99
3.15
00
1.92
1.99
1.89
1.10
2.79

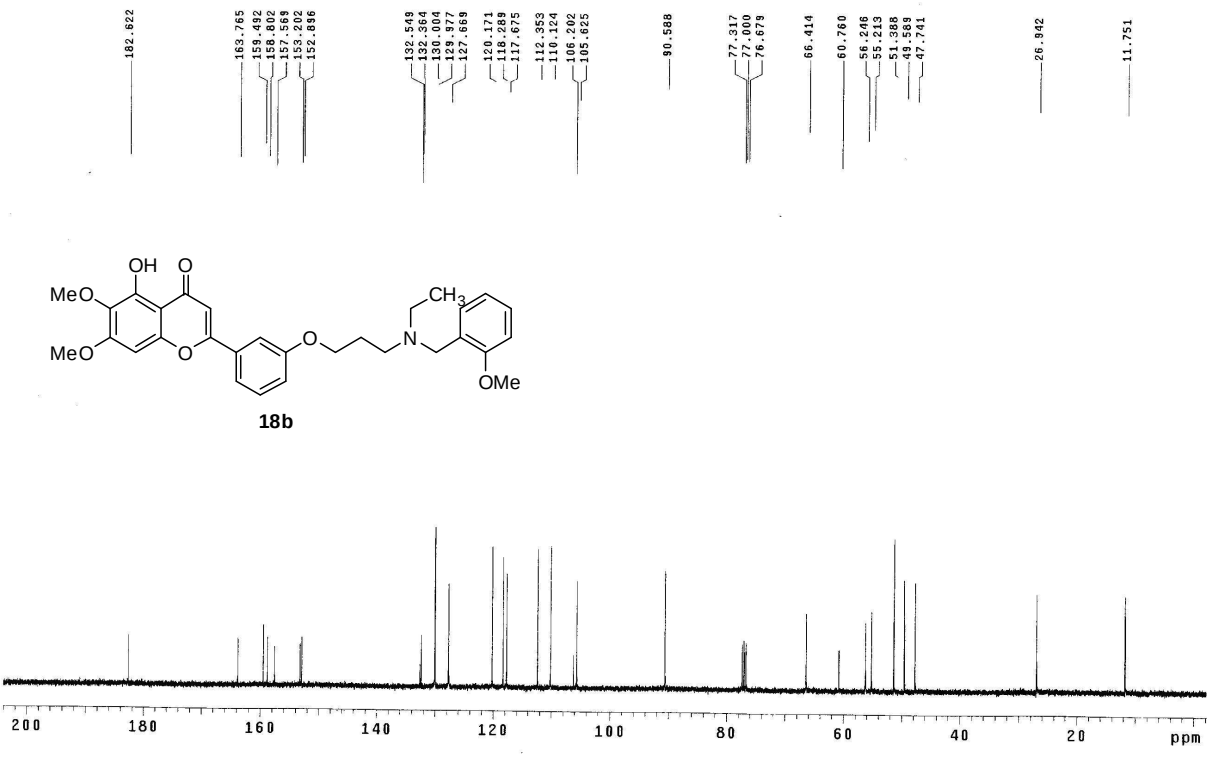
182.622
163.765
159.492
158.802
157.569
153.202
152.856
132.549
132.364
130.004
129.977
127.669
120.171
118.289
117.675
112.353
110.124
106.202
105.625
90.588
77.317
77.000
76.679
66.414
60.760
56.246
55.213
51.388
49.589
47.741
26.942
11.751
OH
O
MeO
MeO
O
O
N
CH3
OMe
18b
200
180
160
140
120
100
80
60
40
20
ppm

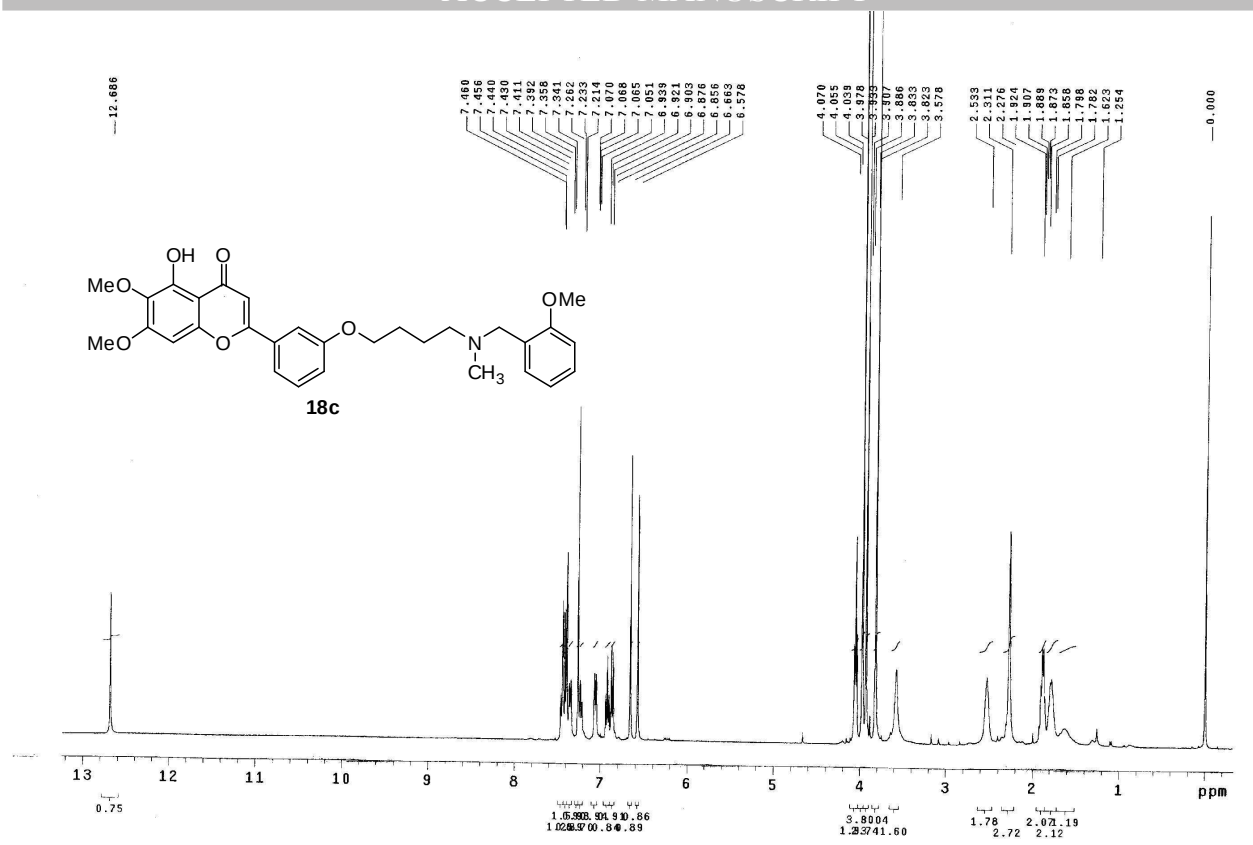
12.686
7.460
7.456
7.440
7.430
7.411
7.392
7.358
7.341
7.262
7.233
7.214
7.070
7.068
7.065
7.051
6.939
6.921
6.903
6.878
6.855
6.668
6.578
4.070
4.055
4.039
3.978
3.933
3.907
3.886
3.853
3.823
3.578
2.533
2.311
2.276
1.924
1.907
1.889
1.873
1.858
1.798
1.782
1.623
1.254
0.000
OH
O
MeO
MeO
O
O
OMe
N
CH3
18c
13
12
11
10
9
8
7
6
5
4
3
2
1
ppm
0.75
3.8004
1.78
2.72
2.07
2.12
1.19

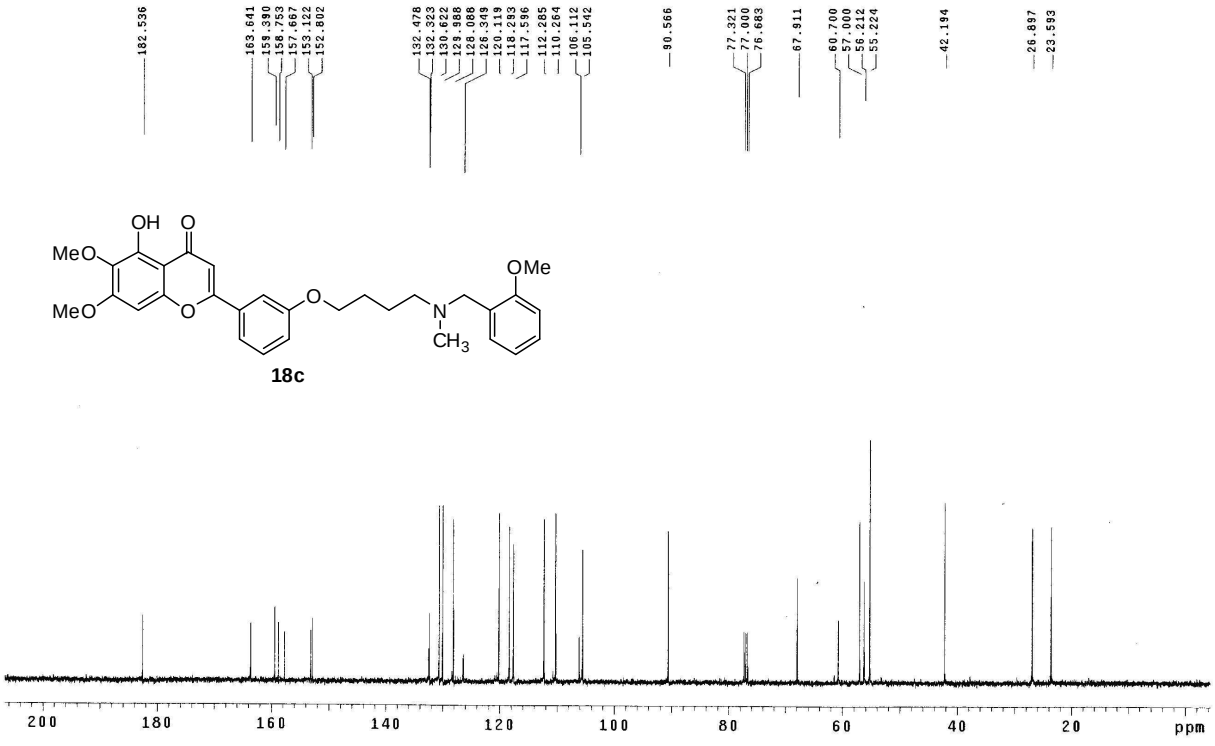
182.536
163.641
159.390
158.753
157.667
153.122
152.802
132.478
132.323
130.622
129.388
128.088
126.349
120.113
118.283
117.596
112.285
110.264
106.112
105.542
90.566
77.321
77.000
76.683
67.911
60.700
57.000
56.212
55.224
42.194
26.897
23.593
OH
O
MeO
MeO
O
O
OMe
N
CH3
18c
200
180
160
140
120
100
80
60
40
20
ppm

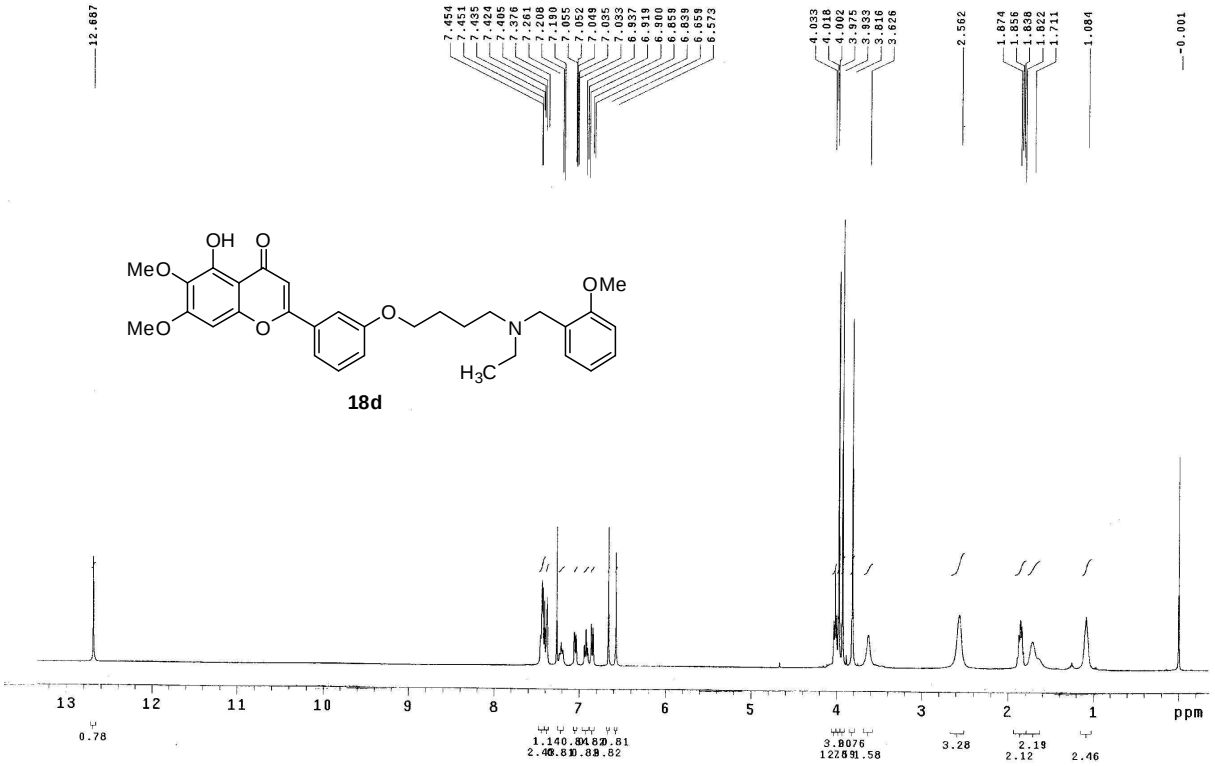
12.687
7.454
7.451
7.435
7.424
7.405
7.376
7.261
7.208
7.190
7.055
7.052
7.049
7.035
7.033
6.937
6.919
6.900
6.859
6.839
6.659
6.573
4.033
4.018
4.002
3.975
3.833
3.816
3.626
2.562
1.874
1.855
1.838
1.822
1.711
1.084
-0.001
OH
O
MeO
MeO
O
O
OMe
N
H3C
13
12
11
10
9
8
7
6
5
4
3
2
1
ppm
0.78
3.28
2.19
2.12
2.46

18d

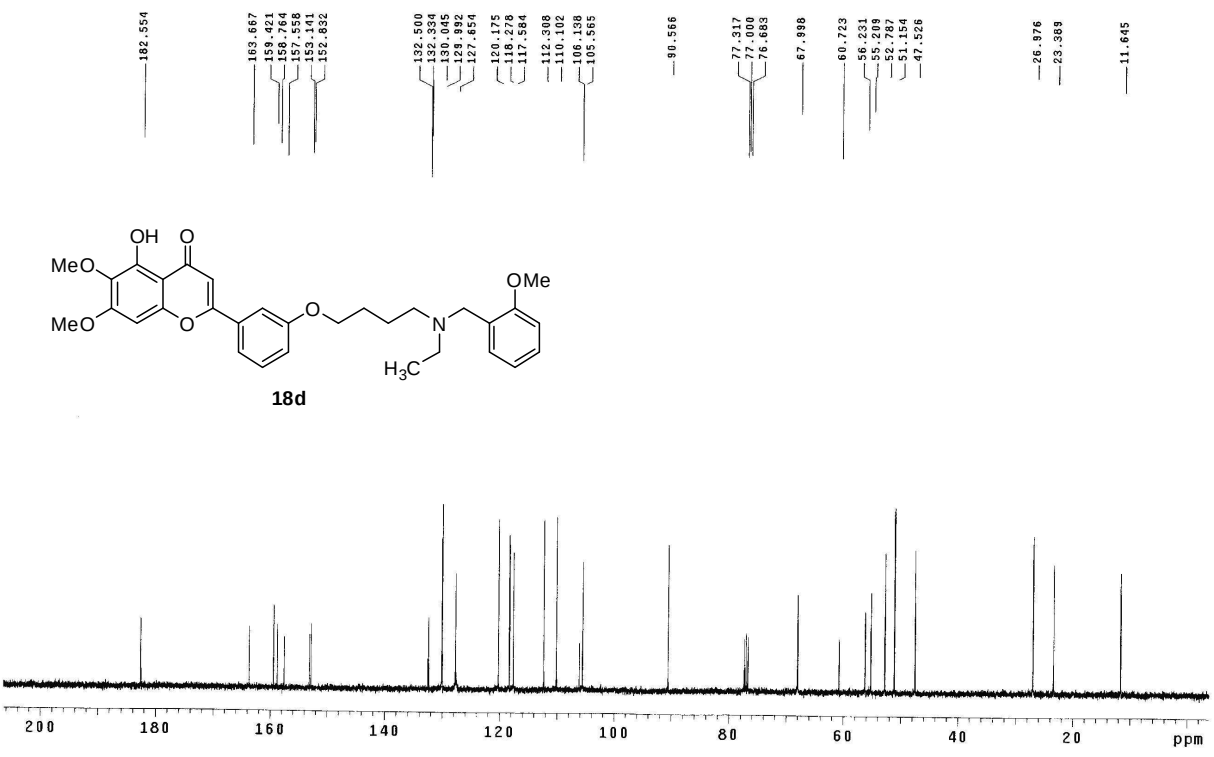
182.554
163.667
159.421
158.764
157.558
153.141
152.832
132.500
132.334
130.045
129.992
127.854
120.175
118.278
117.584
112.308
110.102
106.138
105.565
90.566
77.317
77.000
76.683
67.998
60.723
56.231
55.209
52.787
51.154
47.526
26.976
23.383
11.645
OH
O
MeO
MeO
O
O
OMe
N
H3C
200
180
160
140
120
100
80
60
40
20
ppm

18d

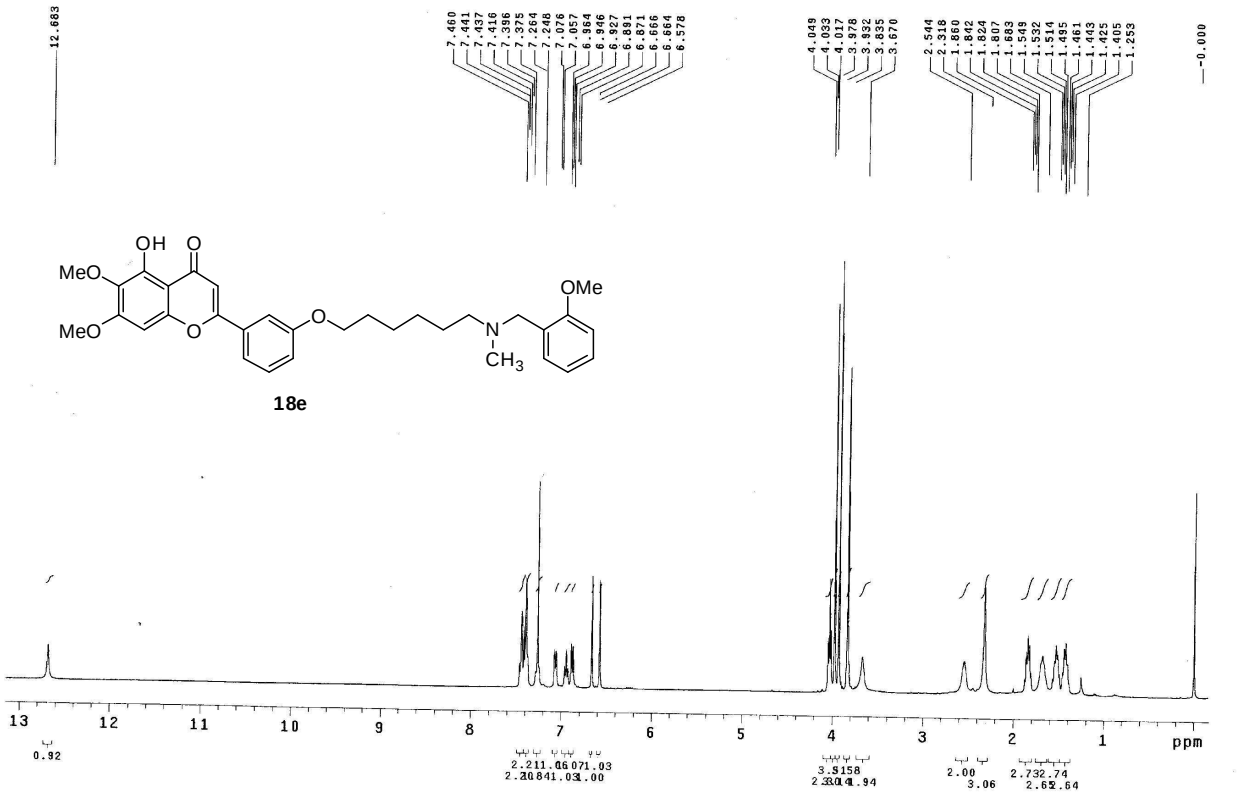
12.663
7.460
7.441
7.437
7.418
7.396
7.375
7.264
7.246
7.076
7.057
6.944
6.926
6.871
6.871
6.666
6.664
6.578
4.049
4.033
4.017
3.878
3.852
3.835
3.670
2.544
2.318
1.860
1.842
1.824
1.807
1.683
1.549
1.532
1.514
1.495
1.461
1.443
1.425
1.405
1.253
-0.000
OH
O
MeO
MeO
O
O
OMe
N
CH3
18e
13
12
11
10
9
8
7
6
5
4
3
2
1
ppm
0.92
2.21
1.06
1.07
1.03
1.00
3.51
58
1.94
2.00
3.06
2.73
2.74
2.64

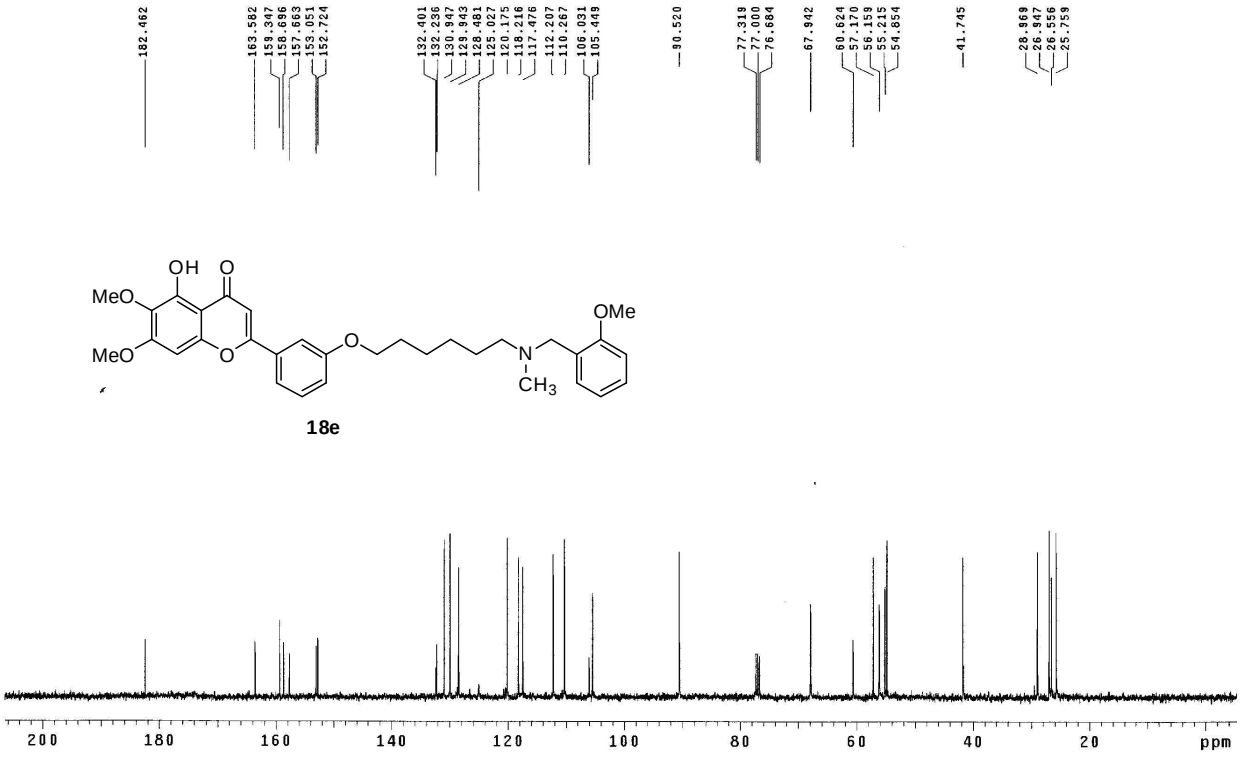
182.462
163.582
159.347
158.696
157.663
153.051
152.724
132.401
132.236
130.947
129.943
128.481
125.027
120.175
118.216
117.476
112.207
110.267
106.031
105.449
90.520
77.319
77.000
76.684
67.942
60.624
57.170
56.159
55.215
54.854
41.745
28.969
26.947
26.556
25.759
OH
O
MeO
MeO
O
O
OMe
N
CH3
18e
200
180
160
140
120
100
80
60
40
20
ppm

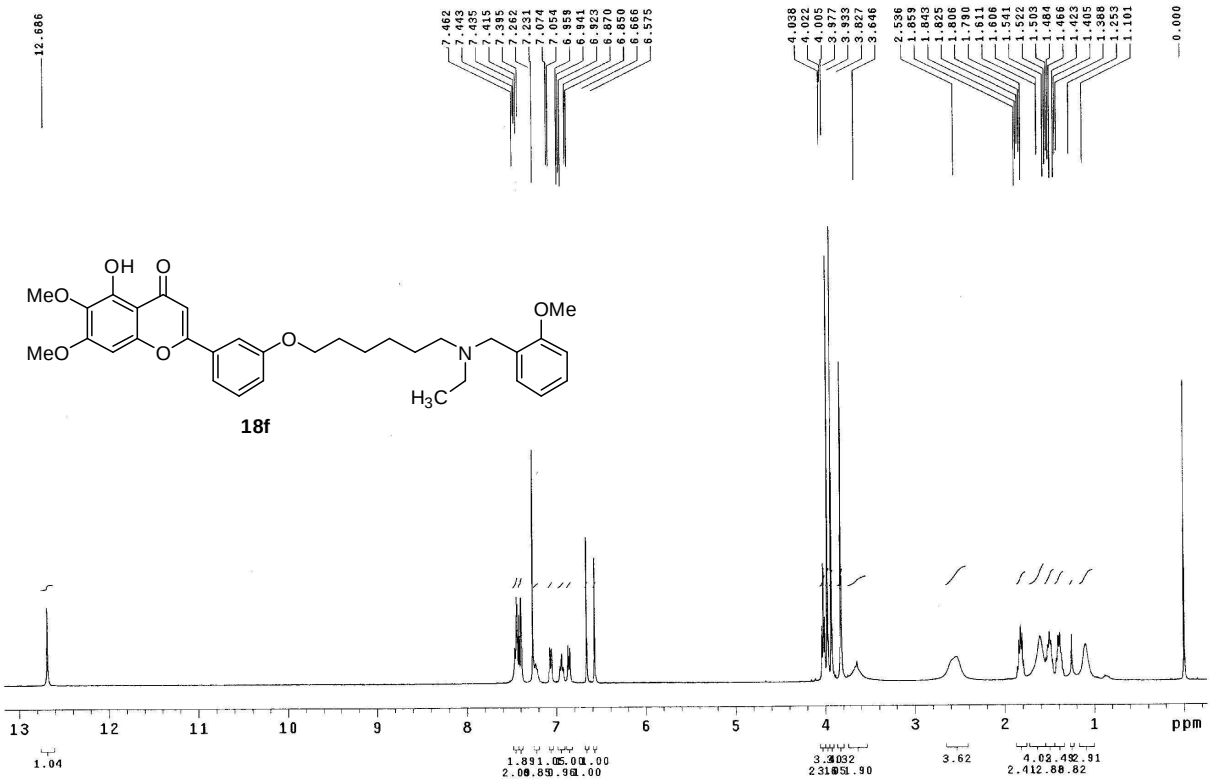
12.686
7.462
7.443
7.435
7.415
7.395
7.262
7.231
7.074
7.054
6.959
6.941
6.923
6.870
6.856
6.656
6.575
4.038
4.022
4.005
3.977
3.933
3.927
3.646
2.536
1.859
1.843
1.825
1.806
1.790
1.611
1.606
1.541
1.522
1.503
1.484
1.466
1.423
1.405
1.388
1.253
1.101
0.000
OH
O
MeO
MeO
O
O
OMe
N
H3C
13
12
11
10
9
8
7
6
5
4
3
2
1
ppm
1.04
3.62

18f

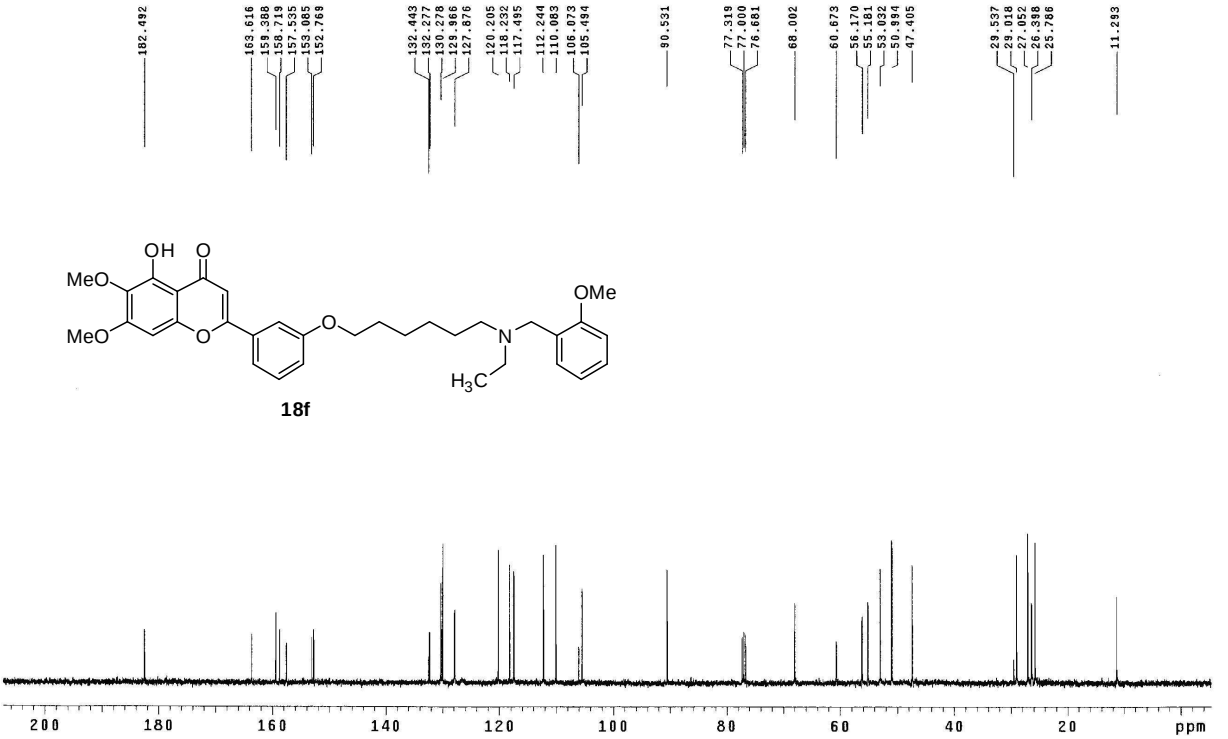
182.492
163.616
159.388
158.719
157.535
153.085
152.769
132.443
132.277
130.278
129.966
127.876
120.205
118.232
117.495
112.244
110.083
106.073
105.494
90.531
77.319
77.000
76.681
68.002
60.673
56.170
55.181
53.032
50.934
47.405
29.537
29.018
27.052
26.388
25.786
11.293
OH
O
MeO
MeO
O
O
OMe
N
H3C
200
180
160
140
120
100
80
60
40
20
ppm

18f